NONLINEAR WAVE MODELLING OVER VARIABLE WATER DEPTH USING EXTENDED BOUSSINESQ EQUATIONS

NIGEL J. WILLIAMS

Nonlinear Wave Modelling over Variable Water Depth using Extended Boussinesq Equations

by

©Nigel J. Williams

A thesis submitted to the School of Graduate Studies in partial fulfillment of the requirements for the degree of

Masters of Engineering

Faculty of Engineering and Applied Science

Memorial University of Newfoundland

December 2012

St. John's Newfoundland

Abstract

Numerical modeling of wave-ship interaction in shallow water over variable depth requires an accurate description of diffraction, refraction, reflection, and nonlinear wave-wave interaction. A computer program has been developed to solve time dependent Boussinesq-type hyperbolic long wave equations. The velocity at an arbitrary depth is expanded into an infinite series for the formulation of the extended Boussinesq equations. The numerical stability and dispersion characteristics are improved for increasing water depths. The partial differential equations are solved by using a fifth-order Adams-Bashforth-Moulton time marching multistep finite difference method. The results are compared with a second-order Crank Nicolson finite difference method and a Galerkin finite element method from previously published results. Results for linear and nonlinear waves are also compared with analytical and experimental data. The program will be integrated with a time-domain seakeeping program to simulate wave-ship interaction in coastal waves. The current research contributes higher order time and space discretizations, and generalizes the numerical algorithm for methods of any order given the coefficients for finite difference equations. The research allows for higher-order Boussinesq equations while minimizing the numerical error from the time and space differential approximations.

Acknowledgements

I would like to thank my supervisors Dr. Heather Peng, Dr. Wei Qiu, and Dr. Brian Veitch for their guidance throughout my research. Their patience and interest in my work was invaluable. I would like to thank the NSERC CREATE research program for Offshore Technology Research for their financial assistance. I would also like to thank my family for their continuous support and encouragement.

My time was made enjoyable from many interesting discussions with my fellow students in the advanced marine hydrodynamics lab. Their humour and enthusiasm was a constant source of inspiration for my work.

There are many people who are responsible for igniting my interest in ocean waves from my experiences in sailing, surfing, and scuba diving. My passion for programming, mathematics, and physics was also nurtured by many people throughout my life.

Table of Contents

List of Tables

List of Figures

Nomenclature

α	aribitrary depth variable
δ	nondimensionalized wave amplitude
η	free surface elevation
λ	wave length
μ	nondimensionalized wave number
ω	angular frequency
ρ	fluid density
τ	stess tensor
θ	phase
a	wave amplitude
a_0	incident wave height
c	wave celerity or phase velocity
F	external forces
g	gravity

h	water depth
h_0	incident wave depth
k	wave number
m	mass of fluid volume
p	pressure
Q	volume flux
S	fluid surface area
T	wave period
t	time
u	horizontal velocity component
U_r	Ursell number
V	fluid volume
v	longitudinal velocity component
w	vertical velocity component
x	horizontal coordinate
y	longitudinal coordinate
z	vertical coordinate
z_α	selected depth for specified value of alpha

Chapter 1

Introduction

1.1 Coastal Wave Propagation

Significant progress has been made in the prediction of the propagation of waves in coastal regions. In deep water, wave motion is not influenced by water depth. Linear wave theories are well understood for small amplitude waves in deep water. Accurately predicting the waveform in the near shore region is still a challenge in coastal engineering. Wave shoaling has been well researched in the past few decades and numerous researchers have taken different approaches in balancing increasing orders of nonlinearity with dispersive terms. The modelling of wave propagation from deep to shallow water is still a challenge, since most dispersive nonlinear long wave equations only have solutions in shallow water and the dispersion relation is not well satisfied in deep water. Wave evolution through the propagation over variable bathymetry is a complex process involving refraction due to the bottom boundary, diffraction from structures, and nonlinear wave-wave interaction from multidirectional waves. Wave shoaling requires high nonlinearity and dispersion for the accurate prediction of long waves. The standard Boussinesq model includes low order effects of frequency disper-

sion and nonlinearity. The equations are widely used for coastal wave propagation to simulate the shoaling action of the wave up to the point where wave breaking occurs and vorticity is induced.

1.2 Non-dimensionalized Variables

The frequency dispersion μ is the wave number non-dimensionalized by the water depth, which represents the dispersive effects of the wave model. The value indicates the range of stability from shallow to deep water for a particular set of Boussinesq equations. The non-dimensionalized wave amplitude, δ, represents the order of nonlinearity for the wave model.

$$\mu = kh \qquad \delta = \frac{a}{h} \qquad k = \frac{2\pi}{\lambda} \qquad c = \frac{\omega}{k}$$

where a is the wave amplitude, k is the wave number, λ is the wave length, h is the water depth, c is the phase velocity, and ω is the angular frequency of the wave.

These non-dimensional variables are used to describe the frequency and amplitude dispersion of the long wave equations. Higher orders of nonlinearity are balanced through increasing orders of dispersion, so these values significantly reflect the accuracy of each particular set of equations.

1.3 Stokes Waves

Stokes (1847) developed wave theory for wave lengths smaller than twice the water depth, which assumes short waves in deep water.

$$\mu = \frac{2\pi h}{\lambda} \approx 1$$

The wave number is a function of wave length and is independent of the water depth for short waves. The flow properties decrease exponentially towards the bottom boundary. Short waves have a circular water particle motion which is due to the phase shift between identical horizontal and vertical flow velocities. These waves exist in deep water or in the form of wind generated capillary waves which are not influenced by the bottom boundary.

$$\frac{h}{\lambda} > \frac{1}{8} \sim \frac{1}{10}$$

1.3.1 Long Waves

Long waves have wave lengths significantly longer than the water depth. Stokes wave theory is not applicable for waves in shallow water. Shallow water is when the vertical water depth is small relative to the horizontal wave length. If $\lambda < 2h$, then the water depth is consider deep relative to the wave length. If $\lambda > 10h$, then the water depth is shallow relative to the wave length. Otherwise, when $1/10 < h/\lambda < 1/2$, the water depth is consider to be of moderate depth. It is the intent of the research to make μ (the correlation between the wave length and the water depth) arbitrary, so that the wave model is stable in all water depths, which adds significant complexity to the physical equations.

$$h \ll \lambda \qquad \mu \ll 1$$

The deep water limit is dependent on the length of the waves and water depth. It assumes that the depth is greater than half of the wave length. In shallow water, the

bottom boundary influences the propagation of the waves, and the phase velocity is dependent on the local water depth. Horizontal velocity is uniform over the water depth, but the vertical velocity decreases linearly. A long wave has a higher magnitude of horizontal velocity relative to the vertical velocity.

1.3.2 Small Amplitude Waves

Linear wave theory accurately describes wave propagation for small amplitude waves. Fluid velocity is linearly proportional to the amplitude of the wave.

$$\delta \ll O(\mu^2)$$

The small amplitude wave assumption significantly reduces the complexity of the wave equations.

1.3.3 Large Amplitude Waves

For large amplitude waves, linear wave theory is no longer accurate at predicting wave propagation. Higher order terms are increasingly significant for larger amplitudes.

$$\delta \gg O(\mu^2)$$

Large amplitude waves require nonlinear wave theory to describe the wave motion. Large amplitude waves are generated through storm swells or from significant shoaling.

1.3.4 Moderate Amplitude Waves

For waves of moderate amplitude, the nonlinear terms are of the same magnitude as the linear terms, so all linear, nonlinear, and dispersive terms are needed, as both

nonlinearity and dispersion are required to accurately model the propagation of long waves of moderate amplitude.

$$\delta \approx O(\mu^2)$$

Nonlinear terms are proportional to the wave amplitude and must be retained. Long waves are no longer predicted through the use of the nonlinear shallow water equations. Boussinesq wave theory is required to accurately model the equations. As defined by Stoker (1947) and Svendsen and Veeramony (1996)

1.4 Types of Waves

A wave is the propagation of a displacement of energy through a volume of fluid. Surface waves exist at the interface between the atmosphere and the fluid region. The restoring forces of gravity and surface pressure exist in an equilibrium for still water. The atmospheric pressure is assumed to be hydrostatic. Internal waves propagate submerged within a fluid instead of on the surface. External forces generate the initial wave forms, such as wind, currents, and other seismic sources. In deep water, surface waves have particles that move in a circular motion. The orbital motion of the particles decrease for lower depths below the surface, which is why the shear stress at the bottom boundary does not influence waves in deep water. For shallow water, the orbital motions of the particles become elliptical due to the rigid ocean floor. Transverse waves have particles that move in a direction perpendicular to the direction of the wave. Longitudinal waves have particles that move parallel to the direction of the wave, such as sound waves.

1.4.1 Gravity Waves

If water is displaced, then due to the isotropic nature of a Newtonian fluid and under the force of gravity, it will return to its state of equilibrium. Pressure and gravity are restoring forces which act upon a fluid to create the hydrostatic equilibrium. Gravity keeps the fluid volume from diffusing due to the dynamic pressure, which inversely keeps gravity from compressing the fluid volume. Surface waves propagate on the interface between water and the atmosphere. The nonlinear wave interaction of long periodic waves generate low frequency propagating waves. Infragravity waves are low frequency waves with long periods. These waves are generated through the nonlinear wave interaction from ocean swells. Ocean swells build up energy over time through the continual repetitive environmental force from storm winds. Non-harmonic waves are generated through transient forces. A tsunamis is sometimes inappropriately referred to as a tidal wave. Tsunamis are generated by intense seismic events or land slides. A tidal bore is generated through a large continuous displacement of water funnelled into still water, such as when the tide rolls into the bay of Fundy. Hydraulic jumps occur when waves of high velocity enter water travelling at a slower velocity, such as the waves generated in rivers.

1.4.2 Other Types of Waves

Wind blowing on a fluid surface generates waves through the forces acting on the fluid. Surface tension controls the dynamics of capillary waves which have a wave length of less than a couple centimetres. Capillary waves differ from gravity waves. They travel faster for shorter wave lengths, while gravity waves increase in speed for longer waves. Capillary waves are still affected by gravity. Sound, light, electromagnetic and seismic waves also have some of the same properties as waves acting in a fluid medium.

Sound waves generate a change in pressure and travel in the form of a wave. Seismic waves occur from an extreme external force and propagate due to the elasticity of particular solids. Photons have elliptical paths and are thought to travel in the form of a wave, but they also exhibit particle theory for which light instead emits in all directions. Other forms of waves have similar properties to gravity water waves and their differential equations can be solved using similar numerical methods.

1.5 Wave Effects

The transformation of shallow water waves are affected by refraction, diffraction, and reflection. Shoaling is the combination of frequency and amplitude dispersion, which influences the wave height and phase velocity. The study investigates the conservation of mass and momentum for an inviscid and incompressible fluid using depth integrated wave equations. The equations of motion for fluid flow are modified to include the effects of varying depths. The nonlinear transformation of long waves in shallow water was investigated by many different researchers. The original Boussinesq equations for shallow water waves account for the low order effects of frequency dispersion, but are only applicable for relatively shallow water depths. The equations produce a dispersion relation from their linear solution, which is not valid in deep water. The equations have been extended to use the velocity variable at an arbitrary distance from the free surface elevation, which improves the linear dispersion properties and allows for the theory to be applied for a wider range of depths while retaining the nonlinear effects of amplitude dispersion.

1.5.1 Shoaling

The transformation from the propagation of long waves is studied for varying bathymetry. As a wave propagates towards a slope with normal incidence from a uniform depth, the wave speed slows down due to the reduction of the water depth, since waves travel slower in shallower depths. As the water depth decreases, the wave height increases due to the physical effects of shoaling, and both the wave celerity and wave length decrease in the shallower water depths. Shoaling requires high order nonlinearity and dispersion for accurate prediction. Reflection significantly affects the shoaling process, and dispersive waves are generated from the tail of the wave. The conservation of flux produces an increase in wave height. Nonlinearity, bottom friction, and wave breaking limit the growth of the wave. Dissipation from vorticity and viscous damping decrease the effects of shoaling. Wave energy is lost due to dissipation from turbulence after a wave breaks.

1.5.2 Refraction

As a wave propagates toward the shore from an oblique direction, or if the angle of inclination is not incident to the direction of the wave, the water wave changes its direction due to refraction. The water depth affects the speed of the wave. A wave will travel slower in shallower depths, and the fluid particles travelling faster in the deeper water will refract towards the shore. Waves of different frequencies will refract to different phase velocities, so dispersion of the waves is formed. Regardless of the incident angle of the wave from the shoreline, a wave always curves toward the normal incident direction from the shore.

1.5.3 Diffraction

Due to diffraction, a wave bends around an obstructing structure or object as it propagates past. Some of the wave energy reflects behind the object, and the fluid particles travel in all directions past the obstruction. Flow separation can be significantly behind the object and a shadowed region may evolve. Wave diffraction reduces the wave amplitude from the diffusion of energy. Diffraction occurs when the obstruction is of the same magnitude as the wave length. Wave diffraction either causes a wave to bend around a structure or spread out from an opening. Secondary wavelets are generated from a point source on the wavefront.

1.5.4 Viscous Damping

Wave amplitude is continuously reduced during propagation. Bottom friction, surface tension, viscosity, and wave breaking significantly increase wave damping. A boundary layer is formed on the floor of the ocean due to the propagation of the wave and the surface friction. The surface of the wave is affected by the shear stress from the wind. The damping is determined by the shear stress from both the surface and bottom boundaries. The bottom roughness, wind speed, and wave amplitude determine the rate of strain, which generates the turbulent energy within the boundary layers. Turbulence increases the effect of shear stress. Energy dissipation occurs in the bottom boundary layer dependent on the friction coefficient and Reynolds number, while the surface tension is also affected by the Froude number of the wave and the wind speed. Porous beds also influence the wave damping. Viscosity is neglected in this research.

1.5.5 Breaking

In the surf zone, wave energy either completely dissipates or reflects back to the open sea. The steepness of the wave is unaffected by dissipation until it reaches the breaking point. Once a wave shoals past the vertical tangent of the wave front, the breaking process is set in motion. Most of the wave energy is reflected back into the domain, but some energy is lost in the breaking process. Excessive wave energy generates turbulence when a wave height grows beyond a maximum height as the wave system becomes unstable. Violent turbulence generates continuous air entrainment within the region of vorticity. The wave energy dissipates and returns to a laminar flow and is reflected back into the domain. A low gradient slope with a steep wave will form a spilling or collapsing breaker. A plunging breaker is formed as the wave steepness is reduced, or the slope increases. A plunging jet will generate strong air entrainment after impacting the fluid below generating mixing layers. As slope increases further a surging breaker is formed as the wave collapses. The surging wave is nearly completely reflected when the slope is steep. An underwater bore may form if the breaking process is long. The breaking process is dominated by the vorticity generated inside a roller region carried along with the wave. The roller thickness defines the mixing length, and the vorticity is generated at the toe of the roller. The vorticty is zero at the free surface and bottom boundaries, but is significant in the roller region. The boundary location of a shoreline changes continuously with the flow of water waves. Bottom friction is significant in the swash zone due to the shallow water depth. The bottom friction and gravitational force causes a minimal amount of water to remain stationary. Once the wave energy is completely dissipated from the shear stress or is reflected from the boundary, the wave runs back down the shore. If the wave over tops the boundary, then inundation occurs and the water floods the region on the opposite side of the boundary.

Wave effects acting on the fluid combine to create a transformation of the initial wave form as it approaches the nearshore region. The mass transport due to inertia induces wave propagation. Varying water depth causes refraction and diffraction which influences wave shoaling. Wave breaking occurs from over reaching waves for which the wavefront becomes a point of inflection. Vorticity controls the turbulent motion of the fluid which is carried with the front of the wave. Runup is the final phase of the process before being reflected back into the domain, unless the region becomes inundated. The transformation of a water wave as it approaches a sloping beach is a complex process of fluid motion. The wave evolution is broken down into different stages to simplify the overall process. Wave shoaling from variable depth is of particular interest because of its nonlinearity and dispersive effects.

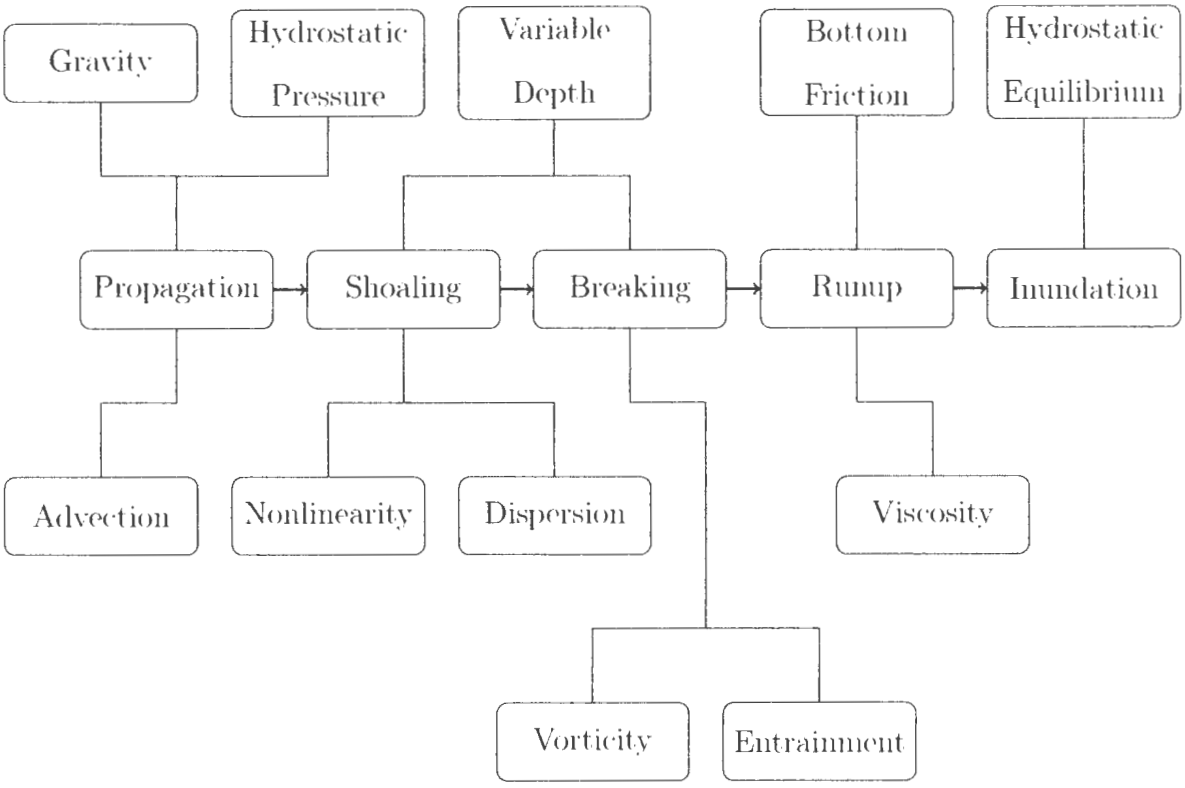

Figure 1.1: Overview of the physical transformation of a wave over varying bahtymetry

1.6 Literature Review

Euler (1757) formulated nonlinear hyperbolic equations which describe the flow of an ideal fluid. The equations are derived from the conservation of mass and momentum of the fluid. Euler derived a set of coupled partial differential equations that describe the motion of an inviscid and incompressible fluid. The Euler equations are composed of the continuity and momentum equations. The momentum equations are three partial differential equations for each velocity component.

1.6.1 Wave Theories

Trochoidal deep water wave theory was first developed by Gerstner (1809). He described wave propagation through the elliptical motion of fluid particles. Gerstner waves are rotational. Deep and shallow water waves are well understood and were thoroughly researched by Airy (1841). Airy (1841) developed differential and analytical equations for linear small amplitude wave theory using surface and bottom boundary conditions. He linearized the propagation of surface water waves to first order and derived analytical solutions. Airy (1841) described the propagation of water waves for intermediate and shallow depths. Stokes (1847) developed a higher order approach. He used a Taylor series expansion through the perturbation of the velocity variable into a power series. He described the propagation of large amplitude short waves with nonlinearity and dispersion. Stokes (1847) described the nonlinear propagation of waves. The Stokes higher order wave equations are valid for relatively short waves with large amplitudes. St. Venant integrated the continuity equation over the water depth to form the nonlinear shallow water equations. St. Venant modelled nonlinear waves of varying form for shallow water to extend the research done by Airy (1841). The nonlinear shallow water equations describe amplitude dispersion but neglect frequency dispersion. It is valid for very long waves or very shallow water depths.

Boussinesq (1871) derived multi-directional nonlinear equations for long waves propagating over a constant depth. The equations give good approximations for waves with moderate amplitudes (Boussinesq (1872)). The equations include weak nonlinearity and low order frequency dispersion. The dispersion relation is derived using a Pade approximant instead of a Taylor series expansion. The equations are valid for long waves. The multi-directional equations accurately predict outgoing reflected and dispersive waves. The Boussinesq equations give a better approximation for larger amplitude

waves in deeper water than the nonlinear shallow water equations. The equations include weak nonlinearity and second order frequency dispersion. The velocity is expanded using a Taylor series. Solitary waves are the characteristic nonlinear solutions for the Boussinesq Equations. Korteweg and Vries (1895) extended the research done by Boussinesq and developed Cnoidal wave theory. The Korteweg-de Vries (KdV) equation is a unidirectional nonlinear and dispersive equation whose solution can be exactly specified by a Cnoidal waveform. Russell (1844) first observed a solitary wave and presented experimental results in his "Report on Waves". Rayleigh (1876) developed analytical equations describing solitary waves, which can be used as solutions to the Boussinesq equations. Korteweg and Vries (1895) developed equations for waves travelling in one direction and derived the exact analytical cnoidal wave solutions to the equations. Since then many alternate forms of the equations and accompanying solutions have been derived. Equations for shallow water waves over variable depth were developed by Lewy (1946), Stoker (1947), and Friedrichs (1948).

Table 1.1: List of Wave Theory

Equation	Frequency Dispersion	Amplitude Dispersion
Airy	first order	first order
Euler	first order	second order
Stokes	first order	second order
St. Vennant	first order	second order
Kortweg-DeVries	second order	second order
Boussinesq	second order	second order
Reynolds	first order	second order
Navier-Stokes	first order	second order

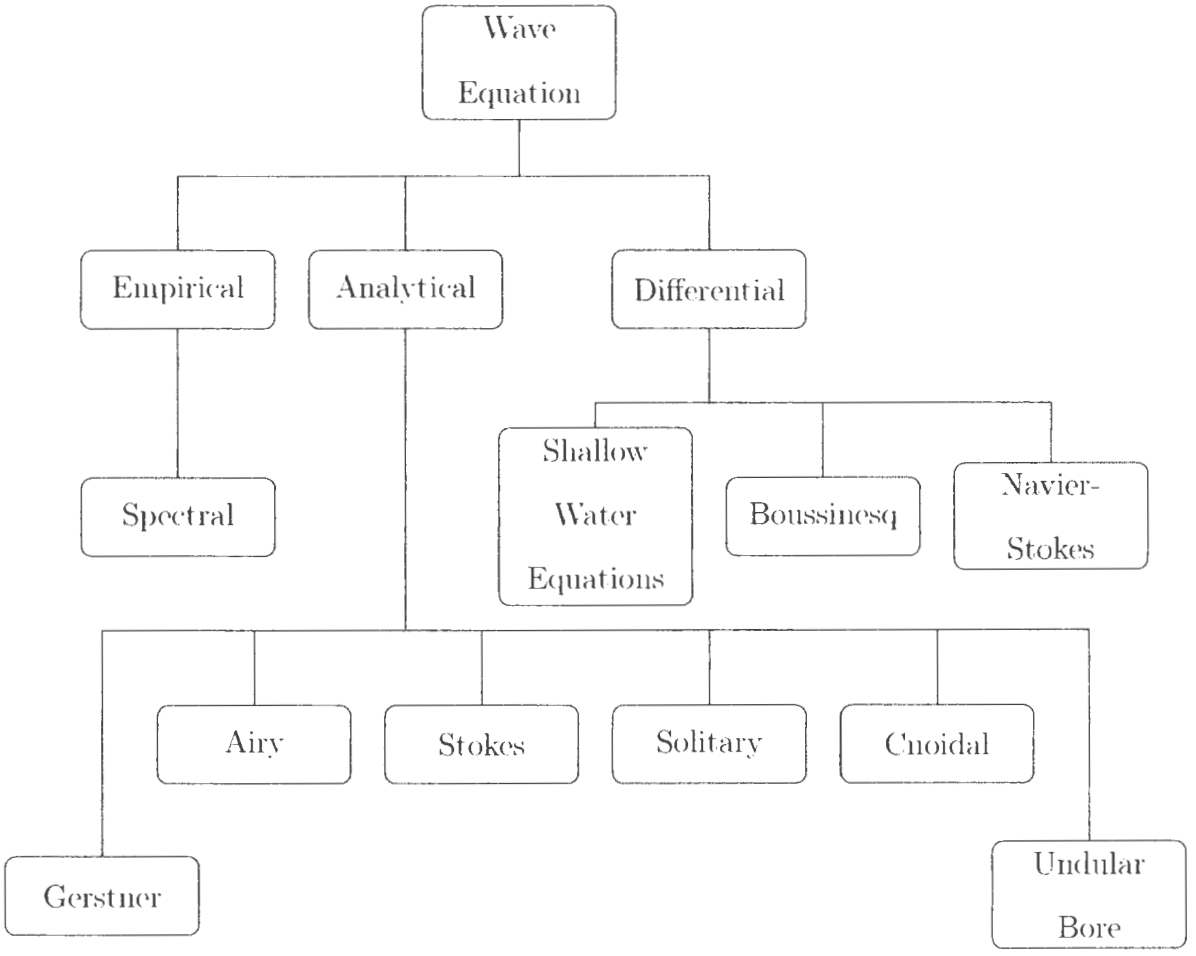

Figure 1.2: Overview of different wave theories

1.6.2 Ursell Number

Stokes (1847) showed the significance of a parameter which represents the ratio of nonlinearity to dispersion. Ursell (1953) also showed a correlation between the frequency dispersion and nonlinearity which determines which wave theory will be applicable. The contribution of both effects determine which model is valid for the selected wave parameters. Ursell (1953) proved the importance of the ratio for the determination of a particular wave theory that is stable for specified wave parameters.

$$U_r = \frac{\delta}{\mu^2} = \frac{a\lambda^2}{h^3} \tag{1.1}$$

If all nonlinear terms are relatively small compared to the linear terms, then linear wave theory is applicable for small amplitude waves.

$$\frac{\delta}{\mu^2} \ll O(1)$$

If the wave heights are of the same magnitude as the water depth and the nonlinear terms are of the same order of magnitude as the linear terms, then the nonlinear SWE are used for large amplitude waves.

$$\frac{\delta}{\mu^2} \gg O(1)$$

If both dispersion and nonlinearity are of the same order, then the Boussinesq wave model is valid for long waves of moderate amplitude. Many different extensions to the Boussinesq theory exist, and some researchers took different approaches than others.

$$\frac{\delta}{\mu^2} = O(1)$$

1.6.3 Boussinesq Models

Specific modifications and shoaling enhancements are of particular interest due to their improvement of accuracy for the prediction of nonlinearity and dispersion for surface waves travelling from deep to shallow water. Mei and Mehaute (1966) and Mei (1989) derived Boussinesq equations for one horizontal direction using the bottom velocity for the propagation of long waves over variable depth with the assumption

that the depth was small compared to the wave length. Mei derived equations for when the cubic depth is of the same order of magnitude as the amplitude. Peregrine (1967) derived Boussinesq equations for variable depth for multiple horizontal directions using depth averaged velocity. The equations provide a better description of the wave steepening from the effect of shoaling, but their major limitation was that they are only applicable to relatively shallow water depth. Efforts have been made to extend the Boussinesq equations to deeper water. Witting (1984) used exact prognostic equations and a high order expansion to compare different velocity variables in the governing equations. He used a Padé approximant to solve the dispersion relation using a power series instead of a Taylor series, which provides better comparisons with the explicit linear result. The dispersion relation is approximate, and the equations are fully nonlinear, but the equations are only derived for constant depth. He used surface velocity as the dependent variable. Grilli and J. Skourup (1989) developed a boundary element method for highly nonlinear waves using potential velocity. Madsen, Murray, and Sorensen (1991) improved the dispersive properties of the Boussinesq equations for constant and variable depth. They included a shoaling operator to accurately predict the dispersive effects and derived equations in terms of the depth integrated velocity. Witting (1984) used a Padé approximant to solve the dispersion relation using a power series instead of a Taylor series, which provides better comparisons with the explicit linear result. The dispersion relation is approximate, and the equations are fully nonlinear, but the equations are only derived for constant depth. He used surface velocity as the dependent variable.

Nwogu (1993) derived Boussinesq equations for an arbitrary depth to derive an approximation to the explicit linear dispersion relation. Nwogu explored deriving different dispersion relations by deriving Boussinesq equations in terms of different velocity

variables. He compared the phase error of the approximate dispersion relations with the explicit linear relation, and determined the optimal depth below the surface at which to take the velocity for the derivation of the equations. Nwogu derived equations for which he could specify an arbitrary depth and showed the equations were convergent for deeper water depths for the specific depth below the surface. Chen and Liu (1995) derived BE for an arbitrary depth in terms of velocity potential. Wei and Kirby (1995) derived fully nonlinear BE for a velocity at an arbitrary depth. They used a fourth-order Adams-Bashforth-Moulton predictor corrector method to reduce the truncation error lower than the order of the dispersive terms. They compared their results to that of the fully nonlinear potential flow model derived by Grilli and J. Skourup (1989). Schäffer and Madsen (1995) extended their research to fourth order accuracy for the dispersion relation using velocity at an arbitrary depth. Frequency domain equations were developed by Kaihatu and Kirby (1998) using a parabolic approximation of the Boussinesq equations. Gobbi and Kirby (1998) derived BE in terms of the fourth order Padé approximation of the dispersion relation by retaining higher order dispersive terms. Gobbi defined a new variable in terms of multiple velocities at arbitrary depths. Research done by Kennedy, Kirby, Chen, and Darymple (2001) improved the equations for runup in the swash zone. Agnon, Madsen, and Schaffer (1999) improved the nonlinearity of the BE by achieving accuracy in the nonlinear terms relative to the linear terms. Kennedy and Gobbi (2002) simplified the high order dispersion equations, while Madsen, Fuhrman, and Wang (2006) improved the velocity profile by retaining the vertical velocity in the equations. Lynett and Liu (2004) used piecewise integration of multiple velocity profiles. The two layer approach significantly increases the accuracy of the Boussinesq model for increasing values of μ. Bingham and Agnon (2005) developed a Fourier method for the Boussinesq model. Madsen, Fuhrman, and Wang (2006) extended the equations for rapidly

varying bathymetry. Bingham, Madsen, and Fuhrman (2009) corrected the vertical velocity distribution to be consistent with the kinematic boundary conditions. The equations were optimized by modifying the free parameters and improving the wave characteristics, which significantly increases the accuracy of the model for increasing depths and higher frequency dispersion. Shi, Dalrymple, Kirby, Chen, and Kennedy (2001) derived Boussinesq equations in curvilinear coordinates. The generalized coordinates allow for irregularly shaped shorelines and more efficient computation for near shore regions. Lin (2008) developed a staggered grid FD method to calculate the velocity at an offset location from the free surface to improve the accuracy of the model. Sorensen and Schaffer (2002) developed a numerical method for an unstructured grid using a finite element method (FEM). Walkley (1999b) separately implemented a Galerkin FEM for the extended BM.

Table 1.2: List of Boussinesq Models

Thoery	Velocity Variable	Method	Nonlinear	Dispersion
Boussinesq	bottom	None	weakly	second order
Mei	bottom	None	weakly	second order
Perregrine	depth averaged	FD	weakly	second order
Nwogu	arbitrary depth	FD	weakly	second order
Liu	potential	parabolic	weakly	second order
Grilli	arbitrary depth	BEM	highly	second order
Madsen	depth integrated	FD	highly	second order
Kirby	arbitrary	FD	highly	second order
Gobbi	arbitrary	FD	highly	fourth order
Agnon	arbitrary	FD	highly	fourth order
Kennedy	arbitrary	FD	highly	fourth order
Lynett	multiple depths	FD	highly	second order
Walkley	arbitrary	FEM	weakly	second order

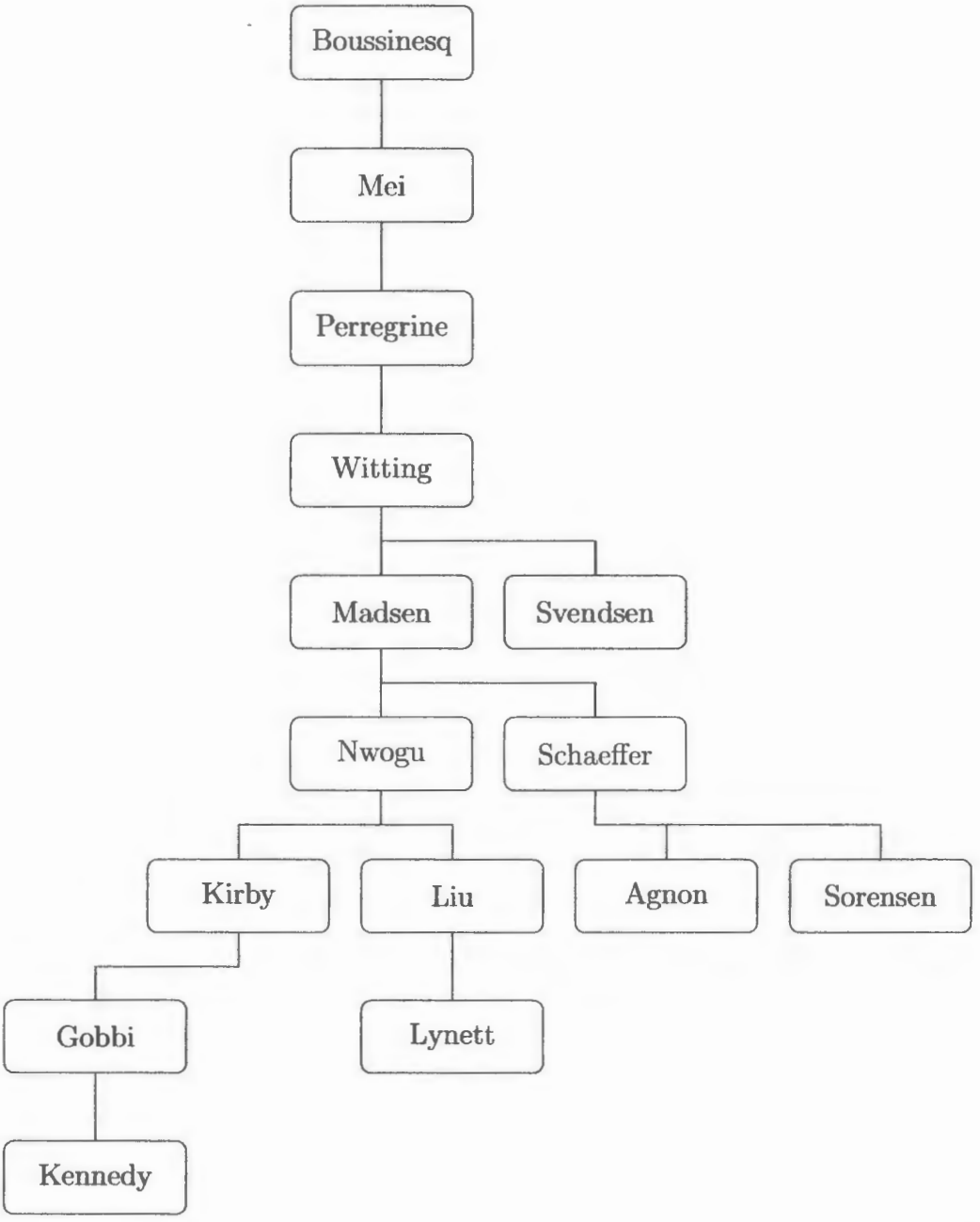

Figure 1.3: Overview of the flow of research in Boussinesq theory

1.6.4 Overview

A weakly nonlinear Boussinesq model is used for nonlinear long wave propagation over variable depth. The dependent velocity variable coupled with the free surface is derived for an arbitrary depth to extend the model to water of intermediate depth using Taylor series expansion and retaining higher order terms. Only second order terms are kept, and other higher order terms are neglected. The appropriate linear dispersion relation is derived using the velocity at the optimum water depth which is selected through comparison with the explicit dispersion relation for intermediate depth. A numerical program was developed for time dependent Boussinesq hyperbolic long wave equations. The governing equations are based on simplified Navier-Stokes equations using depth integration with Euler theory rather than potential theory to allow for the further inclusion of vorticity. No assumption of irrotationality is made. The incorporation of Reynolds equations was investigated for future work in wave breaking. Long wave equations for constant and variable depth are compared using dependent velocity variables at the bottom and surface boundaries, and also using the depth averaged velocity. The phase error in comparing the approximate and exact dispersion relation for each of these derived equations defines the extent to which a solution exists for deeper water. The dispersive properties of the original and standard Boussinesq equations are improved by using a velocity variable at an arbitrary depth which assumes a uniform vertical velocity profile. The equations prove to be stable in intermediate water depths as well as shallow water.

The hyperbolic partial differential equations are discretized using a fifth order time domain finite difference method. The Adams-Bashforth-Moulton (ADM) scheme is used for discretizing the time derivatives. The numerical model was first implemented by Wei and Kirby (1995) for the Boussinesq equations. The fifth order Adams time

marching multi step finite difference method is used to solve the equations. Sixth order spatial difference schemes are used for first order derivatives, and fourth order schemes are used for the second order derivatives which have a lower magnitude of error. The Adams predictor-corrector method is a multi-step time marching scheme. Results for linear and nonlinear shallow water waves, as well as solitary wave conditions, are compared to show the full range of solutions for the Boussinesq equations in regards to the wave parameter defined by Stokes and Ursell for long waves within the shallow water limit. The equations are valid for intermediate water depth as a result from using the extended Boussiensq model for arbitrary depth (Nwogu 1993). Amplitude and frequency dispersion are accurately modelled. Numerical filtering is used to remove short waves generated inside the fluid domain. Solitary wave solutions are studied as they are well represented by the equations and are used as the analytical solutions to the Boussinesq equations. The model is derived to be further extended into full nonlinear, high order dispersion, and wave breaking due to vorticity. Time domain Boussinesq equations are derived to model nonlinear long waves in shallow water. The selection of the optimal velocity variable significantly improves the accuracy of the model in intermediate to deeper waters. Numerical nonlinear waves are compared with experimental data. The solution is found through the construction of a tridiagonal matrix of equations.

1.7 Content of Thesis

In the following chapter, the mathematical formulation is given to derive the equations for long waves over variable depth for different velocity variables. Derivations for constant and variable depth are given for each set of equations. A full overview of the derivation of the Boussinesq equations is described. Analytical deep and shallow water

equations are given as well as for solitary waves. In Chapter Three, the numerical method used in the research is defined. Nine point numerical filtering is described. The algorithm for the numerical method is fully described in detail. The full details for the methods and solvers are given to allow for further research into the topic. In Chapter Four, the numerical results are validated with analytical and previously published results. Solitary wave propagation over variable depth was modelled, as well as the periodic propagation over a breakwater. Both situations generate a train of smaller dispersive waves. Wave Reflection is validated for a solitary wave propagating up a slope and reflecting against a vertical wall. In Chapter Five, the numerical program is described. Other existing dispersive long wave software is discussed and contrasted with the implemented computer program. Performance analysis is done for the computational algorithm. The convergence tolerance is discussed in regards to the order of accuracy and level of precision. Future work and conclusions are given in Chapter Six. Remarks are made about the results of the current method and model, as well recommendations are given for further enhancements. Several enhancements to the current model are discussed in the future work section.

Chapter 2

Mathematical Formulation

Fluid flow is a time dependent physical process which is represented mathematically in the form of differential equations dependent on velocity, acceleration, and dynamic pressure of a fluid volume. Surface waves are generated by external environmental forces. The surface profile generated by external forces may be represented analytically or empirically and used as the initial conditions for the differential equations for specific boundary value problems.

2.1 Coordinate System

An Eularian frame of reference is used in a Cartesian coordinate system and using Einstein and Leibniz notation. A right handed coordinate system is used with the z value being the vertical component, while x and y are the horizontal components. The calm water level is at $z = 0$, and the waves travel in the positive x-direction.

2.1.1 Physical Domain

To numerically simulate the propagation of the water wave over variable depth, the fluid domain is constructed with a free surface, bottom boundary, and lateral boundaries. The varying water depth has a uniform slope. The velocity profile varies with respect to the water depth.

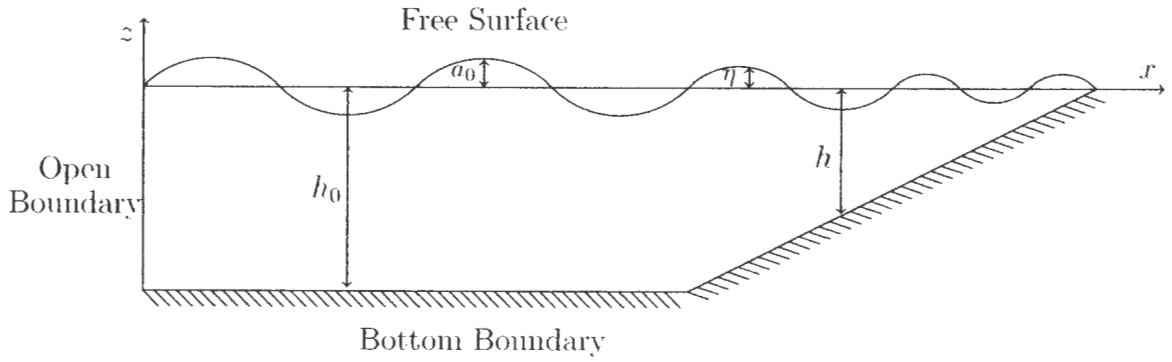

Figure 2.1: Diagram of the fluid domain and boundaries

The domain is enclosed by open or reflective boundaries on both sides of the region of the fluid. The bottom is enclosed by a rigid impermeable boundary, and the top is a free surface. The initial wave amplitude is specified at the incoming boundary and the water depth varies as it approaches the shore. The variables a_0 represents the incident wave height and h_0 represents the initial water depth.

2.2 Hyperbolic Partial Differential Equations

The Boussinesq model is a system of hyperbolic partial differential equations. Free surface and velocity equations represent the physical propagation and shoaling of a nonlinear and dispersive wave. The model includes the dynamic effects of refraction, diffraction, reflection and wave-wave interaction. The Boussinesq equation involves

the velocity expansion of the Euler equations to higher orders. The Euler equations are partial differential momentum equations which represent the fluid flow. The Euler equations are four partial differential equations including the continuity and momentum equations. The wave equation is based on the depth integration of the continuity equation, and the substitution of the hydrostatic pressure into the momentum equation. The wave equation is the simplest form of a hyperbolic partial differential equation. The fluid velocity is coupled with the free surface elevation. The derivation of the wave equation is based on Newton's second law of motion.

2.3 Fluid Assumptions

An ideal Newtonian fluid is assumed to be inviscid and incompressible. A Cartesian coordinate system (x, y, z) is adopted with z pointing upwards from the still water surface, and (u, v, w) are the velocity components, respectively. The bottom boundary is assumed to be rigid and impermeable. The dynamic and kinematic boundary conditions are satisfied at the free surface. Waves are generated specifying an inflow velocity and surface elevation at the incoming boundary. Leibniz notation is used for the formulation of the equations. The atmospheric pressure is zero at the free surface. The normal pressure is assumed to be hydrostatic.

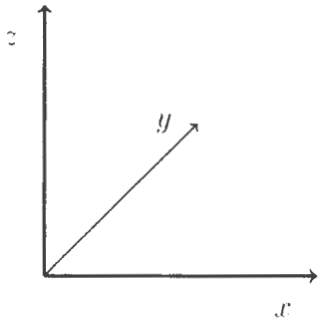

Figure 2.3: Three dimensional Cartesian coordinate system

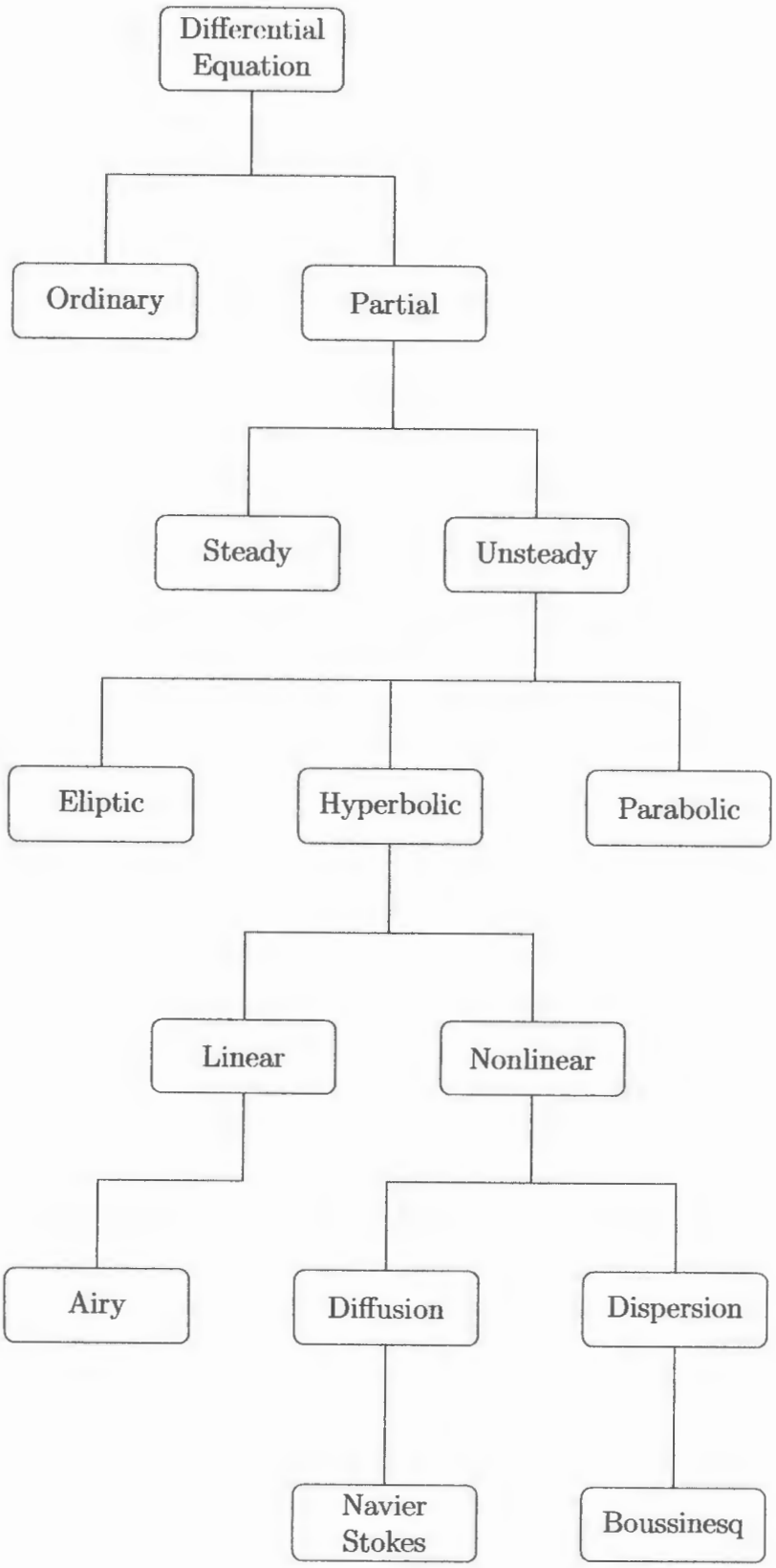

Figure 2.2: Diagram of the differential equation

2.4 Dependent Variables

The free surface elevation η and the horizontal velocity u are interdependent unknown variables. The horizontal velocity may be depth averaged or integrated, or taken at the surface, bottom, or at an arbitrary depth, z_α. The velocity taken at an optimal depth improves the linear dispersion of the equations for increasing values of kh.

2.5 Shallow Water Equations

For horizontal long wave propagation, the problem can be reduced from three to two dimensions by integrating over the water depth with the assumption that vertical velocity varies linearly over the depth. The three dimensional equations of motion and the continuity equation are the governing equations for the shallow water equations.

$$\frac{D\mathbf{u}}{Dt} + \frac{p_x}{\rho} = \mathbf{u}_t + \mathbf{u}\cdot\nabla\mathbf{u} + \frac{p_x}{\rho} = 0 \tag{2.1}$$

$$\frac{\partial u}{\partial t} + u\frac{\partial u}{\partial x} + v\frac{\partial u}{\partial y} + w\frac{\partial u}{\partial z} + \frac{1}{\rho}\frac{\partial p}{\partial x} = 0$$

$$\frac{\partial v}{\partial t} + u\frac{\partial v}{\partial x} + v\frac{\partial v}{\partial y} + w\frac{\partial v}{\partial z} + \frac{1}{\rho}\frac{\partial p}{\partial y} = 0$$

$$\frac{\partial w}{\partial t} + u\frac{\partial w}{\partial x} + v\frac{\partial w}{\partial y} + w\frac{\partial w}{\partial z} + \frac{1}{\rho}\frac{\partial p}{\partial z} + g = 0$$

$$\nabla\mathbf{u} = \frac{\partial u}{\partial x} + \frac{\partial v}{\partial y} + \frac{\partial w}{\partial z} = 0 \qquad for \quad -h \le z \le \eta \tag{2.2}$$

2.5.1 Boundary Conditions

The kinematic bottom boundary condition is due to a rigid impermeable boundary at the bottom of the fluid domain. A no flux condition is used, which implies that the volume flux normal to the rigid boundary is zero.

$$uh_x + vh_y + w = 0 \qquad for \quad z = -h \tag{2.3}$$

A free slip condition is assumed for which there are no restrictions on the tangential velocity of the fluid, where the flow at the bottom is tangent to the rigid boundary.

$$u_x = 0 \qquad for \quad z = -h$$

The kinematic free surface condition implies that the variation of vertical displacement for a fluid particle at the free surface is equivalent to the vertical velocity.

$$\eta_t + u\eta_x + v\eta_y = w \qquad for \quad z = \eta \tag{2.4}$$

The dynamic pressure at the free surface is assumed to be equal to the atmospheric pressure, which is zero at the surface. The normal pressure is assumed to be hydrostatic for the nonlinear shallow water equations.

$$p = \rho g(\eta - z) + p_a \qquad where \quad p_a = 0 \qquad for \quad z = \eta$$

2.5.2 Depth Integration

The continuity equation is integrated vertically over the instantaneous water depth.

$$\int_{-h}^{\eta} \nabla \cdot \mathbf{u} dz = \int_{-h}^{\eta} \frac{\partial u_i}{\partial x_i} dz + w|_{-h}^{\eta} = 0 \qquad for \quad i = 1, 2 \tag{2.5}$$

$$\int_{-h}^{\eta} \frac{\partial u_i}{\partial x_i} dz + w(x, \eta, t) - w(x, -h, t) = 0$$

From the kinematic free surface and bottom boundary conditions, the vertical velocity is substituted into the depth integrated continuity equation.

$$\int_{-h}^{\eta} \frac{\partial u_i}{\partial x_i} dz + \frac{\partial \eta}{\partial t} + u_\eta \frac{\partial \eta}{\partial x_i} + u_b \frac{\partial h}{\partial x_i} = 0 \tag{2.6}$$

Using the Leibniz integral rule with the continuity equation, alternate formulations are derived.

$$\frac{\partial}{\partial x_i} \int_{-h}^{\eta} u dz = u_\eta \frac{\partial \eta}{\partial x_i} + u_b \frac{\partial h}{\partial x_i} + \int_{-h}^{\eta} \frac{\partial u}{\partial x} dz$$

$$\frac{\partial}{\partial x_i} \int_{-h}^{\eta} u_i \, dz - u_i(x_i, \eta) \frac{\partial \eta}{\partial x_i} - u_i(x_i, -h) \frac{\partial h}{\partial x_i} + w(x, \eta, t) - w(x, -h, t) = 0$$

The previous two equations combine to form the new free surface equation.

$$\frac{\partial}{\partial x} \int_{-h}^{\eta} u dz + \frac{\partial \eta}{\partial t} = 0 \tag{2.7}$$

Since u_i are independent of the vertical displacement z, the depth integrated velocity may be simplified.

$$\int_{-h}^{\eta} u_i dz = u_i \int_{-h}^{\eta} dz = u(\eta + h)$$

The depth integrated velocity is substituted into the free surface equation, which

produces an expression for the kinematics of the free surface elevation for variable depth.

$$\frac{\partial \eta}{\partial t} + \frac{\partial [(h+\eta)u_j]}{\partial x_j} = 0 \tag{2.8}$$

The pressure is expressed using the hydrostatic assumption, and the dynamic pressure is $p_a = 0$ at the free surface.

$$p = \rho g(\eta - z)$$

$$\frac{\partial p}{\partial z} = -\rho g$$

The horizontal derivative of the pressure is independent of the vertical component, and substituted into the momentum equation.

$$\frac{\partial p}{\partial x} = \rho g \frac{\partial \eta}{\partial x}$$

$$\frac{\partial u_i}{\partial t} + u_j \frac{\partial u_i}{\partial x_j} + g \frac{\partial \eta}{\partial x_i} = 0 \tag{2.9}$$

The linear propagation of water waves simplifies the equations by removing the non-linear terms. The linear equations are required to derive the linear dispersion relation, and are also useful for determining the stability of the numerical method.

$$\frac{\partial u}{\partial t} + g \frac{\partial \eta}{\partial x} = 0$$

$$\frac{\partial \eta}{\partial t} + \frac{\partial uh}{\partial x} = 0$$

The time derivative of the linear momentum equation.

$$\frac{\partial^2 u}{\partial t^2} = g\frac{\partial^2 \eta}{\partial x \partial t}$$

The horizontal derivative of the linear free surface equation.

$$\frac{\partial^2 \eta}{\partial x \partial t} = g\frac{\partial^2 uh}{\partial x^2}$$

The decoupled velocity equation from the free surface variable results from substituting the horizontal derivative of the time derivative of the linear free surface into the time derivative of the linear momentum equation.

$$\frac{\partial^2 u}{\partial t^2} = g\frac{\partial^2 uh}{\partial x^2}$$

The same process can be done to express the free surface variable independent of the horizontal velocity. The wave equation has characteristic solutions called the Riemann invariants, which are found through factoring the individual waves for each direction.

$$\frac{\partial^2 u}{\partial t^2} - g\frac{\partial^2 uh}{\partial x^2} = 0$$

If we assume a constant depth, the phase velocity is simplified and the equation is easily factored. The two solutions represent waves travelling in alternate directions.

$$\left(\frac{\partial}{\partial t} - c\frac{\partial}{\partial x}\right)\left(\frac{\partial}{\partial t} + c\frac{\partial}{\partial x}\right) u = 0$$

$$\frac{\partial u}{\partial t} - c\frac{\partial u}{\partial x} = 0 \qquad and \qquad \frac{\partial u}{\partial t} + c\frac{\partial u}{\partial x} = 0 \tag{2.10}$$

The linear wave equation in three dimensions.

$$\frac{\partial^2 u}{\partial t^2} = g\left(\frac{\partial^2 uh}{\partial x^2} + \frac{\partial^2 uh}{\partial y^2}\right)$$

For linear theory, $c = \sqrt{gh}$, but for the nonlinear shallow water equations, the phase velocity is proportional to the square root of the total water depth.

$$c = \sqrt{g(\eta + h)}$$

The free surface elevation made be replaced with the propagation speed.

$$\frac{\partial c}{\partial x} = \frac{g\frac{\partial \eta}{\partial x} + g\frac{\partial h}{\partial x}}{2c}$$

$$\frac{\partial c}{\partial t} = g\frac{(\frac{\partial \eta}{\partial x})}{2c}$$

The equations may now be formulated with respect to the phase velocity.

$$\frac{\partial u}{\partial t} + u\frac{\partial u}{\partial t} + 2c\frac{\partial c}{\partial x} - g\frac{\partial h}{\partial x} = 0$$

$$2\frac{\partial c}{\partial t} + 2u\frac{\partial c}{\partial x} + c\frac{\partial u}{\partial x} = 0$$

The characteristic shallow water equations for a uniform slope.

$$\left[\frac{\partial}{\partial t} + (u-c)\frac{\partial}{\partial x}\right]\left(u - 2c - g\frac{\partial h}{\partial x}\right) = 0$$

$$\left[\frac{\partial}{\partial t} + (u+c)\frac{\partial}{\partial x}\right]\left(u + 2c - g\frac{\partial h}{\partial x}\right) = 0$$

2.5.3 Radiation

A radiation boundary condition is used to absorb wave energy for an open boundary. The wave propagating through the computational domain needs to be completely absorbed without any reflection. An exact radiation boundary condition without wave reflection is defined. For waves travelling in the opposite direction, the Riemann invariant is used. Sommerfeld (1949) defined the open boundary condition for outgoing waves.

$$\eta_t + c\eta_x = 0$$

$$\eta_t - c\eta_x = 0$$

If the incident wave direction, θ, is known a priori, then the absorbing boundary is modified for the appropriate angle of incidence.

$$\eta_t + c\cos\theta\eta_x = 0 \tag{2.11}$$

For two dimensional boundaries, the wave direction is unknown. A parabolic approximation for the absorbing boundary condition was proposed by Engquist and Majda (1977).

$$\eta_{tt} + c\eta_{xt} - \frac{c^2}{2}\eta_{yy} = 0 \tag{2.12}$$

2.5.4 Reflection

Wave reflection is generated from a vertical rigid boundary, where the water volume flux across the vertical wall is zero. The no flux condition is used to force the horizontal velocity normal to the surface of a vertical wall to be zero. After reflections occurs, the wave velocity reverses direction, and the wave propagates back into the domain. A free slip condition for the flow along the boundary is required, where the flow velocity is tangential. The horizontal velocity component perpendicular to the boundary is zero. A free slip with no flux Cauchy boundary condition is used at the wall.

$$u \cdot n = 0 \qquad \nabla\eta \cdot n = 0 \qquad w_z = 0$$

Each reflected wave has its own phase speed, which are unknown, and cannot be well represented with a single value, so an approximation still generates waves back into the domain. The generating absorbing boundary condition allows for the generation of waves into the domain, but still absorbs reflected or dispersive waves. The incident and outgoing waves are combined at the boundary, where η_I is the incident wave elevation. The reflected wave is subtracted from the incident wave using an approximate phase

speed for the reflected waves which is unknown a priori.

$$(\eta_I)_t + c(\eta_I)_x = 0$$

$$(\eta_R)_t - c(\eta_R)_x = 0$$

$$\eta = \eta_I - \eta_R$$

$$\eta_t - c\eta_x - 2(\eta_I)_t = 0 \tag{2.13}$$

Wave reflection is generated back into the domain from the above boundary condition, since the phase speed is an approximation and the reflected wave directions are unknown. A sponge layer should be used as given in appendix E to absorb all of the low frequency waves.

2.6 Dispersion Relation

The substitution of a linear wave solution into the linear Boussinesq equations leads to an approximate form of the dispersion relation. The dispersion relation relates the phase velocity to the wave number and water depth. The explicit linear dispersion relation is derived by substituting the linear solution into the free surface boundary condition.

$$\eta = a\cos\theta \tag{2.14}$$

$$u = \frac{agk}{\omega}\frac{\cosh k(z+h)}{\cosh kh}\cos(kx - \omega t + \epsilon) \tag{2.15}$$

$$\eta_t + u\eta_x + v\eta_y = w \qquad for \quad z = \eta$$

$$\omega^2 \cosh kh - gk \sinh kh = 0$$

$$\omega^2 = gk \tanh kh \tag{2.16}$$

This dispersion relation is only valid for linear wave theory. The nonlinear dispersion relation may be found similarly for using Stokes wave theory.

2.6.1 Pade Approximation

Witting (1984) thought of using a Pade approximation instead of Taylor series expansion to derive the approximate velocity for dispersive wave theory. The Pade approximant is equivalent (to the same order of error) to the taylor series of the same function.

$$f(x) = \sum_{i=0}^{\infty} c_i x^i = \frac{\sum_{i=0}^{n} a_i x^i}{1 + \sum_{j=1}^{m} b_j x^j}$$

$$\frac{1}{gh}\frac{\omega^2}{k^2} = \frac{c^2}{gh} = \frac{\tanh(kh)}{kh}$$

The Taylor series expansion of the dispersion relation defines the explicit linear dispersion relation.

$$\frac{c^2}{gh} = 1 - \frac{1}{3}(kh)^2 + \frac{2}{15}(kh)^4 + O((kh)^6) \tag{2.17}$$

The Pade approximant of the explicit dispersion relation is used instead of the Taylor series expansion.

$$1 - \frac{1}{3}(kh)^2 + \frac{2}{15}(kh)^4 = \frac{1}{1 + b_1 kh + b_2(kh)^2}$$

The first order Pade approximation of the exact linear dispersion relation is substituted for the Taylor series approximation.

$$\frac{\tanh(kh)}{kh} = 1 - \frac{1}{3}(kh)^2 + O(\mu^4)$$

$$1 + b_1 kh + \left(b_2 - \frac{1}{3}\right)(kh)^2 \frac{1}{3} b_1 (kh)^3 = 1$$

$$b_1 = 0$$

$$b_2 - \frac{1}{3} = 0 \quad \Longrightarrow \quad b_2 = \frac{1}{3}$$

$$\frac{\tanh(kh)}{kh} = \frac{1}{1 + \frac{1}{3}(kh)^2} + O(\mu^4) \tag{2.18}$$

Similarly, the second order Pade approximation of the dispersion relation may also be derived.

$$\frac{\tanh(kh)}{kh} = 1 - \frac{1}{3}(kh)^2 + \frac{2}{15}(kh)^4 + O(\mu^6)$$

$$\frac{\tanh(kh)}{kh} = \frac{1 + \frac{1}{15}(kh)^2}{1 + \frac{2}{5}(kh)^2} + O(\mu^6)$$

The Pade approximation for the linear dispersion relation takes the form:

$$\frac{c^2}{gh} = \frac{1 + b(kh)^2}{1 + \left(\frac{1}{3} + b\right)(kh)^2} \tag{2.19}$$

As $kh \to 0$, the pade approximant is asymptotically equivalent to the exact linear dispersion relation. As the water depth increases, the dispersion relation diverges from the linear theory. The velocity taken at a reference water depth instead of the depth averaged velocity significantly improves the linear dispersive properties. (nwogu) redefined the linear dispersion relation using the second order pade approximation.

$$\omega^2 = gk^2h\frac{1 - (\alpha + \frac{1}{3})(kh)^2}{1 - \alpha(kh)^2}$$

Where α is relative to the reference depth, Z_α.

$$\alpha = \frac{1}{2}\left(\frac{z_\alpha}{h}\right)^2 + \frac{z_\alpha}{h}$$

In deep water, where $kh > 3$, the dispersion relation deviates from linear theory and is no longer convergent. The dispersion relation can be refined to match the linear theory by choosing an optimized value for α in deep water. Nwogu (1993) found that a value of $\alpha = -0.39$ produces results closest to the linear theory. The standard Boussinesq equations represent a value of $\alpha = -\frac{1}{3}$, which corresponds to the first order pade approximant, but is limited to shallow water where $kh < 2$. A value of $\alpha = -0.4$ reduces the dispersion relation to the second order Pade approximation. The intent is to minimize the relative error between the exact solution and the Pade approximants for the linear dispersion relation. A forth order Pade approximation was derived by Gobbi and Kirby (1998).

$$\omega^2 = \frac{1 + \frac{1}{9}(kh)^2 + \frac{1}{945}(kh)^4}{1 + \frac{4}{9}(kh)^2 + \frac{1}{63}(kh)^4} + O((kh)^4) \tag{2.20}$$

2.7 Boussinesq Equations

The Boussinesq equations introduce dispersion through velocity expansion into the nonlinear shallow water equation to stabilize increasing orders of nonlinearity for deeper water relative to the wave length. Peregrine (1969) derived multidimensional weakly nonlinear long wave equations over varying depth using depth averaged velocity. The standard Boussinesq equations in terms of the depth averaged velocity have better convergence with the linear dispersion relation. The main drawback is they are only applicable to relatively shallow water. Nwogu (1993)developed extended Boussinesq equations for variable depth in terms of the velocity at an arbitrary water depth. The dispersive effects are significantly improved for deeper water. The extended Boussinesq equations for an arbitrary depth derived by Nwogu are used in this paper. where z_a is the arbitrary water depth. Nwogu's model is accurate up to $kh \approx 0.5$, and convergent up to $kh \approx 3.0$. The Boussinesq equations are derived using a Taylor power series expansion of the chosen velocity variable.

$$u = \sum_{i=0}^{\infty} (z + h)^i u$$

The vertical variation of the velocity is represented by an infinite series. which can be truncated to specific order.

$$u = u_0 + (z + h)u_1 + (z + h)^2 u_2 + ...$$

The derivative of the velocity variables are derived with respect to x and z.

$$u_x = u_{0x} + (z+h)u_{1x} + (z+h)^2 u_{2x} + ...$$

$$w_z = 2u_2 + 6(z+h)u_3 + 12(z+h)^2 u_4 + ...$$

The derivatives of the velocity expansions are substituted into the continuity equation.

$$u_x + w_z = u_{0x} + (z+h)u_{1x} + (z+h)^2 u_{2x} + ... + 2u_2 + 6(z+h)u_3 + 12(z+h)^2 u_4 + ... = 0$$

$$\sum_{i=0}^{\infty} (u_{ix} + (i+1)(i+2)u_{i+2})(z+h)^i = 0$$

The equation represents a polynomial which is zero for all values of $z+h$, which requires all terms to be zero, which may be generalized in a recursive formula.

$$u_{i+2} = \frac{u_{ix}}{(i+1)(i+2)}$$

The horizontal velocity may now be expressed in terms of the first two variables from the bottom.

$$u = u_0 + (z+h)u_1 - \frac{(z+h)^2}{2}u_{0x} + \frac{(z+h)^3}{6}u_{1x} + O(\mu^4)$$

$$u = \sum_{i=0}^{\infty} (i+1)(z+h)^i u_i = 0 \qquad for \quad z = -h$$

Since all the terms are zero at the bottom, $u_1 = 0$.

$$u = u_0 - \frac{1}{2}(z+h)^2 u_{xx} + \frac{1}{24}(z+h)^4 u_{xxxx} + O(\mu^6)$$

The solution for the fluid velocity represented be an infinite series.

$$u = \sum_{i=0}^{\infty} \frac{(-1)^i}{2i!}(z+h)^{2i} \frac{\partial^i u}{\partial x^{2i}}$$

The equation is substituted into kinematic free surface and bottom boundary conditions.

$$w = \eta_t + u\eta_x \qquad for \quad z = \eta$$

$$uh_x + w = 0 \qquad for \quad z = -h$$

$$w = -((\eta+h)u_0)_x + \frac{(\eta+h)^3}{6} u_{0xxx} + O(\mu^4)$$

$$w = -h u_{0x} - \frac{h^3}{6} u_{0xxx}$$

The solutions for the vertical velocity at the surface and bottom boundaries are used as before for the derivation of the depth integrated continuity equation.

$$\frac{\partial \eta}{\partial t} + \frac{\partial[(h+\eta)u]}{\partial x} = \frac{h^3}{6}\frac{\partial^3 u}{\partial x^3} \tag{2.21}$$

The momentum equation is derived through substitution into the Euler equation using dynamic free surface condition.

$$\frac{\partial u}{\partial t} + u\frac{\partial u}{\partial x} + g\frac{\partial \eta}{\partial x} = \frac{h^2}{2}\frac{\partial^3 u}{\partial x^2 \partial t} \tag{2.22}$$

Differentiation of the free surface equation in terms of the bottom velocity with respect to time, and differention of the momentum equation in terms of the bottom velocity with respect to x and multiplying by the water depth derives the following multidirectional equation in terms of the free surface velocity.

$$\frac{\partial^2 \eta}{\partial t^2} - gh\frac{\partial^2 \eta}{\partial x^2} - c^2\left(\frac{3\eta^2}{2h} + \frac{h^2}{3}\frac{\partial^2 \eta}{\partial x^2}\right)_{xx} = 0$$

2.7.1 Dispersion Relation

The Taylor series approximation of the dispersion relation.

$$\frac{c^2}{gh} = \frac{\tanh kh}{kh} = 1 - \frac{(kh)^2}{3} + \frac{2}{15}k^4h^4 \tag{2.23}$$

Substitution of the small amplitude wave solution into the free surface and momentum equations.

$$\eta = ae^{i(kx - \omega t)}$$

$$u = u_0 e^{i(kx - \omega t)}$$

$$\omega a - kh(1 - \frac{(kh)^2}{6})u_0 = 0$$

$$-ka - \omega(1 + \frac{(kh)^2}{2})u_0 = 0$$

The previous equations form a system of linear equations:

$$A = \begin{pmatrix} \omega & -kh(1+\frac{(kh)^2}{6} \\ -k & \omega(1+\frac{(kh)^2}{2} \end{pmatrix}$$

The system of equations has a solution when the determinant is zero.

$$\omega^2\left(1+\frac{(kh)^2}{2}\right)-k^2h\left(1+\frac{(kh)^2}{6}\right)=0$$

The disperion relation for the Boussinesq equation in terms of the horizontal velocity at the bottom boundary.

$$\frac{c^2}{gh}=\frac{1+\frac{1}{6}(kh)^2}{1+\frac{1}{2}(kh)^2} \tag{2.24}$$

The Boussinesq equations in terms of the bottom velocity has poor convergence with the linear dispersion relation. It is convergent up to $O(kh) \approx 1.0$. Madsen, Murray, and Sorensen (1991) determined a generic solution of the disperion relation for the Boussinesq equation in terms of Witting's Pade approximation of the phase velocity.

$$\frac{c^2}{gh}=\frac{1+b(kh)^2}{1+\left(\frac{1}{3}+b\right)(kh)^2} \tag{2.25}$$

$$\frac{\partial u}{\partial t}+u\frac{\partial u}{\partial x}+g\frac{\partial \eta}{\partial x}=\left(\frac{1}{3}+b\right)h^2\frac{\partial^3 u}{\partial x^2\partial t} \tag{2.26}$$

$$\frac{\partial \eta}{\partial t}+\frac{\partial[(h+\eta)u]}{\partial x}=bh^3\frac{\partial^3 u}{\partial x^3} \tag{2.27}$$

For Boussinesq equations in terms of the velocity at the bottom boundary, $b = \frac{1}{6}$.

2.7.2 Variable Depth

For variable depth, the equations must include the variation of depth into the spatial derivatives. The fluid velocity expansion in terms of the bottom velocity is used to derive the equations for variable depth. The equations become significantly more complicated for variable depth for higher orders of nonlinearity and dispersion. The variation in depth is assumed to be of second order magnitude. Fourth order terms are neglected. The velocity expansion must include the depth derivatives.

$$\mathbf{u} = \mathbf{u}_b - (z+h)\nabla\cdot(h\mathbf{u}_b) - \frac{(z+h)^2}{2}\nabla^2\cdot\mathbf{u}_b + O(\mu^4)$$

Boussinesq equations in three dimensions for variable depth using the bottom velocity as the dependent variable are derived by generalizing the method of derivation for constant depth.

$$\mathbf{u}_t + \mathbf{u}\cdot\nabla\mathbf{u} + g\nabla\eta + \frac{h^2}{6}\nabla(\nabla\cdot\mathbf{u}_t) - \frac{h}{2}\nabla[\nabla\cdot(h\mathbf{u}_t)] = 0 \tag{2.28}$$

$$\eta_t + \nabla\cdot[(h+\eta)\mathbf{u}] + \frac{h^3}{3}\nabla(\nabla\cdot\mathbf{u}) - \frac{h^2}{2}\nabla[\nabla\cdot(h\mathbf{u})] = 0 \tag{2.29}$$

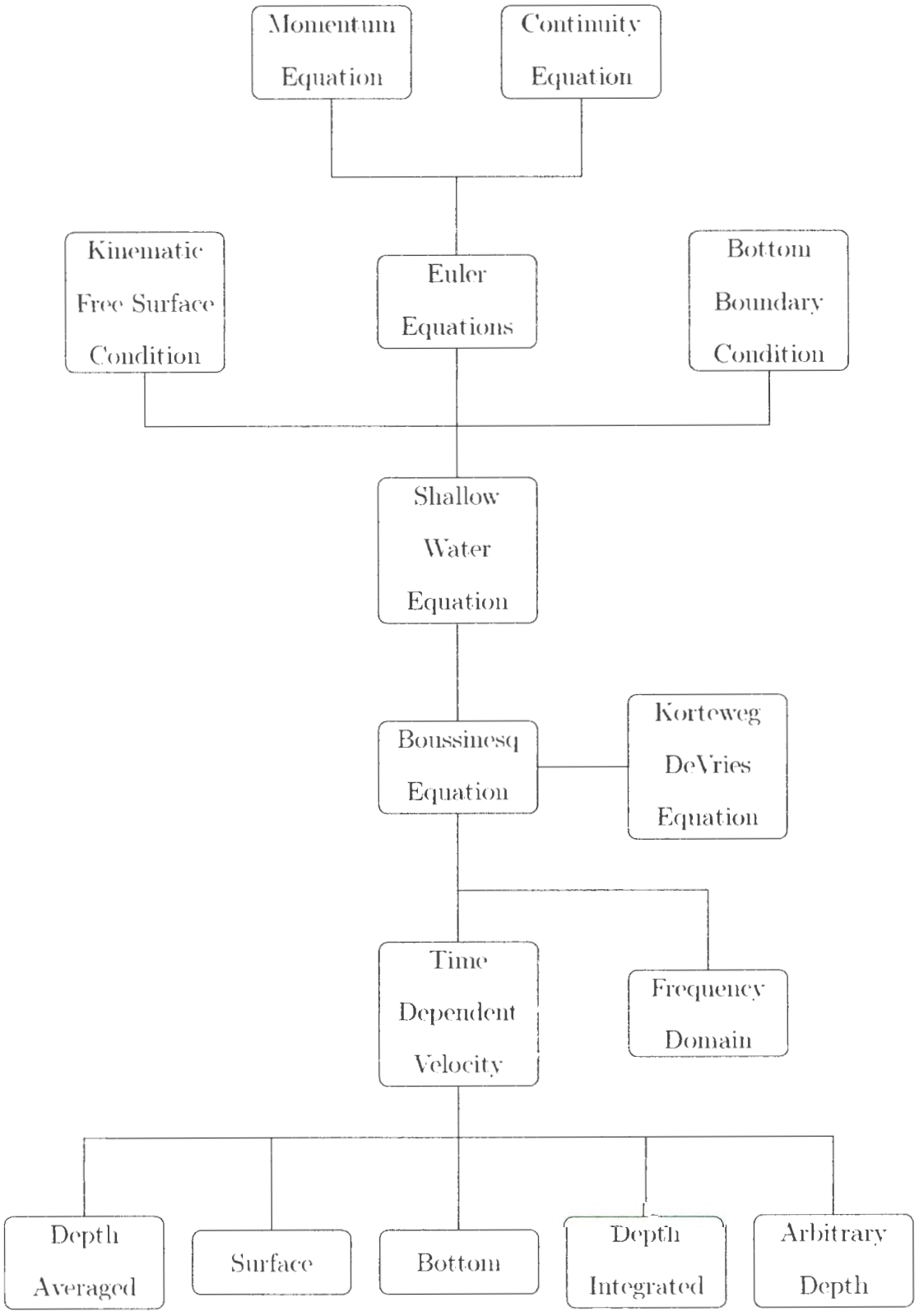

Figure 2.4: Overview of the derivation of the Boussinesq equations

2.7.3 Surface Velocity

The fluid velocity expansion in terms of the bottom velocity is used to derive the equations in terms of the surface velocity. The surface velocity variable is substituted for the velocity at the bottom.

$$u = u_0 - \frac{1}{2}(z+h)^2 u_{0xx}$$

$$u_\eta = u_0 - \frac{h^2}{2} u_{\eta xx} \qquad for \quad z = \eta$$

The velocity at the bottom is solved to derive the equation in terms of the surface variable. The bottom velocity in terms of the surface variable is substituted into the surface velocity expansion.

$$u_0 = u_\eta + \frac{h^2}{2} u_{\eta xx}$$

$$u_0 = u_\eta + \frac{h^2}{2}\left(u_\eta + \frac{h^2}{2} u_{\eta xx}\right)$$

Substitution of the equation for the bottom velocity in terms of the velocity at the surface yields the Boussinesq equation for the velocity at the surface.

$$\eta_t + [(h+\eta)u]_x + \frac{h^3}{3} u_{xxx} = 0 \tag{2.30}$$

$$u_t + \eta_x + u u_x = 0 \tag{2.31}$$

The dispersion relation for Boussinesq equations in terms of the surface velocity.

$$\frac{c^2}{gh} = 1 - \frac{1}{3}(kh)^2 \tag{2.32}$$

The Boussinesq equations in terms of the surface velocity has the worst convergence with the linear dispersion relation. It is convergent up to $O(kh) \approx 0.5$.

2.7.4 Depth Averaged Velocity

Peregrine (1967) developed weakley nonlinear small amplitude long wave motion over varying depth using the depth averaged velocity.

$$\bar{u} = \frac{1}{\eta + h} \int_{-h}^{\eta} u dx$$

The second order velocity expansion is used to solve for the depth average velocity. The averaged velocity expansion is expressed in terms of the bottom velocity. The bottom velocity is solved from the equation for the averaged velocity.

$$u = u_0 - \frac{1}{2}(z + h)^2 u_{xx}$$

$$\bar{u} = u_0 - \frac{(\eta + h)^2}{6} u_{0xx}$$

$$u_0 = \bar{u} + \frac{(\eta + h)^2}{6} \bar{u}_{xx}$$

Substitution of the equation for the bottom velocity in terms of the depth averaged velocity into the horizontal velocity expansion yields the Boussinesq equation in terms of depth averaged velocity.

$$\frac{\partial \eta}{\partial t} + \frac{\partial [(h+\eta)u]}{\partial x} = \frac{h^3}{6}\frac{\partial^3 u}{\partial x^3} \tag{2.33}$$

$$\frac{\partial u}{\partial t} + u\frac{\partial u}{\partial x} + g\frac{\partial \eta}{\partial x} = \frac{h^2}{2}\frac{\partial^3 u}{\partial x^2 \partial t} \tag{2.34}$$

The dispersion relation is calculated for depth averaged velocity.

$$c = \sqrt{\frac{gh}{1 + \frac{1}{3}(kh)^2)}} \tag{2.35}$$

Three dimensional Boussinesq equations over a variable depth for depth averaged velocity may also be obtained.

$$\mathbf{u}_t + \mathbf{u}\cdot\nabla u + g\nabla\eta + \frac{h^2}{6}\nabla(\nabla\cdot\mathbf{u}_t) - \frac{h}{2}\nabla[\nabla\cdot(h\mathbf{u}_t)] = 0 \tag{2.36}$$

$$\eta_t + \nabla\cdot[(h+\eta)\mathbf{u}] = 0 \tag{2.37}$$

The Boussinesq equations in terms of the depth averaged velocity has better convergence with the linear dispersion relation. It is convergent up to $O(kh) \approx 1.5$.

2.7.5 Depth Integrated Velocity

Madsen, Murray, and Sorensen (1991) derived Boussinesq in terms of a depth integrated velocity variable, which represents the instantaneous flux of the fluid volume.

$$Q = \int_{-h}^{\eta} u dz$$

The depth integration of the continuity equation may be expressed in terms of depth

integrated velocity.

$$\frac{\partial}{\partial x}\int_{-h}^{\eta} u dz + \frac{\partial \eta}{\partial t} = 0$$

$$\frac{\partial}{\partial x} Q + \frac{\partial \eta}{\partial t} = 0$$

$$Q = (h + \eta)u$$

The depth averaged velocity is expressed in terms of the depth integrated velocity. The depth averaged velocity expressed with respect to the integrated velocity is substituted into the depth averaged velocity equation. The equations may also be derived for variable depth.

$$u = \frac{Q}{h + \eta}$$

$$\left(\frac{Q}{h+\eta}\right)_t + \frac{Q}{h+\eta}\left(\frac{Q}{h+\eta}\right)_x + \eta_x = \frac{h^2}{3}\left(\frac{Q}{h+\eta}\right)_{xxt}$$

$$\left(\frac{Q}{h+\eta}\right)_t + \frac{Q}{h+\eta}\left(\frac{Q}{h+\eta}\right)_x + \eta_x = \frac{1}{2}\left[h\left(\frac{Q}{h+\eta}\right)_{xx} - \frac{h^2}{3}\left(\frac{Q}{h+\eta}\right)_{xx}\right]_t$$

Madsen's equations in terms of depth integrated velocity.

$$\eta_t + Q_x = 0 \tag{2.38}$$

$$Q_t + \left(\frac{Q}{\eta + h}\right)_x^2 + g(\eta + h)\eta_x - \frac{h^2}{3} Q_{xxt} = 0 \tag{2.39}$$

Madsen's derivations for Boussinesq equations in terms of depth integrated velocity have the same order of accuracy as Nwogu's arbitray depth equations.

2.8 Arbitrary Depth Velocity

Nwogu (1993) developed three dimensional Boussinesq equations for variable depth in terms of the velocity at an arbitrary depth. The dispersion effects were significantly improved by the modification to the Boussinesq equations. Madsen, Murray, and Sorensen (1991) also determined the convergence towards linear theory in terms of the optimal selection of appropriate coefficients for the derivation of the equations.

$$\mathbf{u} = \mathbf{u}_b - (z+h)\nabla[\nabla\cdot(h\mathbf{u}_b)] + \frac{(z^2+h^2)}{2}\nabla(\nabla\cdot\mathbf{u}_\alpha) + O(\mu^4)$$

The arbitrary depth velocity for a specified α and calculated reference depth, z_α.

$$\mathbf{u} = \mathbf{u}_\alpha + (z_\alpha - z)\nabla[\nabla\cdot(h\mathbf{u}_\alpha)] + (z_\alpha^2 - z^2)\nabla(\nabla\cdot\mathbf{u}_\alpha) + O(\mu^4)$$

$$u = \sum_{i=0}^{\infty}(z+h)^i\frac{\partial^i u}{\partial x^i}$$

$$u = u + (z+h)u_x + \frac{(z+h)^2}{2}u_{xx} + \frac{(z+h)^3}{4}u_{xxx} + \frac{(z+h)^4}{8}u_{xxxx} + O(\mu^6)$$

$$w = -\nabla\cdot[(z+h)\mathbf{u}_\alpha] + \nabla\frac{(z+h)^2}{2}(\nabla\cdot\mathbf{u}_\alpha\nabla h + \nabla\cdot\mathbf{u}\nabla h) + O(\mu^6)$$

The velocity at the bottom is derived in terms of the velocity at an arbitrary depth. The equation for u_0 is solved in terms of u_α. The fluid velocity is derived in terms of the velocity at an arbitrary depth.

$$\mathbf{u} = \mathbf{u}_\alpha + \left(\frac{z_\alpha^2}{2} - \frac{z^2}{2}\right)\nabla(\nabla\cdot\mathbf{u}_\alpha) + (z_\alpha - z)\nabla\left[\nabla\cdot(h\mathbf{u}_\alpha)\right] + O(\mu^4)$$

$$w = -\nabla\cdot h\mathbf{u}_\alpha - z\nabla\cdot\mathbf{u}_\alpha + O(\mu^4)$$

$$p = \eta - z + z\nabla\cdot(h\mathbf{u}_{\alpha t}) + \frac{z^2}{2}\nabla\cdot\mathbf{u}_{\alpha t} + O(\delta^2, \delta\mu^2, \mu^4)$$

Three dimensional Boussinesq equations for varaible depth in terms of the velocity at an arbitrary depth.

$$\eta_t + \nabla\cdot\left[(h+\eta)\mathbf{u}\right] + \nabla\cdot\left(\frac{z^2}{2} - \frac{h^2}{6}\right)h\nabla(\nabla\cdot\mathbf{u}) + \nabla\cdot\left(z + \frac{h}{2}\right)h\nabla\left[\nabla\cdot(h\mathbf{u})\right] = 0 \quad (2.40)$$

$$\mathbf{u}_t + g\nabla\eta + \mathbf{u}\cdot\nabla\mathbf{u} + \frac{z^2}{2}\nabla(\nabla\cdot\mathbf{u}_t) + z\nabla\left[\nabla\cdot(h\mathbf{u}_t)\right] = 0 \quad (2.41)$$

The linear Boussinesq equations in terms of a velocity variable at an arbitrary depth in one dimension.

$$\eta_t + hu_x + (\alpha + \frac{1}{3})h^3 u_{xxx} = 0$$

$$u_t + g\eta_x + \alpha h^2 u_{xxt} = 0$$

$$\alpha = \frac{1}{2}\left(\frac{z_\alpha}{h}\right)^2 + \frac{z_\alpha}{h}$$

z_α is the reference water depth.

$$\eta = ae^{i(kx-\omega t)}$$

$$u = u_0 e^{i(kx-\omega t)}$$

Substitute the small amplitude wave solution into the conservation equations

$$\omega^2 + \omega^2 \left(1 + \left(\frac{1}{3} + b\right)\right)(kh)^2 - k^2 k^2 b(kh)^2)gh$$

$$\frac{c^2}{gh} = \frac{1 + b(kh)^2}{1 + \left(\frac{1}{3} + b\right)(kh)^2}$$

The Pade approximation of the explicit linear dispersion relation for the velocity at an arbitary depth.

$$\frac{c^2}{gh} = \frac{1 - (\alpha + \frac{1}{3})(kh)^2}{1 - \alpha(kh)^2} \tag{2.42}$$

The Boussinesq equations in terms of an arbirary depth velocity has the best convergence with the linear dispersion relation. It is convergent up to $O(kh) \approx 3.0$. The Padé approximant is asymptotically equivalent to the exact linear dispersion relation as the depth approaches zero, but as water depth increases, the approximate dispersion relation diverges from linear theory. The velocity taken at a reference water depth instead of the depth averaged velocity significantly improves the dispersive properties. In significantly deep water, the dispersion relation deviates from linear theory for the extended Boussinesq equations. The coefficients for the dispersion relation are refined to match the linear theory through the selection of an optimized value for α in deep water. Nwogu found that a value of α = -0.39 produces results relatively close to lin-

ear theory for moderate depth. The standard Boussinesq equations represent a value of α = -1/3, which corresponds to the first order Padé approximant. A value of α = -0.4 reduces the dispersion relation to the second order Padé approximation. In this paper, a value of α = -0.39 is used in accordance with Nwogu's theory. The intent is to minimize the relative error between the exact solution and the Padé approximants for the explicit dispersion relation.

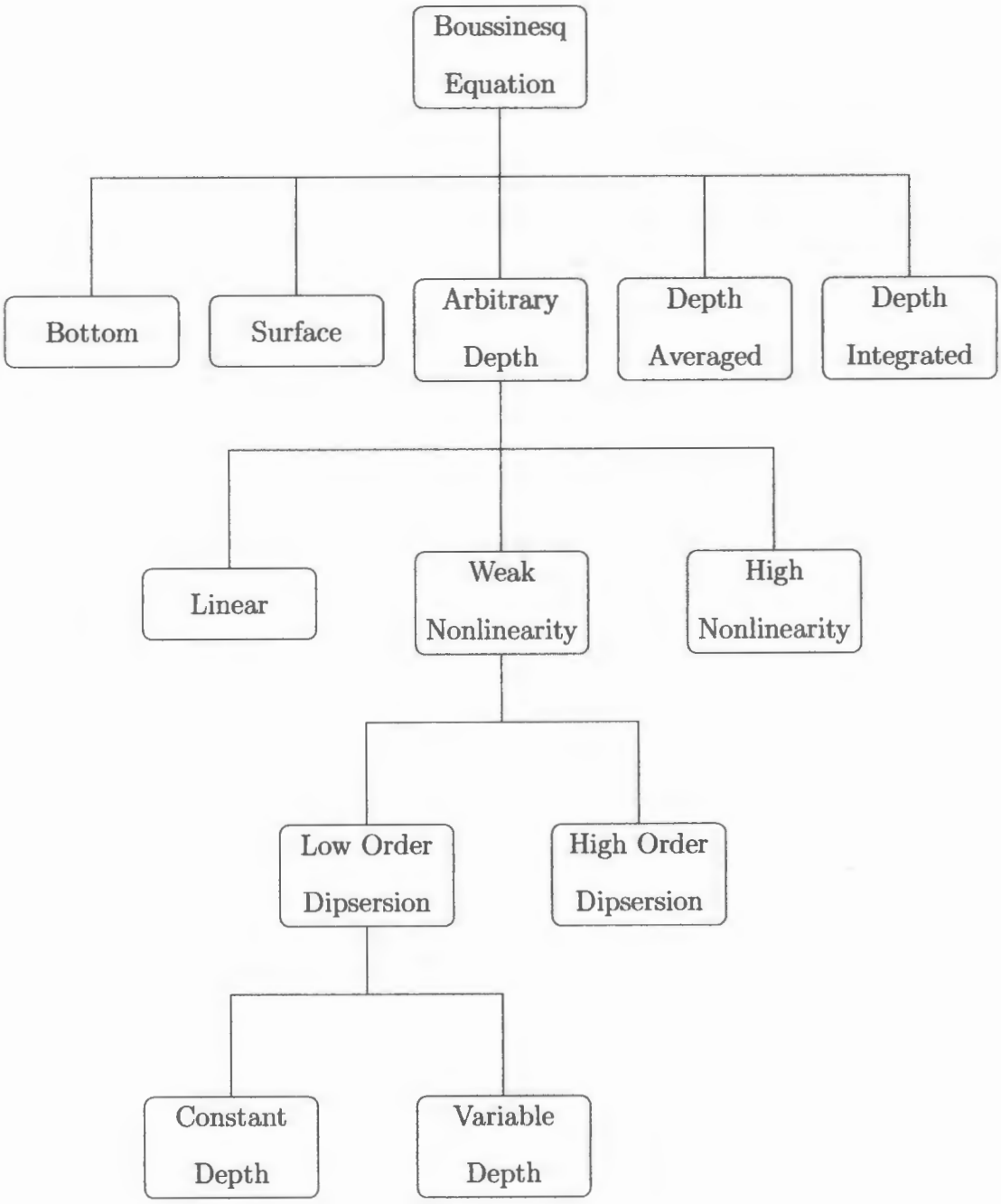

Figure 2.5: Overview of Boussinesq wave theory

2.9 Korteweg-DeVries Equation

The equations derived by Korteweg and Vries (1895) are modified unidirectional Boussinesq equations. The equations may either be derived in terms of the velocity or free surface elevation variable. The equations have several alternate forms depending on whether the time or spatial derivatives are taken.

2.9.1 Constant Depth

The KdV equation in terms of velocity variable for constant depth can be derived in either the free surface or velocity variables.

$$\mathbf{u}_t + c\nabla \cdot \mathbf{u} + \frac{3c}{2h}\mathbf{u} \cdot \nabla\mathbf{u} - c\frac{h2}{2}\nabla(\nabla \cdot \mathbf{u}_t) = 0$$

$$\eta_t + c\nabla\eta + \frac{3c}{2h}\eta\nabla\eta + c\frac{h^2}{6}\nabla\nabla\nabla\eta = 0$$

2.9.2 Variable Depth

The KdV equations may also be derived for variable depth in terms of both the velocity and free surface variables.

$$\mathbf{u}_t + c\mathbf{u} \cdot \nabla\mathbf{u} + \frac{3c}{2h}\nabla \cdot \mathbf{u} + c\frac{h^2}{6}\nabla(\nabla \cdot \mathbf{u}_t) - \frac{h}{2}\nabla[\nabla \cdot (h\mathbf{u}_t)] = 0$$

$$\eta_t + c\nabla\eta + + \frac{3c}{2h}\eta\nabla\eta + c\frac{h^2}{6}\nabla\nabla\nabla\eta - c\frac{h}{2}\nabla\nabla[\nabla(h\eta)] = 0$$

2.10 Analytical Wave Solutions

There are a wide range of solutions for which the Boussinesq equations can be used to model wave propagation. The strength of the nonlinear and dispersive equations is the generality of the solutions for the equations. Many different types of waves require specific initial conditions that may be specified for different wave setups.

2.10.1 Airy Linear Wave Theory

Airy (1841) derived the linear propagation of waves in terms of the free surface elevation and velocity.

$$\eta = a\cos(k_x x + k_y y - \omega t + \epsilon)$$

Where ϵ is the initial phase, a is the wave amplitude, k is the wave number,ω is the wave angular frequency, and θ is the wave heading in radians.

$$k_x = k\cos\theta \qquad k_y = k\sin\theta$$

The deep water limits $x \to \infty$ and $\tanh x \to 1$ for small amplitude waves. Equations for horizontal and vertical velocities are given.

$$u = a\omega e^{kz}\cos(kx - \omega t + \epsilon)$$

$$w = a\omega e^{kz}\sin(kx - \omega t + \epsilon)$$

The dispersion relation and pressure equations specific to deep water theory.

$$\omega^2 = gk$$

$$p = -\rho g(z - e^{kz}\eta)$$

Finite amplitude sets $\delta = \mathrm{O}(1)$. The amplitudes are of the same order as the water depth.

$$u = \frac{agk}{\omega}\frac{\cosh k(z+h)}{\cosh kh}\cos(kx - \omega t + \epsilon)$$

$$w = \frac{agk}{\omega}\frac{\sinh k(z+h)}{\cosh kh}\sin(kx - \omega t + \epsilon)$$

The dispersion relation and pressure equation for finite depth.

$$\omega^2 = gk\tanh kh$$

$$\frac{\tanh kh}{kh} = \frac{\omega^2}{k^2 gh}$$

$$p = -\rho g(z - \frac{\cosh k(z+h)}{\cosh kh}\eta)$$

In shallow water, the motion of the fluid is linear isntead of being elliptical. Shallow water limit assumes $x \to 0$ and $\tanh x \to x$. The theory is for applicable long waves with moderate amplitudes.

$$u = a\sqrt{\frac{g}{h}}\cos(kx - \omega t + \epsilon)$$

$$w = a\omega\frac{z+h}{h}\sin(kx - \omega t + \epsilon)$$

The dispersion relation and pressure equation for shallow water.

$$\omega^2 = gk^2h$$

$$p = -\rho g(z - \eta)$$

2.10.2 Stokes Nonlinear Water Theory

Stokes' expansions of the free surface elevation and the according dispersion relation were derived from Airy's small amplitude wave theory. Stokes (1847) expanded the equations for higher orders of nonlinearity.

$$\eta = a\cos\theta + \frac{1}{2}ka^2cos2\theta + \frac{3}{8}k^2a^3cos3\theta$$

$$\omega^2 = gk(1 + a^2k^2 + \frac{5}{4}a^4k^4)$$

Where θ is the phase angle where $\theta = kx - \omega t$

The second order theory for intermediate water depth is given.

$$\eta = a\cos\theta + \frac{ka^2}{4}\frac{\cosh kh}{\sinh^3 kh}(2 + \cosh 2kh)cos2\theta$$

$$u = \frac{agk}{2\omega}\frac{coshk(h+z)}{\cosh kh}\cos\theta + \frac{3}{4}ck^2a^2\frac{\cosh 2k(z+h}{\sinh^4 kh}\cos 2\theta$$

$$\omega^2 = gk(1 + a^2k^2)$$

2.10.3 Solitary Wave

The solitary wave solution for depth averaged velocity is given. Rayleigh, St. Vennant, and Korteweg-Devries all contributed to the derivation of solitary wave equations. The given equations are taken from Peregrine (1967).

$$\eta = a\,\mathrm{sech}^2\left[\sqrt{\frac{a}{2h^3}}(x - ct)\right]$$

$$u = \sqrt{\frac{g}{h}}\eta$$

$$c = \sqrt{gh}(1 + \frac{a}{2h})$$

The solitary wave solution for arbitrary depth velocity is also given. The analytical equations for Boussinesq equations in terms of an arbitrary velocity become significantly more complex. The equations are taken from Wei and Kirby (1995).

$$\eta = a_1\,\mathrm{sech}^2[b(x - ct)] + a_2\,\mathrm{sech}^4[b(x - ct)]$$

$$u = a\,\mathrm{sech}^2[b(x - ct)]$$

$$a = \frac{c^2 - gh}{c} \qquad b = \sqrt{\frac{c^2 - gh}{4[(\alpha + \frac{1}{3})gh^3 - \alpha h^2c^2]}}$$

$$a_1 = \frac{c^2 - gh}{3[(\alpha + \frac{1}{3})gh - \alpha c^2]}h$$

$$a_2 = -\frac{(c^2 - gh)^2}{2ghc^2}\frac{(\alpha + \frac{1}{3})gh + 2\alpha c^2}{(\alpha + \frac{1}{3})gh - \alpha c^2}h$$

2.10.4 Undular Bore

The evolution of an undular bore is an excellent observation of the effects of nonlinearity and dispersion. After wave breaking, a wave resembles the nature of an undular bore, which can be used for measurements and the creation of empirical data. A bore wave propagates into still water and generates dispersive waves. The equations are taken from Wei, Kirby, Grilli, and Subramanya (1995).

$$u = \frac{u_0}{2}\left(1 - \tanh\frac{x}{a}\right)$$

$$\eta = u + \frac{u^2}{4}$$

The bore wave conserves mass and momentum across the wave. The wave heights increase over time and a uniform wave train is generated. Vertical acceleration in the point of inflection between the two asymptotes from the transition from uniform flow to still water generates the dispersive waves.

Chapter 3

Numerical Method

A time dependent finite difference method of lines is used to solve the hyperbolic partial differential equations. The extended Boussinesq equations are discretized using a fifth order multistep time marching method. The Adams-Bashforth-Moulton (ABM) predictor-corrector scheme is used to discretize the time derivatives. Sixth order spatial difference schemes are used for first order derivatives, and fourth order schemes are used for the second order derivatives which have a lower magnitude of error. The ABM predictor-corrector method is a multi-step time marching scheme, which uses fourth order explicit forward time difference methods and fifth order implicit backwards time methods. The numerical method used by Wei and Kirby (1995) is extended for higher order methods. The spatial differencing truncation error for first and second order terms needs to be small relative to the dispersive third order terms. The first order terms are solved with a higher order accuracy than the dispersive terms to reduce the relative error. The predictor corrector method was used to minimize the truncation error and estimate a corrective term on every iteration.

$$y(t_{k+1}) = y(t_k) + \int_{t_k}^{t_{k+1}} f(t, y(t))dt$$

3.1 Overview of Computational Methods

All of the finite difference methods that were used over the course of the research are given in the following table. Other popular methods like Beam Warming and MacCormack were excluded due to their similarity of stability to other methods.

Table 3.1: List of Finite Difference Methods

Method	Scheme	Time	Space	Stability	Convergence
FTFS	explicit	first	first	$-1 \leq CFL \leq 0$	yes
FTBS	explicit	first	first	$0 \leq CFL \leq 1$	yes
FTCS	explicit	first	second	none	no
Lax-Friedrichs	explicit	first	second	$CFL \leq 1$	yes
BTCS	implicit	first	second	unconditional	yes
CTCS	implicit	second	second	unconditional	yes
Lax-Wendroff	implicit	second	second	$CFL \leq 1$	yes
Crank Nicolson	implicit	second	second	$CFL \leq 1$	yes
Adams	implicit	fifth	fourth	unconditional	yes

F = forward, B = backward, C = center, T = time, S = space

CFL = Courant Friedrichs Lewy condition

3.1.1 Adams-Bashforth Predictor

A low order approximation is calculated by an explicit extrapolation method as an initial guess for the instantaneous value of the differential equations. The first order method is the forward Euler method. The second to fourth order explicit extrapolation

methods are given.

$$y_{k+1} = y_k + \frac{h}{2}(-f_{k-1} + 3f_k)$$

$$y_{k+1} = y_k + \frac{h}{12}(5f_{k-2} - 16f_{k-1} + 23f_k)$$

$$y_{k+1} = y_k + \frac{h}{24}(-9f_{k-3} + 37f_{k-2} - 59f_{k-1} + 55f_k)$$

3.1.2 Adams-Moulton Corrector

The second-order implicit interpolation scheme is the trapezoidal finite difference method which is similar to the Crank Nicolson temporal discretization. The second to fifth order corrector methods are given.

$$y_{k+1} = y_k + \frac{h}{2}(f_{k-1} + f_k)$$

$$y_{k+1} = y_k + \frac{h}{12}(-f_{k-1} + 8f_k + 5f_{k+1})$$

$$y_{k+1} = y_k + \frac{h}{24}(f_{k-2} - 5f_{k-1} + 19f_k + 9f_{k+1})$$

$$y_{k+1} = y_k + \frac{h}{720}(-19f_{k-2} + 106f_{k-1} - 264f_k + 646f_{k+1} + 251f_{k+2})$$

3.2 Difference Equations

The conservation equations are rearranged to facilitate the time and spatial differencing. Wei and Kirby (1995) rewrote the equations to handle high order time marching schemes. The equations are divided up into different components representing the left and right hand side of the system of equations. The model constructs a tridiagonal system of equations, which is then solved using a tridagonal solver. The momentum

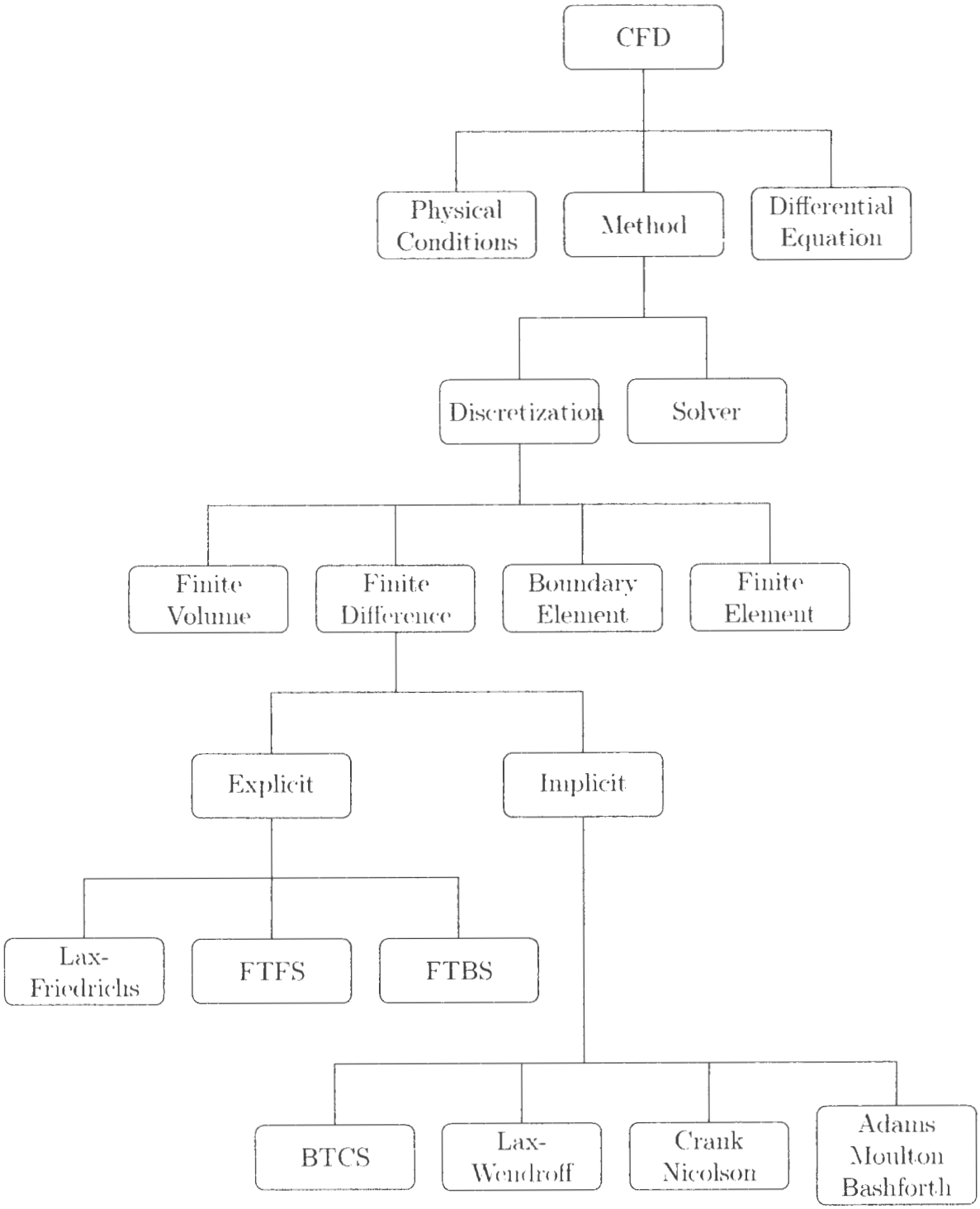

Figure 3.1: CFD Overview

and continuity equations are much more difficult to solve using an implicit scheme, and the new variable facilitate the computations.

$$\eta_t = E(\eta, u, v)$$

$$\begin{aligned} E(\eta, u, v) = &- [(h+\eta)u]_x - \{a_1 h^3 (u_{xx} + v_{xy}) + a_2 h^2 [(hu)_{xx} + (hv)_{xy}]\}_x \\ &- [(h+\eta)v]_y - \{a_1 h^3 (u_{xy} + v_{yy}) + a_2 h^2 [(hu)_{xy} + (hv)_{yy}]\}_y \end{aligned}$$

$$U_t = F(\eta, u, v) + [F_1(v)]_t$$

$$V_t = G(\eta, u, v) + [G_1(u)]_t$$

$$U = u + h[b_1 h u_{xx} + b_2 (hu)_{xx}]$$

$$V = v + h[b_1 h v_{yy} + b_2 (hv)_{yy}]$$

$$F = -g\eta_x - (uu_x + vu_y)$$

$$G = -g\eta_y - (uv_x + vv_y)$$

$$F_1 = -h[b_1 h v_{xy} + b_2 (hv)_{xy}]$$

$$G_1 = -h[b_1 h u_{xy} + b_2 (hu)_{xy}]$$

where $a1$, $a2$, $b1$, $b2$ are constants proportional to the reference water depth, Z_α.

$$a1 = \frac{Z_\alpha^2}{2h^2} - \frac{1}{6} \qquad a2 = \frac{Z_\alpha}{h} + \frac{1}{2} \qquad b1 = \frac{Z_\alpha^2}{2h^2} \qquad b2 = \frac{Z_\alpha}{h}$$

3.2.1 Time Discretization

A fifth-order predictor corrector method is used to solve the Boussinesq equations. A fourth-order Adams-Bashforth explicit predictor method gives an initial approximation and a fifth order Adams-Moulton implicit corrector method is used to iterate over the results to converge to a specified tolerance of error. The third and fourth-order Adams-Bashforth predictor methods are given for reference.

$$\eta_{ij}^{n+1} = \eta_{ij}^n + \frac{\Delta t}{12}[23E_{ij}^n - 16E_{ij}^{n-1} - 5E_{ij}^{n-2}]$$

$$U_{ij}^{n+1} = U_{ij}^n + \frac{\Delta t}{12}[23F_{ij}^n - 16F_{ij}^{n-1} - 5F_{ij}^{n-2}] + 2(F_1)_{ij}^n - 3(F_1)_{ij}^{n-1} + (F_1)_{ij}^{n-2}$$

$$V_{ij}^{n+1} = V_{ij}^n + \frac{\Delta t}{12}[23G_{ij}^n - 16G_{ij}^{n-1} - 5G_{ij}^{n-2}] + 2(G_1)_{ij}^n - 3(G_1)_{ij}^{n-1} + (G_1)_{ij}^{n-2}$$

$$\eta_{ij}^{n+1} = \eta_{ij}^n + \frac{\Delta t}{24}[55E_{ij}^n - 59E_{ij}^{n-1} + 37E_{ij}^{n-2} - 9E_{ij}^{n-3}]$$

$$U_{ij}^{n+1} = U_{ij}^n + \frac{\Delta t}{24}[55F_{ij}^n - 59F_{ij}^{n-1} + 37F_{ij}^{n-2} - 9F_{ij}^{n-3}] + 2(F_1)_{ij}^n - 3(F_1)_{ij}^{n-1} + (F_1)_{ij}^{n-2}$$

$$V_{ij}^{n+1} = V_{ij}^n + \frac{\Delta t}{24}[55G_{ij}^n - 59G_{ij}^{n-1} + 37G_{ij}^{n-2} - 9G_{ij}^{n-3}] + 2(G_1)_{ij}^n - 3(G_1)_{ij}^{n-1} + (G_1)_{ij}^{n-2}$$

The fourth and fifth order Adams-Moulton corrector method are also given. The implicit method is used to increase the accuracy of the results from the less accurate explicit method.

$$\eta_{ij}^{n+1} = \eta_{ij}^n + \frac{\Delta t}{24}[9E_{ij}^{n+1} + 19E_{ij}^n - 5E_{ij}^{n-1} + E_{ij}^{n-2}]$$

$$U_{ij}^{n+1} = U_{ij}^{n} + \frac{\Delta t}{24}[9F^{n+1} + 19F_{ij}^{n} - 5F_{ij}^{n-1} + F_{ij}^{n-2}] + (F_1)_{ij}^{n+1} - (F_1)_{ij}^{n}$$

$$V_{ij}^{n+1} = V_{ij}^{n} + \frac{\Delta t}{24}[9G^{n+1} + 19G_{ij}^{n} - 5G_{ij}^{n-1} + G_{ij}^{n-2}] + (G_1)_{ij}^{n+1} - (G_1)_{ij}^{n}$$

$$\eta_{ij}^{n+1} = \eta_{ij}^{n} + \frac{\Delta t}{720}[251E_{ij}^{n+1} + 646E_{ij}^{n} - 264E_{ij}^{n-1} + 106E_{ij}^{n-2} - 19E_{ij}^{n-3}]$$

$$U_{ij}^{n+1} = U_{ij}^{n} + \frac{\Delta t}{720}[251F^{n+1} + 646F_{ij}^{n} - 264F_{ij}^{n-1} + 106F_{ij}^{n-2} - 19F_{ij}^{n-2}] + (F_1)_{ij}^{n+1} - (F_1)_{ij}^{n}$$

$$V_{ij}^{n+1} = V_{ij}^{n} + \frac{\Delta t}{720}[251G^{n+1} + 646G_{ij}^{n} - 264G_{ij}^{n-1} + 106G_{ij}^{n-2} - 19G_{ij}^{n-3}] + (G_1)_{ij}^{n+1} - (G_1)_{ij}^{n}$$

The time derivative for F_1, which is similarly for G_1, is calculated using lower order predictor corrector methods. The second order predictor method and the third order corrector schemes are given.

$$[(F_1)_t]_{ij}^{n} = \frac{1}{2\Delta t}[3F_{1ij}^{n} - 4F_{1ij}^{n-1} + F_{1ij}^{n-2}]$$

$$[(F_1)_t]_{ij}^{n-1} = \frac{1}{2\Delta t}[F_{1ij}^{n} - F_{1ij}^{n-2}]$$

$$[(F_1)_t]_{ij}^{n-2} = -\frac{1}{2\Delta t}[3F_{1ij}^{n} - 4F_{1ij}^{n-1} + F_{1ij}^{n-2}]$$

$$[(F_1)_t]_{ij}^{n+1} = \frac{1}{6\Delta t}[11F_{1ij}^{n+1} - 18F_{1ij}^{n} + 9F_{1ij}^{n-1} - 2F_{1}^{n-2}]$$

$$[(F_1)_t]_{ij}^{n} = \frac{1}{6\Delta t}[2F_{1ij}^{n+1} + 3F_{1ij}^{n} - 6F_{1ij}^{n-1} + F_{1}^{n-2}]$$

$$[(F_1)_t]_{ij}^{n-1} = \frac{1}{6\Delta t}[2F_{1ij}^{n-2} + 3F_{1ij}^{n-1} - 6F_{1ij}^{n} + F_{1}^{n+1}]$$

$$[(F_1)_t]_{ij}^{n+1} = \frac{1}{6\Delta t}[11F_{1ij}^{n-2} - 18F_{1ij}^{n-1} + 9F_{1ij}^{n} - 2F_{1}^{n+1}]$$

3.2.2 Spatial Differencing

The spatial derivatives were discretized using general seven point finite difference schemes to allow for higher orders of nonlinearity and dispersion. The time and space derivatives need to be discretized to an order higher than the order of the hyperbolic equations. The magnitude of error from the truncation of the Taylor series of the finite difference method should be lower than the truncation of the Taylor series for the velocity expansion. A five point differencing scheme is given for first order spatial derivatives. These are the numerical equations used by Wei, Kirby, Grilli, and Subramanya (1995). A three point difference scheme is used for the second order derivatives. Second order difference methods are used for the mixed derivatives. The accompanying boundary and corner difference equations are also given.

$$(u_x)_{1,j} = \frac{1}{12\Delta x}(-25u_{1,j} + 48u_{2,j} - 36u_{3,j} + 16u_{4,j} - 3u_{5,j})$$

$$(u_x)_{2,j} = \frac{1}{12\Delta x}(-3u_{1,j} - 10u_{2,j} + 18u_{3,j} - 6u_{4,j} + u_{5,j})$$

$$(u_x)_{ij} = \frac{1}{12\Delta x}(8(u_{i+1,j} - u_{i-1,j}) - (u_{i+2,j} - u_{i-2,j})) \qquad \text{for} \quad i = 3, 4, \ldots, M-2$$

$$(u_x)_{M-1,j} = \frac{1}{12\Delta x}(3u_{M,j} + 10u_{M-1,j} - 18u_{M-2,j} + 6u_{M-3,j} - u_{M-4,j})$$

$$(u_x)_{M,j} = \frac{1}{12\Delta x}(25u_{M,j} - 48u_{M-1,j} + 36u_{M-2,j} - 16u_{M-3,j} + 3u_{M-4,j})$$

$$(u_{xx})_{1,j} = \frac{1}{(\Delta x)^2}(2u_{1,j} - 5u_{2,j} + 4u_{3,j} - u_{4,j})$$

$$(u_{xx})_{i,j} = \frac{1}{(\Delta x)^2}(u_{i+1,j} - 2u_{ij} + u_{i-1,j}) \qquad \text{for} \quad i = 2, 3, \ldots, M-1$$

$$(u_{xx})_{M,j} = \frac{1}{(\Delta x)^2}(2u_{M,j} - 5u_{M-1,j} + 4u_{M-2,j} - u_{M-3,j})$$

$$(u_{xy})_{1,1} = \frac{1}{4\Delta x \Delta y}[9u_{1,1} + 16u_{2,2} + u_{3,3} - 12(u_{1,2} + u_{2,1}) + 3(u_{1,3} + u_{3,1}) - 4(u_{2,3} + u_{3,2})]$$

$$(u_{xy})_{1,j} = \frac{1}{4\Delta x \Delta y}[-3(u_{1,j+1} - u_{1,j-1}) + 4(u_{2,j+1} - u_{2,j\ -1}) - (u_{3,j+1} - u_{3,j-1})]$$

$$\text{for} \quad j = 2, 3, ..., N-1$$

$$(u_{xy})_{ij} = \frac{1}{4\Delta x \Delta y}(u_{i+1,j+1} + u_{i-1,j-1} - u_{i-1,j+1} - u_{i+1,j-1})$$

$$\text{for } i = 2, 3, ..., M-1 \text{ and } j = 2, 3, ..., N-1$$

The current research implements a higher order difference method in preparation for higher orders of nonlinearity and dispersion. The order of the truncation error for the difference methods should be higher than the truncation error in the derivation of the velocity variable, so that the numerical method does not introduce error of the same order of magnitude. It is also intuitive for the spatial discretization to have a lower magnitude of truncation error than the time discretization, since the spatial difference scheme is independent of the temporal method, but the temporal method is dependent on the spatial differences. A sixth-order seven point difference method is used for the first order spatial derivatives.

$$(u_x)_{1,j} = \frac{1}{60\Delta x}(-147u_{1,j} + 360u_{2,j} - 450u_{3,j} + 400u_{4,j} - 225u_{5,j} + 72u_{6,j} - 10u_{7,j})$$

$$(u_x)_{2,j} = \frac{1}{60\Delta x}(-10u_{1,j} - 77u_{2,j} + 150u_{3,j} - 100u_{4,j} + 50u_{5,j} - 15u_{6,j} + 2u_{7,j})$$

$$(u_x)_{3,j} = \frac{1}{60\Delta x}(2u_{1,j} - 24u_{2,j} - 35u_{3,j} + 80u_{4,j} - 30u_{5,j} + 8u_{6,j} - u_{7,j})$$

$$(u_x)_{ij} = \frac{1}{60\Delta x}(-u_{i-3,j} + 9u_{i-2,j} - 45u_{i-1,j} + 45u_{i+1,j} - 9u_{i+2,j} + u_{i+3,j})$$

$$\text{for} \quad i = 4, 5, ..., M-3$$

$$(u_{xx})_{1,j} = \frac{1}{180(\Delta x)^2}(812u_{1,j} - 3132u_{2,j} + 5265u_{3,j} - 5080u_{4,j} + 2970u_{5,j} - 972u_{6,j} + 137u_{7,j})$$

$$(u_{xx})_{2,j} = \frac{1}{180(\Delta x)^2}(137u_{1,j} - 147u_{2,j} - 255u_{3,j} + 470u_{4,j} - 285u_{5,j} + 93u_{6,j} - 13u_{7,j})$$

$$(u_{xx})_{3,j} = \frac{1}{180(\Delta x)^2}(-13u_{1,j} + 228u_{2,j} - 420u_{3,j} + 200u_{4,j} + 15u_{5,j} - 12u_{6,j} + 2u_{7,j})$$

$$(u_{xx})_{i,j} = \frac{1}{180(\Delta x)^2}(2u_{i-3,j} - 27u_{i-2,j} + 270u_{i-1,j} - 490u_{i,j} + 270u_{i+1,j} - 27u_{i+2,j} + 2u_{i+3,j}$$

$$\text{for} \quad i = 4, 5, \ldots, M-3$$

The finite difference scheme for a vertical reflective wall bounding the domain.

$$u_{i,N} = \frac{1}{25}(48u_{i,N_1} - 36u_{i,N_2} + 16u_{i,N_3} - 3u_{i,N_4})$$

$$\eta_{i,N} = \frac{1}{25}(48\eta_{i,N_1} - 36\eta_{i,N_2} + 16\eta_{i,N_3} - 3\eta_{i,N_4})$$

$$\text{for } i = 1, 2, 3, \ldots, M$$

3.3 Convergence

The numerical method iterates between the predicted and corrected values. The results for each step in time converges towards a solution for a specific range of water depth proportional to the wave length. The error between k and k + 1 subsequent time steps is calculated to assure that the numerical solution is convergent to a specified tolerance.

$$\Delta\eta = \frac{\sum_i \sum_j |\eta_{ij}^{k+1} - \eta_{ij}^{k}|}{\sum_i \sum_j |\eta_{ij}^{k+1}|}$$

$$\Delta u + \Delta v = \frac{\sum_i \sum_j |u_{ij}^{k+1} - u_{ij}^{k}| + |v_{ij}^{k+1} - v_{ij}^{k}|}{\sum_i \sum_j |u_{ij}^{k+1}| + |v_{ij}^{k+1}|}$$

The convergence speed is increased by using a relaxation method to blend the values between the previous time step and the current time step being evaluated. The adjusted value is used in the subsequent time step to speed up the convergence.

$$\eta^{k+1} = (1 - R)\eta^{k+1} + R\eta^{k}$$

R is a constant value between 0.0 and 1.0. Wei and Kirby (1998) used a value of 0.2 which produced satisfactory results. The same method is used similarly for the velocity components, u and v.

3.4 Stability

The Adams-Bashforth-Moulton multi-step finite difference method is implemented up to fifth order accuracy. A general formula is used to show the order of all linear multistep methods. The von Neumann linear stability analysis is applied for fourth order accuracy. The linearized Boussinesq equations for wave propagation in one dimension are given. The equations are derived into the associated left and right hand sides for the implicit finite difference schemes.

$$\eta_t + hu_x + (\alpha + \frac{1}{3})h^3 u_{xxx} = 0$$

$$u_t + g\eta_x + \alpha h^2 u_{xxt} = 0$$

$$\eta_t = -hu_x - (\alpha + \frac{1}{3})h^3 u_{xxx}$$

$$U_t = -g\eta_x$$

$$U = u + \alpha h^2 u_{xx}$$

3.4.1 von Neumann Analysis

The von Neumann method is applied to perform linear stability analysis for constant water depth in one dimension. The stability analysis is only performed on one iteration of the predictor and corrector methods. This method was used by Wei and Kirby (1998). The finite difference equations are represented using their Fourier components.

$$\eta_j^n = \eta_0 exp[i(kj\Delta x - \omega n\Delta t)]$$

$$u_j^n = u_0 exp[i(kj\Delta x - \omega n\Delta t)]$$

The finite difference expressions for the predictor and corrector schemes are given.

$$\eta_j^{n+1} = \eta_j^n + \frac{\Delta t}{12}(23E_j^n - 16E_j^{n-1} + 5E_j^{n-2})$$

$$U_j^{n+1} = U_j^n + \frac{\Delta t}{12}(23F_j^n - 16F_j^{n-1} + 5F_j^{n-2})$$

$$\eta_j^{n+1} = \eta_j^n + 46pu_j^n - 32pu_j^{n-1} + 10pu_j^{n-2}$$

$$u_j^{n+1} = u_j^n + 46q\eta_j^n - 32q\eta_j^{n-1} + 10q\eta_j^{n-2}$$

$$\eta_j^{n+1} = \eta_j^n + \frac{\Delta t}{24}(9E_j^{n+1} + 19E_j^n - 5E_j^{n-1} + E_j^{n-2})$$

$$U_j^{n+1} = U_j^n + \frac{\Delta t}{24}(9F_j^{n+1} + 19F_j^n - 5F_j^{n-1} + F_j^{n-2})$$

$$\eta_j^{n+1} = \eta_j^n + 9pu_j^{n+1} + 19pu_j^n - 5pu_j^{n-1} + pu_j^{n-2}$$

$$u_j^{n+1} = u_j^n + 9q\eta_j^{n+1} + 19q\eta_j^n - 5q\eta_j^{n-1} + q\eta_j^{n-2}$$

The Fourier solutions are substituted into the difference equations, and the variables.

p and q. are are solved for one step in the solution to the linear Boussinesq equations. The following solution of the equations is from the derivation by Wei and Kirby (1998).

$$p = -\frac{ih\Delta t}{24\Delta x}\sin k\Delta x\left[\frac{4-\cos k\Delta x}{3} - \frac{4(\alpha+\frac{1}{3})h^2}{\Delta x^2}\sin^2\left(\frac{k\Delta x}{2}\right)\right]$$

$$q = -\frac{\frac{ig\Delta t}{24\Delta x}\sin k\Delta x\left[\frac{1-\cos k\Delta x}{3}\right]}{1-\frac{4\alpha h^2}{\Delta x^2}\sin^2\left(\frac{k\Delta x}{2}\right)}$$

The substitution of the predictor expressions for the $n+1$ values into the corrector equation defines an amplification matrix for which there exists eigenvalues. The eigenvalues are the wavenumber $k\Delta x$, the Courant/Friedrichs/Lewy number $CFL = \sqrt{gh}\Delta t/\Delta x$, and the ratio between depth and grid unit $\frac{h}{\Delta x}$. If the modulus of each eigenvalue is less than or equal to one, then the numerical scheme is stable. It was further found by Wei and Kirby (1998) that the finite difference scheme is stable independent of the wavenumber and depth to grid ratio, if $CFL \leq 0.8$. The current research goes to a much higher order of difference equations, and the resulting linear stability equations are significantly more complex.

3.4.2 Numerical Filtering

Short wave components generated from nonlinear effects create stability problems for the prediction of long wave propagation. A nine point numerical filter was used to filter out nonphysical low frequency waves which would otherwise propagate through the domain and blow up the solution. Weighted averages of neighbouring points are used to eliminate these components, which would otherwise create discontinuities in the wave form. Short wave components create potential stability concerns for the prediction of long waves. These waves are generated by wave reflection and dispersion. A numerical filter as defined by Wei and Kirby (1998) which uses weighted averages to eliminate these components. A nine point filter is used instead of the seven point filter

used by Wei and Kirby (1998). The truncation error of the numerical filter should be lower than the truncation error of the spatial derivatives, so that the numerical filter does not introduce any error into the numerical model.

$$\eta_j^* = \frac{1}{4}[2\eta_j + \eta_{j+1} + \eta_{j-1}] \qquad \text{for} \quad j = 2, M-1$$

$$\eta_j^* = \frac{1}{16}[10\eta_j + 4(\eta_{j+1} + \eta_{j-1}) - (\eta_{j+2} + \eta_{j-2})] \qquad \text{for} \quad j = 3, M-2$$

$$\eta_j^* = \frac{1}{64}[44\eta_j + 15(\eta_{j+1} + \eta_{j-1}) - 6(\eta_{j+2} + \eta_{j-2}) + \eta_{j+3} + \eta_{j-3}] \qquad \text{for} \quad j = 4, M-3$$

$$\eta_j^* = \frac{1}{256}[186\eta_j + 56(\eta_{j+1} + \eta_{j-1}) - 28(\eta_{j+2} + \eta_{j-2}) + 8(\eta_{j+3} + \eta_{j-3}) - (\eta_{j+4} + \eta_{j-4})]$$

$$\text{for } j = 5, 6, ..., M-4$$

3.5 Solver

There are many different types of solvers that can be used which make marginal difference to the accuracy of the solution. The advantage of using certain solver algorithms over others is due to their improved speed and space efficiency. The slowest solver is Gaussian elimination, but it is a generic algorithm that can be used for any system of equations. Row by row permutations are made to the matrix until the left hand side only has one variable for each corresponding row. The Jacobian and Gauss Seidel solvers are significant improvements over Gaussian elimination, but more efficient methods can be used to solve tridiagonal of symmetric matrices. Cyclic reduction was also implemented, but the generic Thomas tridiagonal matrix algorithm (TDMA) is used. A tridiagonal matrix is formed from the left and right hand sides of the equations.

$$b_N = \begin{pmatrix} b_1 & c_1 & & & & 0 \\ a_2 & b_2 & c_2 & & & \\ & a_3 & b_3 & c_3 & & \\ & & \ddots & \ddots & \ddots & \\ & & & a_{M-1} & b_{M-1} & c_{M-1} \\ 0 & & & & a_M & b_M \end{pmatrix} \cdot u$$

The tridiagonal values of the equations, which are the left hand side of the differential equation with respect to the final form used in the numerical method. The tridiagonal values of the equations are given for multiple dimensions as well.

$$a_i = \frac{h_i}{(\Delta x)^2}(b_1 h_i + b_2 h_{i-1})$$

$$b_i = 1 - \frac{2h_i^2}{(\Delta x)^2}(b_1 + b_2)$$

$$c_i = \frac{h_i}{(\Delta x)^2}(b_1 h_i + b_2 h_{i+1})$$

$$a_{ij} = \frac{h_{ij}}{(\Delta x)^2}(b_1 h_{ij} + b_2 h_{i-1,j})$$

$$b_{ij} = 1 - \frac{2h_{ij}^2}{(\Delta x)^2}(b_1 + b_2)$$

$$c_{ij} = \frac{h_{ij}}{(\Delta x)^2}(b_1 h_{ij} + b_2 h_{i+1,j})$$

$$a_{ij} = \frac{h_{ij}}{(\Delta y)^2}(b_1 h_{ij} + b_2 h_{i,j-1})$$

$$b_{ij} = 1 - \frac{2h_{ij}^2}{(\Delta y)^2}(b_1 + b_2)$$

$$c_{ij} = \frac{h_{ij}}{(\Delta y)^2}(b_1 h_{ij} + b_2 h_{i,j+1})$$

Thomas tridiagonal matrix algorithm uses LU (lower and upper triangular matrices) decomposition. The algorithm is slower than the cyclic reduction method, but the accuracy is sufficient. The algorithm is divided into forward elimination and backward substitution.

for $i = 2$ to M **do**

$b_i = b_i - \frac{a_i}{b_{i-1}} c_{i-1}$

end for

$d_1 = b_1$

for $i = 2$ to M **do**

$d_i = d_i - \frac{a_i}{b_{i-1}} d_{i-1}$

end for

$x_M = \frac{d_M}{b_M}$

for $i = M - 1$ to 1 **do**

$x_i = \frac{d_i - c_i x_{i+1}}{b_i}$

end for

For periodic boundary conditions, the TDMA needs to be modified by perturbing the original matrix and solving using the original tridiagonal algorithm. The Sherman Morrison Woodbury formula is used.

$$A \cdot x = b \qquad (A + x \cdot v)u = b$$

where $A \cdot y = b$ and $A \cdot z = u$

$$x = y\left(\frac{vy}{1+vz}\right)z$$

$$u = \begin{pmatrix} b_1^* \\ 0 \\ \vdots \\ 0 \\ c_n \end{pmatrix} \qquad v = \begin{pmatrix} 1 \\ 0 \\ \vdots \\ 0 \\ \frac{a_1}{b_1} \end{pmatrix}$$

$$b_1' = b_1 - b_1^*$$

$$b_n' = b_n - \frac{c_n a_1}{b_1}$$

$$A = \begin{pmatrix} b_1 & c_1 & & & & a_1 \\ a_2 & b_2 & c_2 & & & \\ & a_3 & b_3 & c_3 & & \\ & & \ddots & \ddots & \ddots & \\ & & & a_{n-1} & b_{n-1} & c_{n-1} \\ c_n & & & & a_n & b_n \end{pmatrix} \cdot u$$

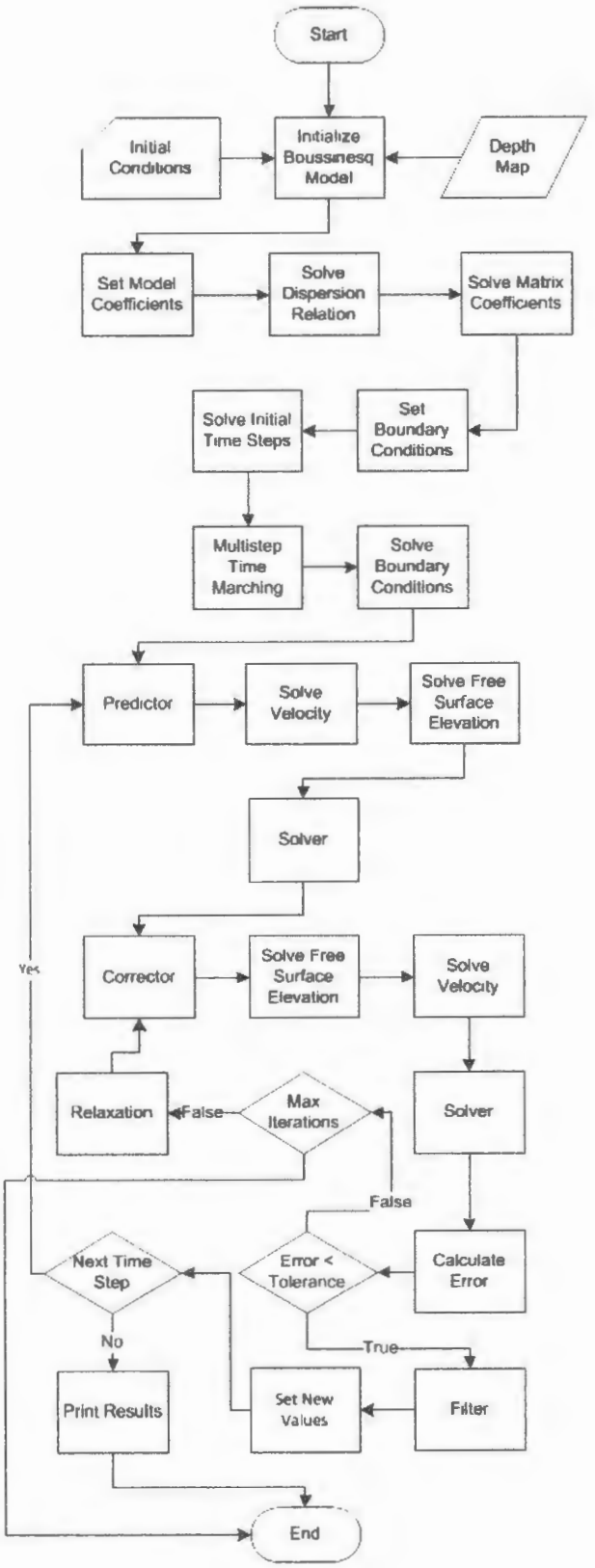

Figure 3.2: Computational flow of the numerical program

Chapter 4

Numerical Results

Several different wave setups are studied to illustrate the accuracy of the Boussinesq equations in modelling wave effects in the near shore region where shallow water conditions are significant. The nonlinearity and dispersive nature of shoaling waves exemplifies the application of the Boussinesq equations for coastal engineering. The equations are solved using initial and generating boundary conditions for regular and solitary waves over varying bathymetry. Several finite difference methods were used to model wave propagation for different time and space discretizations. Nwogu (1993) used a Crank-Nicolson finite difference method for his research, but it is not stable enough for wave propagation from deep to shallow water. An Adams-Bashforth-Moulton time marching method was developed by Wei and Kirby (1995) extending the stability for increasing CFL numbers. The solution to the Boussinesq equations was built up from the simple wave equation. Eventually nonlinearity and dispersion were included, and then modified to permit variable bathymetry and velocity from an arbitrary depth.

4.1 Regular Wave

The Crank-Nicolson finite difference method, including many other low order methods, were analyzed by solving the standard wave equation. A standing wave solution was used as the initial condition to handle multidirectional wave propagation. For two dimensions, the Crank-Nicolson method gave highly accurate results, which are compared with their analytical solutions.

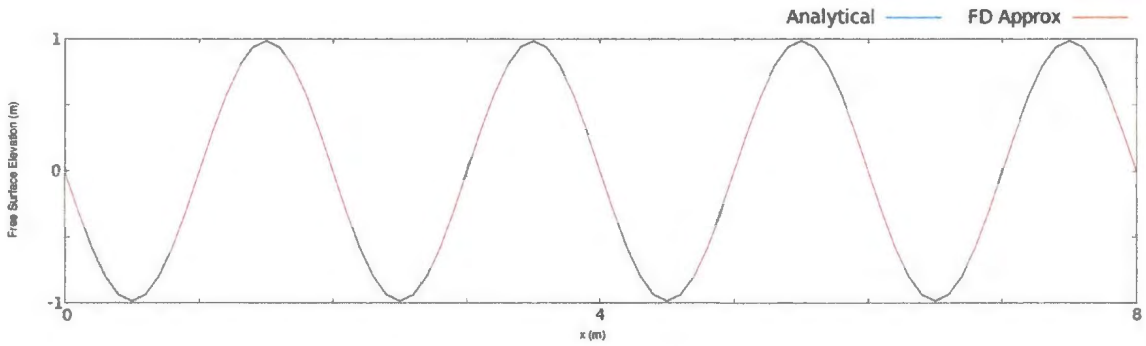

Figure 4.1: Comparison of finite difference and analytical results for initial wave amplitude, a = 1.0m, and wave length, $\lambda = 4.0$

In Figure 4.1, the linear wave equation was solved in three dimensions to test the stability of the model for multiple dimensions. An oblique wave was given as initial conditions to test the boundary conditions for the fluid domain. A three dimensional standing wave solution was given as an initial condition to examine wave interaction within the fluid domain, as seen in Figure 4.2.

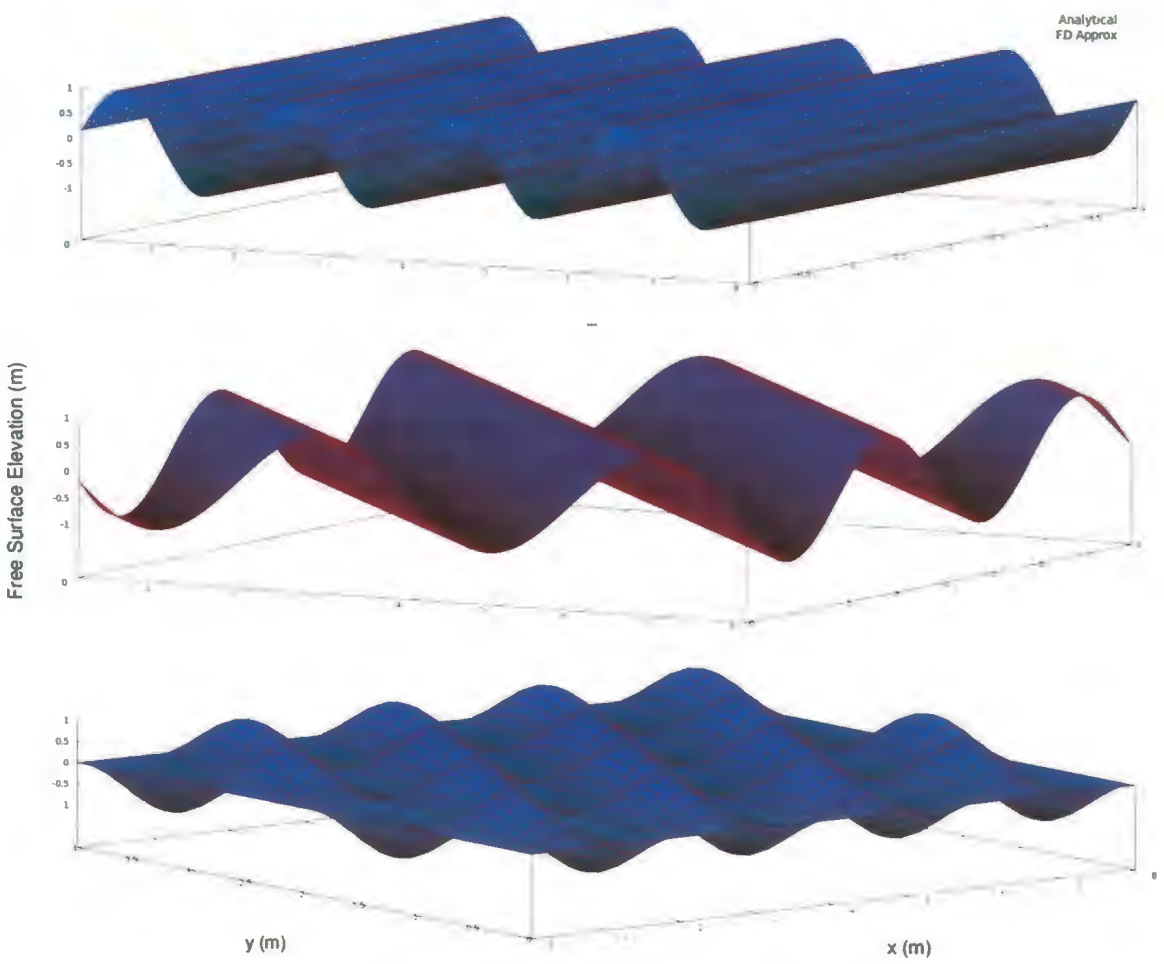

Figure 4.2: Comparison of finite difference and analytical results for initial wave amplitude a = 1.0m, and wave length, $\lambda = 2.0$

A plane wave propagates up a sloping bathymetry in Figure 4.3 and generates amplitude dispersion, which increases in wave height as it approaches the shore. The phase velocity is not dependent on the wave length, so there is no phase dispersion of the wave.

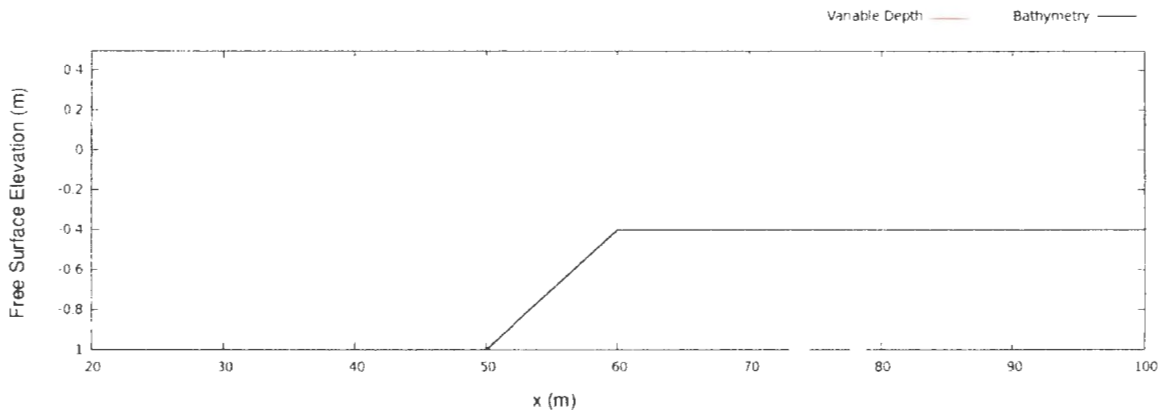

Figure 4.3: A linear plane wave propagates up a sloping bathymetry Shoaling for initial wave amplitude is a = 0.2m, and wave length, $\lambda = 10.0$

4.2 Solitary Wave

Russell (1844) was the first to observe and report a solitary wave. Rayleigh (1876) furthered Russell's research, and came to similar conclusions made by Stokes. Nonlinear solitary waves are compared with analytical and experimental data, which is a classical example of a nonlinear and dispersive water wave, as seen in Figure 4.4. The numerical results from the Adams-Bashforth-Moulton finite difference method are compared with the analytical solution for constant depth.

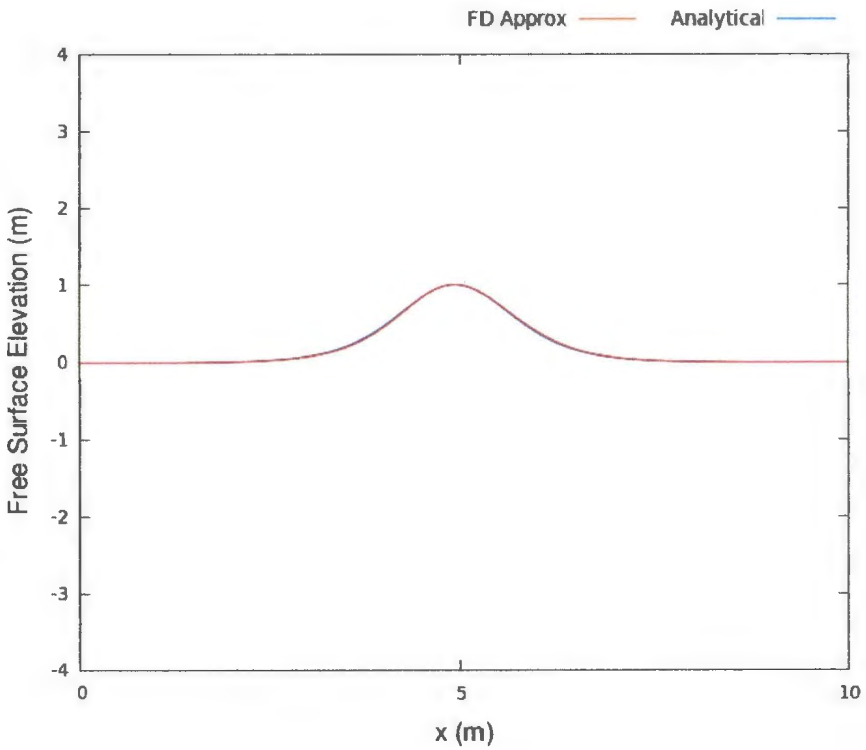

Figure 4.4: Solitary wave representation for constant depth, where wave amplitude, a = 1m

The wave develops forward shoaling and a dispersive oscillating tail is generated following the front wave. The nonlinear equations provide accurate results for moderately shallow water, but for deeper water, a discontinuity due to instability appears at the peak of the wave as the wave shoals over a moderate slope due to the high amplitude dispersion, which would occur in Figure 4.5 in the proceeding time steps.

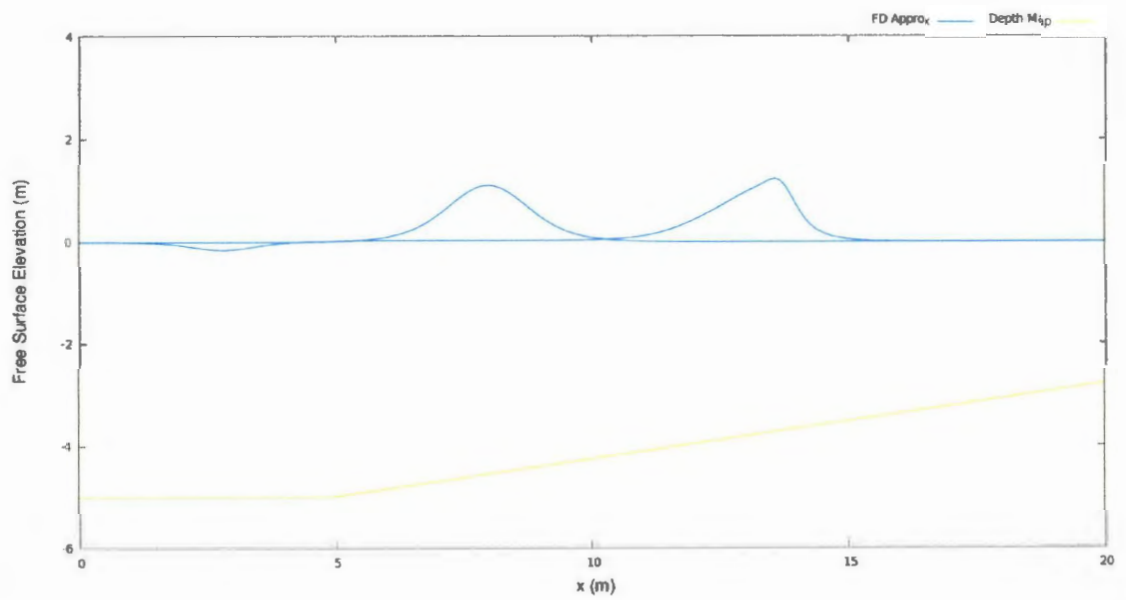

Figure 4.5: Nonlinear propagation of a solitary wave without dispersion, where the wave amplitude is a = 1m, and the water depth is $h_0 = 5m$

Once the discontinuity forms, the error slowly propagates throughout the domain, and the solution blows up. The dispersive effects of the Boussinesq equations balances the high nonlinearity. The extended Boussinesq equations for variable depth were solved using a solitary wave as the initial condition. The Korteweg-deVries equation was developed after the Boussinesq equation, but it is a simplification to waves propagating only in one direction, so it is a good test to validate the numerical method with the KdV before the multidirectional Boussinesq equations.

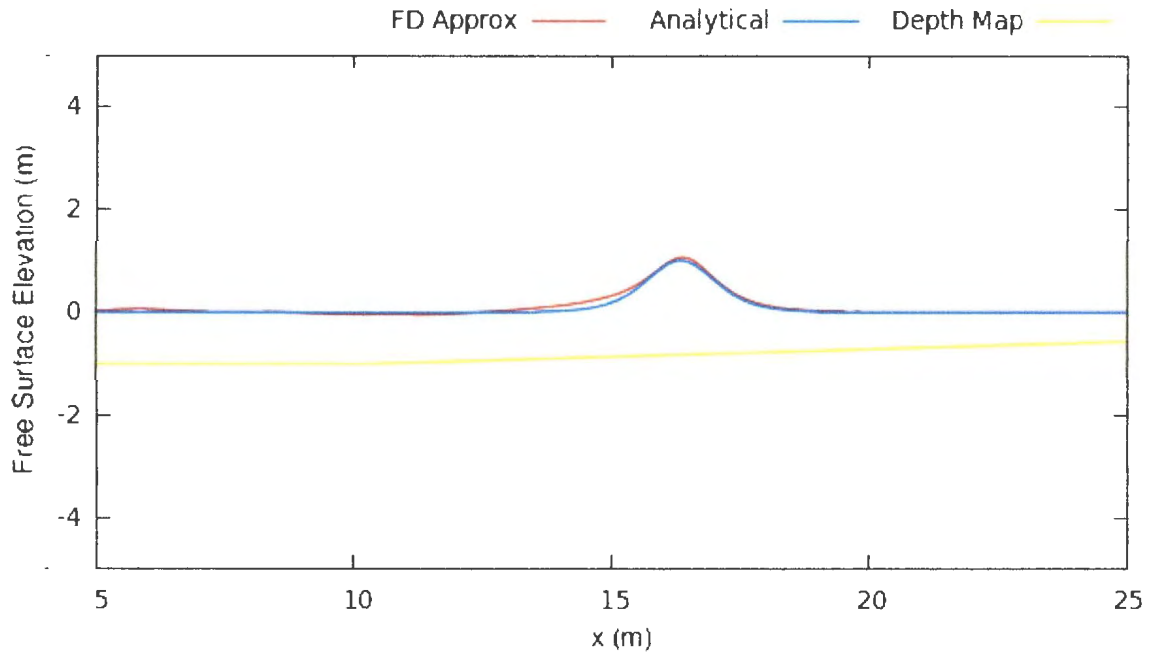

Figure 4.6: Comparison of analytical and numerical results for KdV equation, where the wave amplitude is a = 1m, and the water depth is $h_0 = 1m$

The KdV equation was solved for multiple dimensions, which is shown in Figure 4.7. The dispersive terms for varying bahtymetry create a stable solution for increasing water depth. The wave retains the forward shoaling, and a dispersive oscillating tail is generated following the main wave. The balance of nonlinearity and dispersion is the elegance of the solution for numerical stability in the wave form.

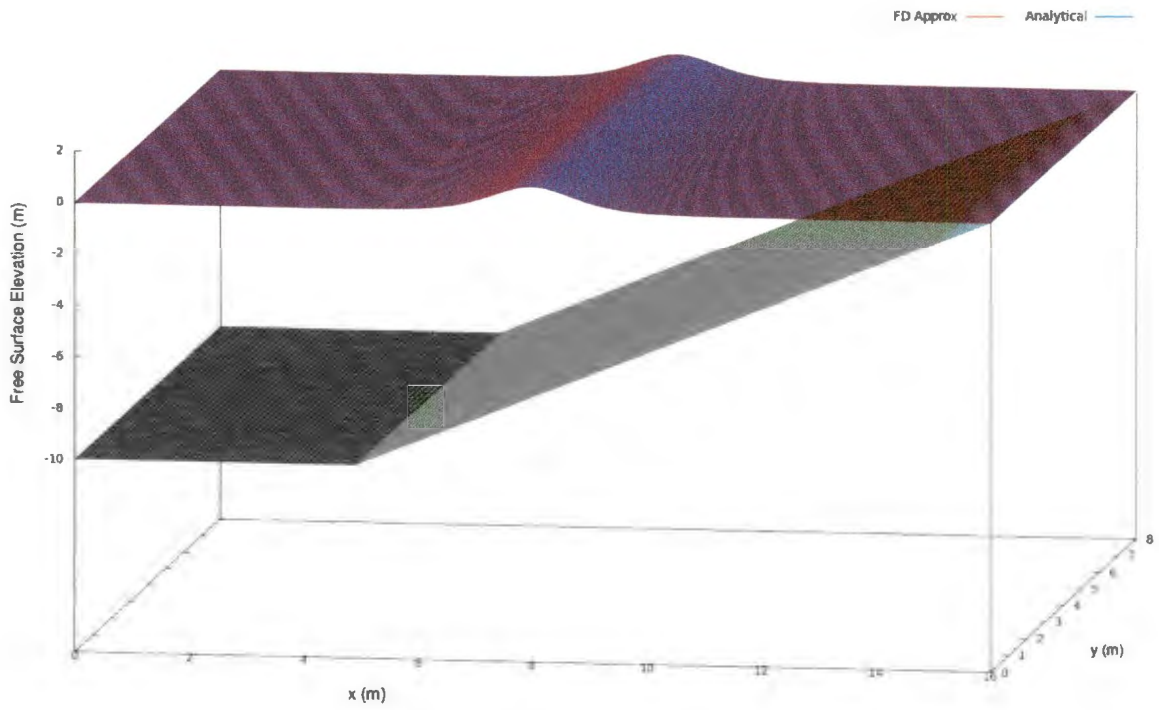

Figure 4.7: Solitary wave in three dimensions using the KdV equation, where the wave amplitude is a = 1m, and the water depth is $h_0 = 10m$

4.2.1 Boussinesq Equation

The extended Boussinesq equations for variable depth are solved using a solitary wave as the initial wave conditions. The results from the numerical code are compared with the numerical data generated by Wei and Kirby (1995). The extended Boussinesq equations allow for the prediction of waves for increasing slope of the bathymetry. A good comparison is made with their weakly nonlinear theory, and the slight magnitude of error is due to digitizing the data from graphical plots. Wave amplitude dispersion is over predicted in the weakly nonlinear theory compared with the fully nonlinear theory, as seen in Figure 4.8. Figure 4.9 shows the evolution of a solitary wave propagating up a slope with the formation of dispersive waves travelling at an alternate

phase speed.

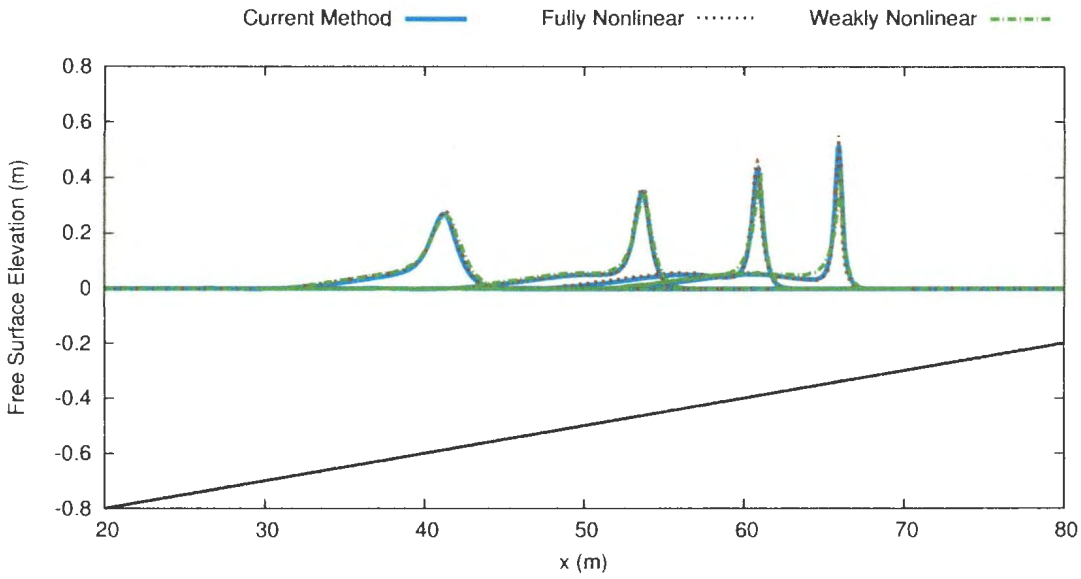

Figure 4.8: Comparison with results from Wei and Kirby, where the water depth $h_0 = 1.0$, the depth gradient is 0.01, and the wave amplitude is a = 0.2

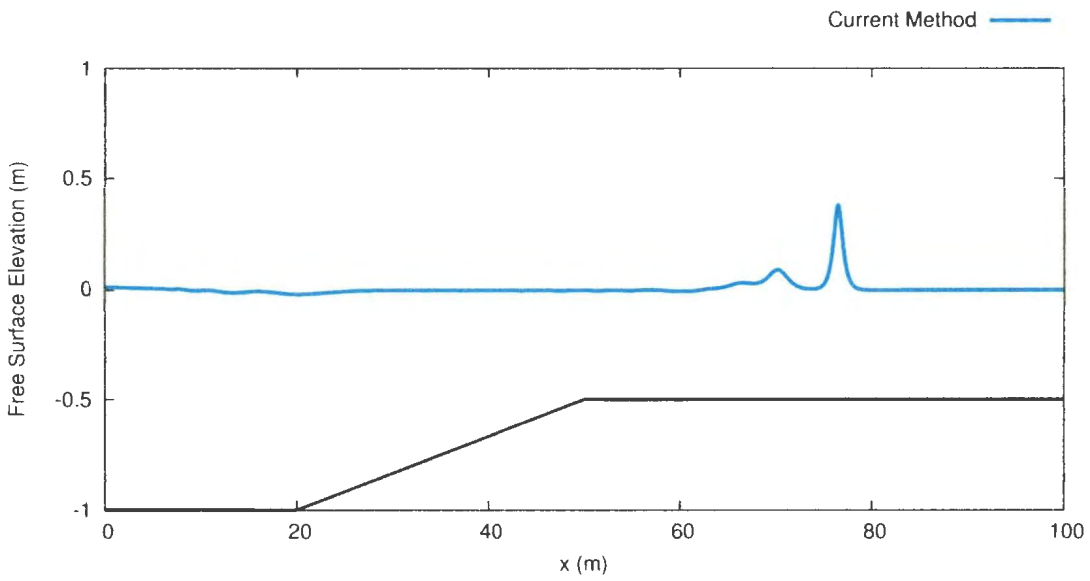

Figure 4.9: Stabilization of a solitary wave after a change in water depth, where the wave amplitude, a = 0.2, the water depth, $h_0 = 1.0$, and the depth gradient is 0.05

4.2.2 Wave Reflection

A solitary wave is modelled as it propagates up a moderate slope and reflects off of a vertical wall. The significant nonlinearity of wave shoaling is difficult for the reflective boundary to accurately predict. The multidirectional Boussinesq equations provide an excellent nonlinear and dispersive solution to the problem of wave reflection for solitary waves. The nonlinearity peaks at the highest point of the shore where the reflective boundary is positioned. When the shoaling solitary wave is incident with the vertical wall, the horizontal velocity is reduced to zero, and the wave momentum is reflected back into the domain. There is no flux through the vertical boundary, but a free slip condition is applied to the tangential/vertical velocity. The dispersive waves generated from the shoaling of the wave form are also reflected from the vertical wall. Every dispersive wave generated that propagates over the sloping bathymetry

also recursively generates smaller dispersive waves as they undergo shoaling which are in turn reflected from the vertical boundary. In Figure 4.10, the propagation and reflection of a solitary wave is shown.

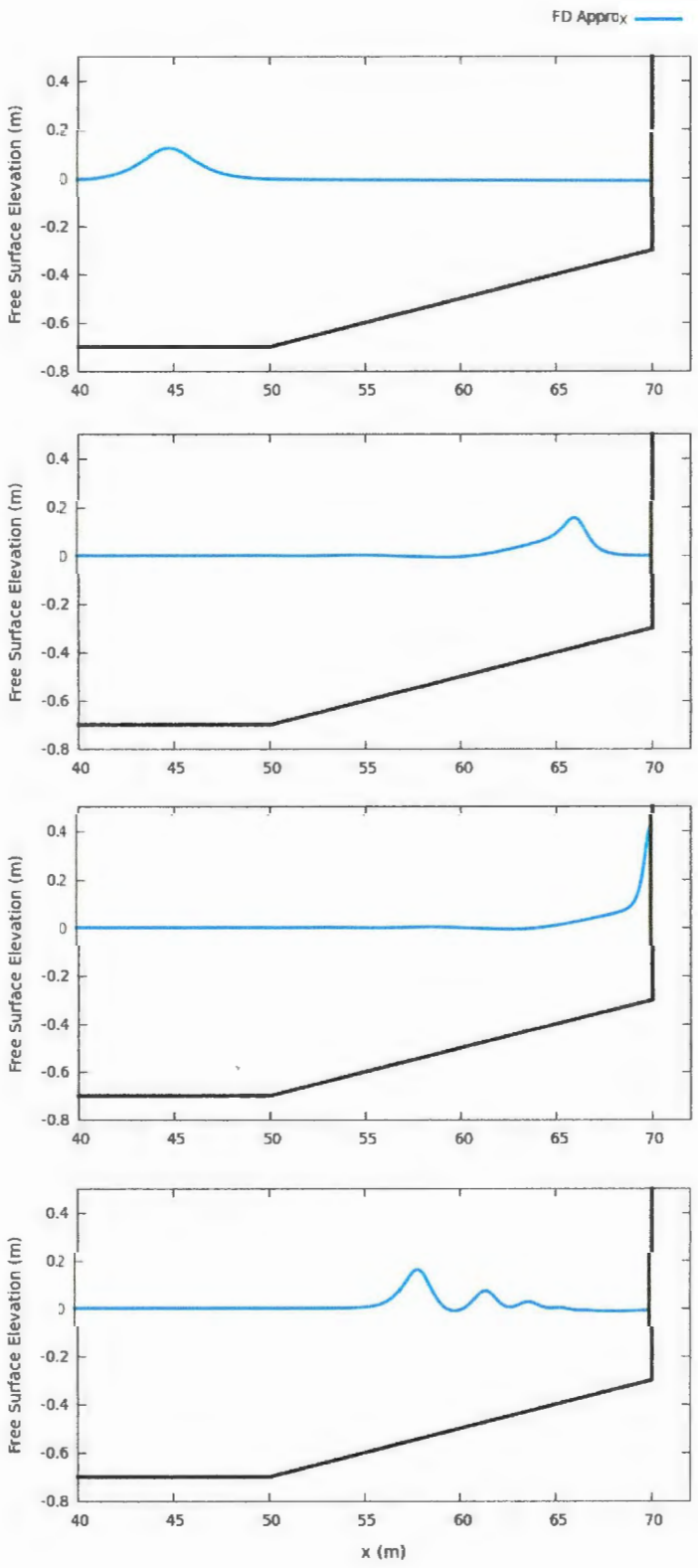

Figure 4.10: Propagation of a reflected solitary wave where the amplitude is a = 0.12m, and the water depth is h = 0.6m

As the wave returns to a constant depth a permanent wave form is once again produced for the solitary and dispersive waves. Wave reflection is validated and compared with experimental data and with published results from a FEM developed by Walkley (1999).

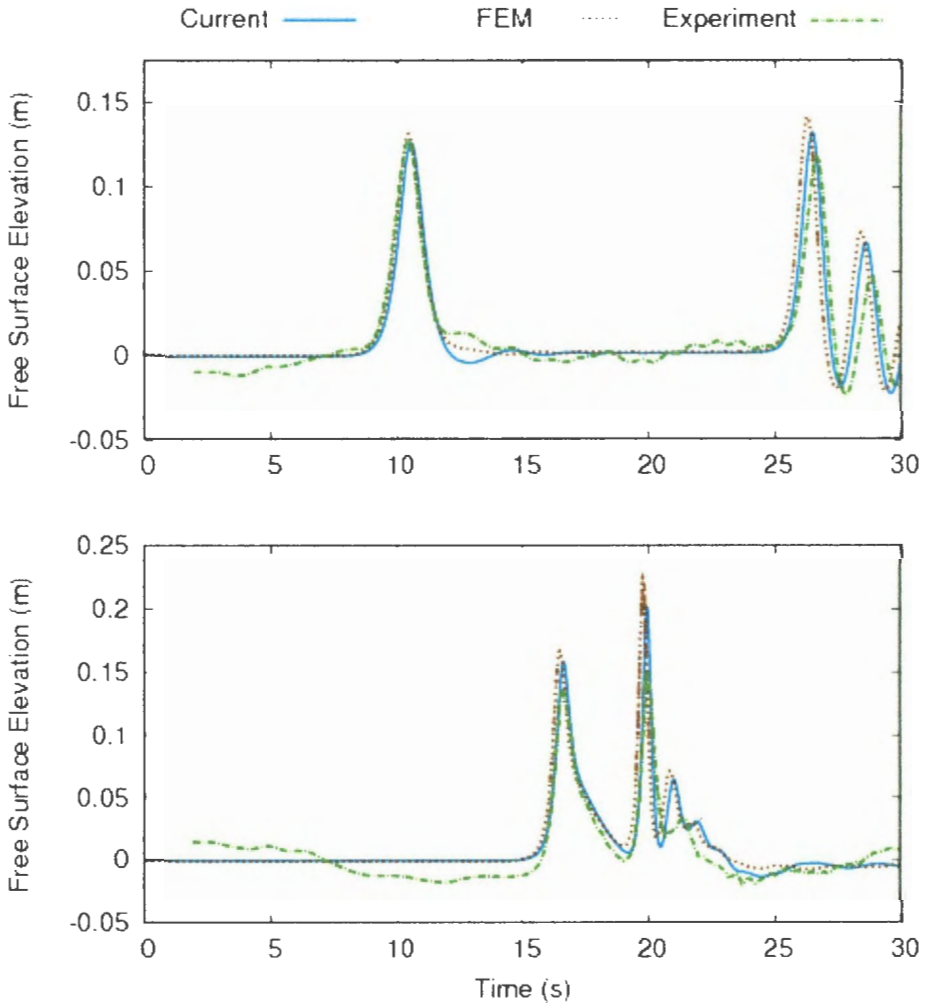

Figure 4.11: Time series of solitary wave reflection for a = 0.07m, taken at x = 50m and x = 66.2m

In Figures 4.11 and 4.12, the time series of the reflected solitary wave is plotted against the FEM model and experimental data. The high-order finite difference method shows

excellent results in comparison with both the FEM model and the experimental data. The main disadvantage is the slight over-prediction of the frequency dispersion, which is seen from the dip in the follow following the front wave.

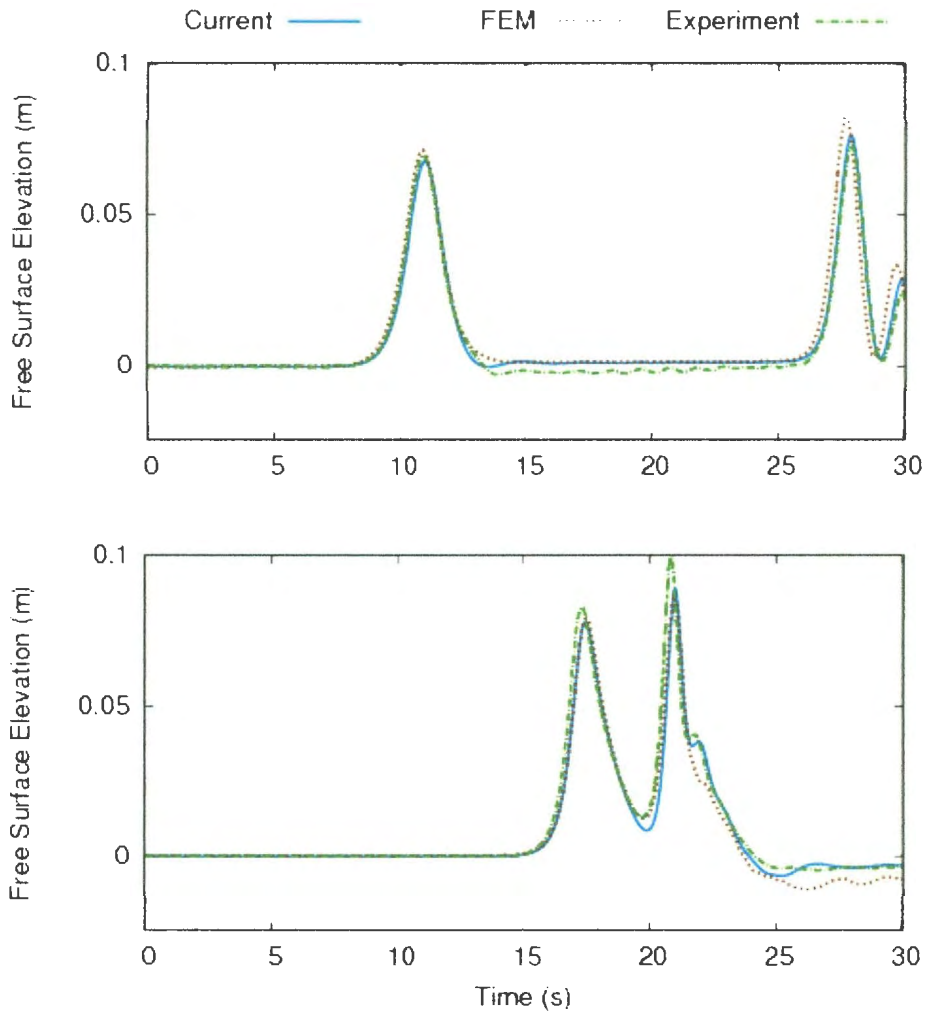

Figure 4.12: Time series of solitary wave reflection for a = 0.12m taken at x = 50 and x = 66.25

4.3 Periodic Propagation over a Breakwater

A periodic wave propagating up a sloping bathymetry and over a breakwater was modelled numerically. The regular periodic wave generates amplitude dispersion, and increases the wave height as it approaches the shore. Smaller dispersive waves are generated in the troughs of the wave. The numerical results are compared with a Galerkin finite element method developed by Walkley (1999b). The experimental setup was constructed by Dingemans (1994), and was further investigated by Beji and Battjes (1994). The propagation of a periodic wave over a submerged breakwater is shown in Figure 4.13. The time series of the periodic wave is shown in Figure 4.14. The current model shows excellent results when compared with the experimental data.

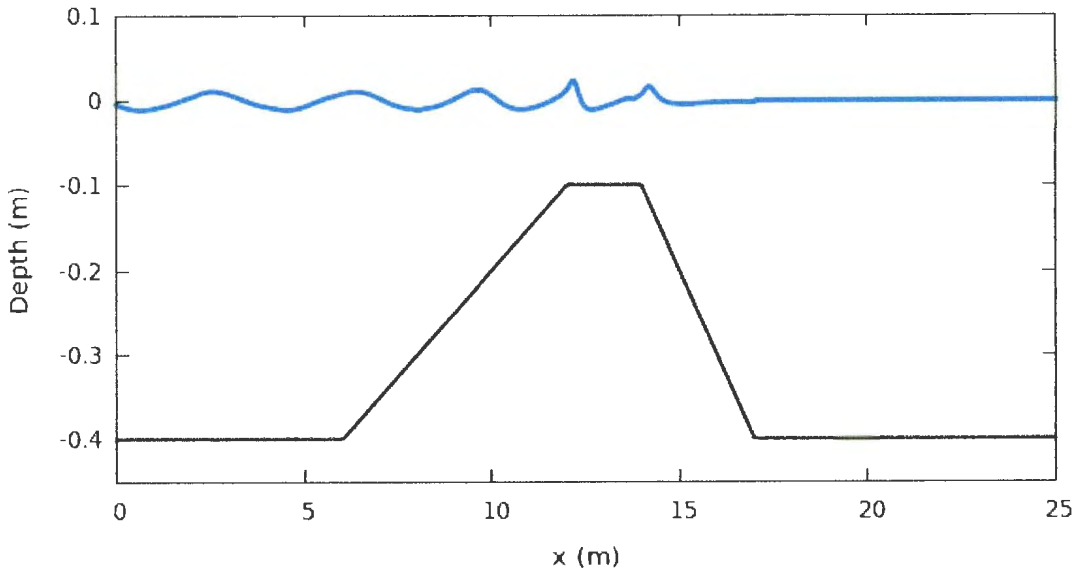

Figure 4.13: Periodic wave propagation over a breakwater, where the wave amplitude is a = 0.01m, and the water depth is $h_0 = 0.4m$, and the top of the breakwater is at h = 0.1m

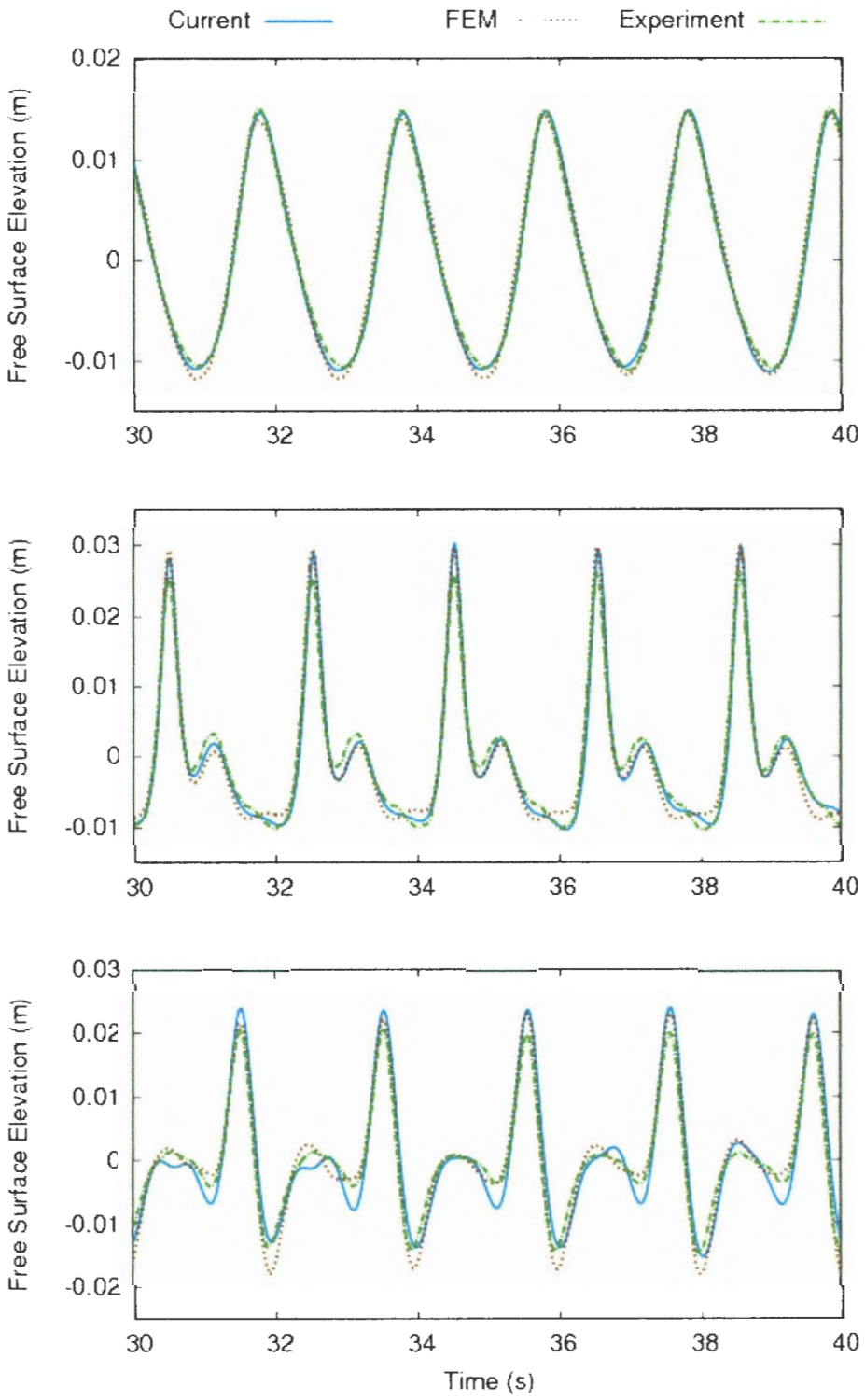

Figure 4.14: Time series of regular wave shoaling over a breakwater at x = 10.5, x = 13.5, and x = 17.3, where a = 0.01, λ = 3.73, and T = 2.02

The propagation of a solitary wave over a breakwater is of particular interest. As the wave propagates over the breakwater, wave shoaling occurs and dispersive waves are generated from the tail of the solitary wave. Once the wave is past the breakwater, the waves return to a permanent form. Each resulting dispersive wave undergoes the effects of shoaling. The waves steepen and generate even smaller dispersive waves. A train of shoaling solitary waves is formed as the numerical process is continued, which is shown in Figure 4.15.

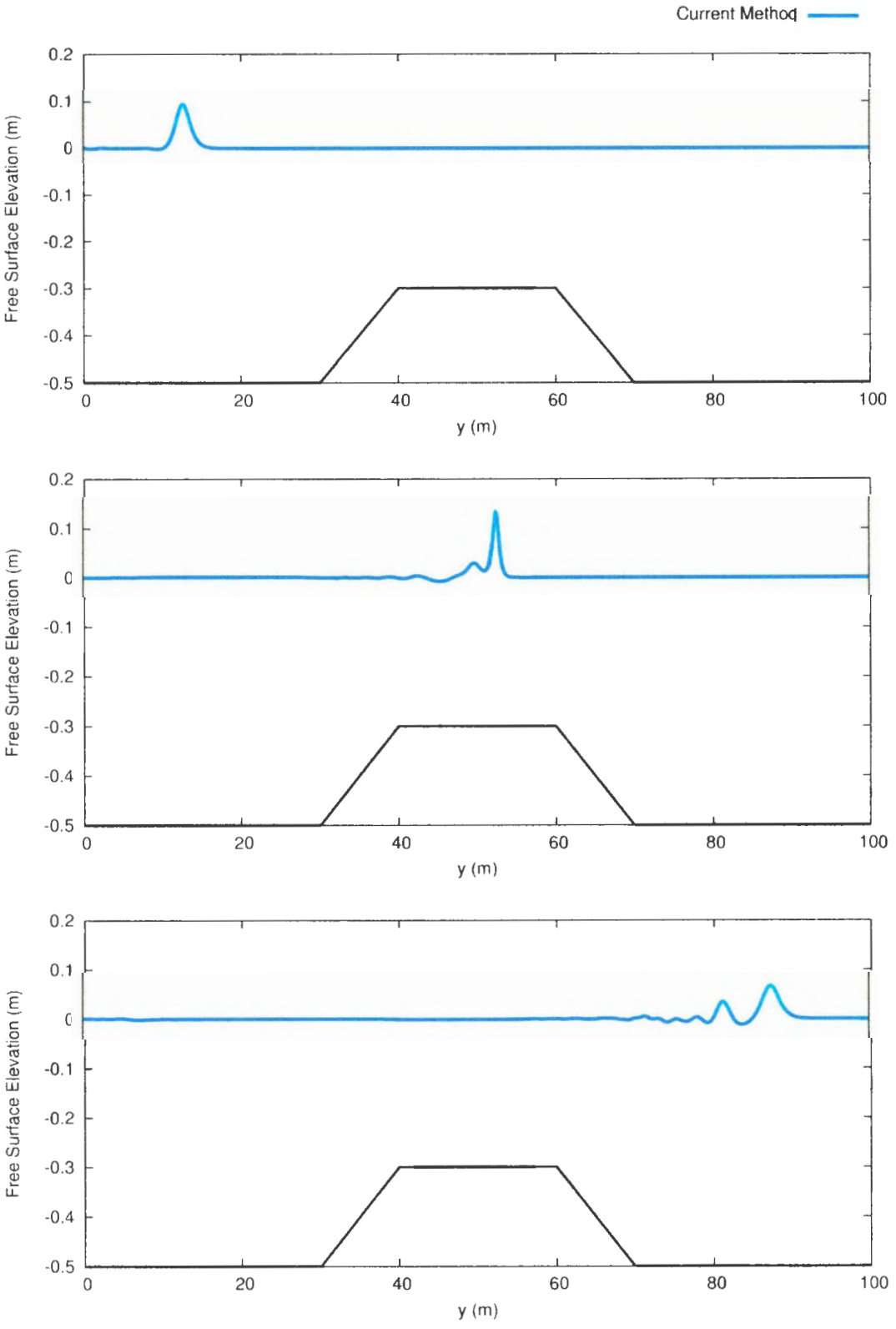

Figure 4.15: Solitary wave propagation over a breakwater, where wave amplitude is a = 0.1m, and water depth is $h_0 = 0.5m$, and the top of the breakwater is at h = 0.3m

4.4 Undular Bore

An undular bore generates oscillatory waves as it propagates into still water. Conversely to solitary waves, the dispersive waves are generated at the front of the bore wave. The wave propagation and evolution of a bore require both nonlinearity and dispersion, which is well represented by the Boussiensq wave model. Airy's nonlinear wave theory describes the steepening of the wave front, but does not accurately predict the oscillating dispersive waves. The prediction of the wave crests and troughs requires significant nonlinearity. The propagation of an undular bore wave requires the stabilizing effect of dispersion due to its high nonlinearity. The bore wave propagates into still water generating dispersive waves while conserving mass and momentum. Wave height increases over time and uniform wave trains are generated. Vertical acceleration at the point of inflection between the two asymptotes from the transition of uniform flow to still water generates dispersive waves. The bore wave, shown in Figure 4.16, is compared with fully nonlinear data from Wei and Kirby (1998).

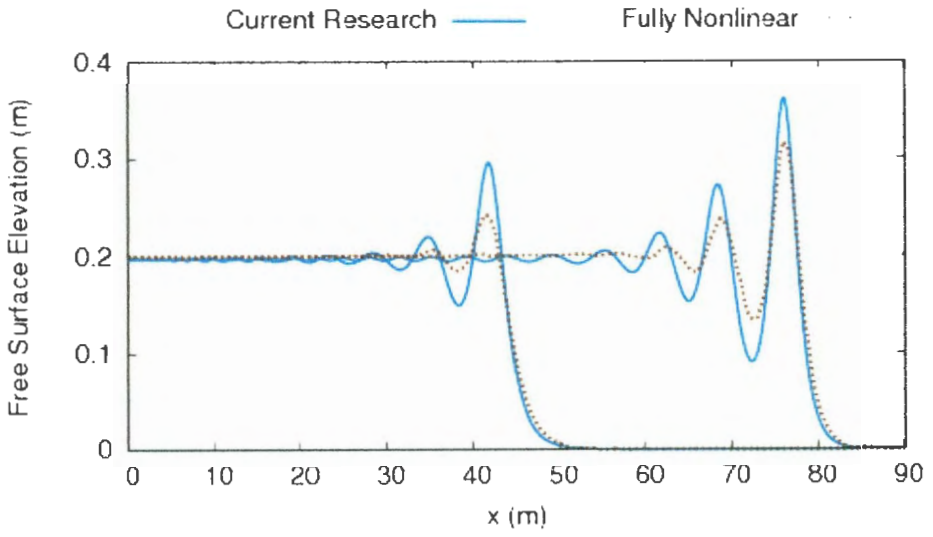

Figure 4.16: Undular bore wave propagation, where the initial wave elevation is a = 0.2m

4.5 Numerical Program

A numerical program was developed to solve the Boussinesq equations. The program is very efficient computationally, and handles very large computational domains. The finite difference method that was used is very fast, but the higher magnitude of error causes trouble in the swash zone, when very fine grid resolution is used. In very shallow regions, a very fine granularity is required for the grid resolution to accurately predict the waves in the swash zone. If the truncation error from the finite difference method is large relative to the shallow water depth and small wave heights in the swash zone, then convergence is lost.

4.5.1 Coastal Wave Simulation

The entire program was modularized into separate objects and files. A controller was designed to manage input, output, and the system initialization. A numerical module was used to implement the time domain finite difference method. All of the independent spatial derivative discretizations were implemented in a single file separate from the time domain method. A hierarchy of classes was constructed for the derivation of the logic for the Boussinesq and shallow water equations. Individual time dependent finite difference methods were implemented in every equation class from the basic wave equations to the Boussinesq equations.

4.5.2 Main Program

The main program application was written in C++. C++ provides extensive object orientation, and high efficiency, which are both essential for the numerical and graphical components of the program. C++ is a modern programming language that is extremely well suited for numerical programming if the user understands memory management well enough. It eliminates some of the overhead inherent in languages like Fortran, although recent versions of Fortran may be accelerated by calling c routines, or an accelerator like Cuda. Fortran's intrinsic functions and complex arithmetic make it a popular choice for numerical programming. The acceleration for the current program is being done using OpenCL called from C++ to access the CPU and GPU cores heterogeneously. The main advantage of Fortran is that it handles sophisticated array access, though there is some overhead when compared to a bare metal memory managed language like C or C++.

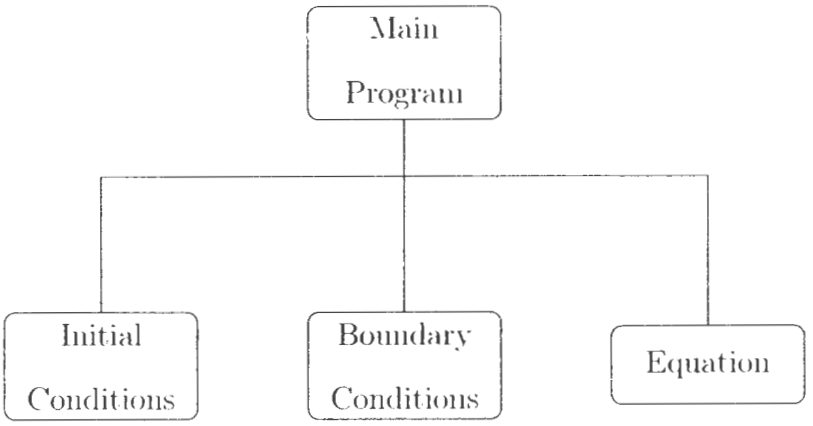

Figure 4.17: Overview of the numerical software

4.5.3 Precision

Double precision significantly increases the accuracy of the solution, and also speeds up the iteration to convergence since it reduces the overall floating point error. The tolerance value used in the convergence test for each step of the predictor corrector numerical method is 1.0×10^{-10}. Computer programs for numerical computation are inherently vulnerable to floating point error. If single precision is used for approximate variables for real numbers, and there is a lot of conversion between single and double precision variables, then there is a significant round off error, which may amplify and propagate throughout the fluid domain over time. Double precision is used throughout the program for the numerical method. Single precision may be used for some constant input parameters for which double precision is not necessary, or where only a few significant digits are required, but all instantaneous variables are kept in double precision.

4.5.4 Performance

Table 4.1: Run-Time Performance

# of Nodes	# of Time Steps	Run-Time
1000	1000	1.39 s
1000	5000	6.37 s
1000	10000	15.79 s
2000	10000	30.24 s
3000	10000	48.13 s
4000	10000	106.64 s
5000	10000	120.37 s
10000	10000	1091.95 s
10000	20000	2634.35 s

4.6 Other Software

Other software is available to simulate coastal wave propagation. A commercial software program, SMS, integrated Bouss2D, which was implemented by Nwogu and Demirbelik (2001) in conjunction with the U.S. Army Corps of Engineers at the Engineer Research and Development Center. The Bouss2D software program implements a Crank-Nicolson method for fully nonlinear BE for arbitrary depth. Internal or external wave generation is used for the initial conditions. Wave breaking and the effects of bottom friction are modelled with artificial dissipative terms. Flow through porous structures and the simulation of wave runup are also included. Kirby, Wei,

Chen, Kennedy, and Dalrymple (1998) and Kirby, Long, and Shi (2003) contributed to the software project Funwave created at the university of Delaware. The program differs from Bouss2D in that it implements a fourth order ABM predictor-corrector method. It allows specification of the BE in curvilinear coordinates, and retains high order dispersive and nonlinear terms. Liu, Lynnett, Sitanggang, and Kim developed a parallel long wave modeling program called Coulwave at Cornell University. The model is accurate up to fourth order in time and space. The difference in the software is that the program uses a multiple layer equation model, where velocities are taken at two or more reference water depths to further optimize the accuracy. Ferrant, Skourup, and Buchman developed the Xwave program which modelled fully nonlinear potential velocity equations. Engsig-Karup, Bingham, and Lindberg (2009) and Ducrozet, Bingham, Ensig-Karup, and Ferrant (2010) further developed the software into Oceanwave3D, a general purpose GPU software program for nonlinear long wave propagation with fully nonlinear potential flow equations. The software uses a parallel algorithm using a multi-grid domain and improved iterative solver. It models nonlinear wave-wave interaction, diffraction due to wave-structure interaction, and refraction from the bottom boundary.

Chapter 5

Conclusions and Recommendations

A high-order numerical scheme was applied to the extended Boussinesq equations, and a computer program was developed using the discretized equations. Validation of the numerical code has been done for many situations in which high nonlinearity and wave dispersion become increasingly important for the accurate prediction of waves travelling over changing water depth. The equations are applicable in increasing depths for long waves over steep slopes. Solitary and regular wave examples were shown with good agreement with analytical and experimental results. The extended Boussinesq equations accurately models frequency and amplitude dispersion and the ABM numerical method is stable for large CFL numbers. The high-order finite difference method gave very accurate values in the comparisons with experimental data. The method better predicts the amplitude dispersion than the FEM model, but the frequency dispersion is over predicted, which is seen in the small oscillations following the front wave form. The Boussinesq equations are flexible and has low complexity solutions for the propagation of waves from deep to shallow water. The Boussinesq equations have been well researched and validated for many different situations in which wave propagation and breaking occur. Several cases of wave

shoaling over variable bathymetry has been validated in the current research. Wave reflection of solitary waves is validated for the Boussinesq equations using the finite difference method, which is accurately predicted by the method. Undular bore wave propagation is also validated for the Boussinesq equations. Significant progress has been made by several researchers in the field of Boussinesq theory, but the collective research is spread over several different physical models and numerical methods. The current research is an attempt at consolidating the different theories while adding further enhancements to the methods and models.

5.1 Future Work

More investigation needs to be done regarding the numerical boundary conditions for the fluid domain, as for higher amplitudes the absorbing boundary conditions are not consistent. Fully absorbing boundary conditions using sponge layers or perfectly matching layers (PML) are required to absorb all of the dispersive and reflected waves. Full nonlinearity, high order dispersion, and vorticity from breaking waves are required to increase the accuracy of the extended Boussinesq wave model past the breaking point and into the surf zone. After significant shoaling, a vertical tangent exists on the face of the wave where wave breaking needs to be physically modelled with vorticity. Other breaking models which involve artificial dissipation through viscous terms in the momentum equations do not model the true physics of the wave motion. It is not an accurate representation of the real forces acting on the fluid during wave breaking. Dissipation from bottom friction is generated due to shear stress acting on the fluid from the impermeable and rigid boundary, but viscosity is only significant in extremely shallow water where shear forces are required to model wave runup in

the swash zone.

5.1.1 Physical Improvements

Vorticity transport generated from the wave breaking process was modeled in the surf zone by Yu and Svendsen (1995), and Veeramony and Svendsen (2000). They split the velocity equation into rotational and irrotational components. A volume of water is carried by the waveform at the front of the wave where the physical vorticity is generated. Fully nonlinear equations including vorticity were developed by Musumeci, Svendsen, and Veeramony (2005). The equations were further extended for the swash zone in extremely shallow water regions by Lo Re, Musumeci, and Foti (2012). Schaffer, Madsen, and Deigaard (1993) and Svendsen and Veeramony (1996) provided a well researched method to including vorticity by using simplified Reynolds equations given in Appendix B. Several other enhancements may be made to the Boussinesq model to improve the accuracy of the extended Boussinesq equations. Wave amplitude dispersion is over predicted in the current model. Higher nonlinearity and high order dispersion are increasingly important for larger amplitude waves and steeper shoaling waves.

Additional terms could be included in the numerical method to represent the generation of waves using a source function, and energy dissipation through wave breaking, bottom friction, and wind stress. The method should be extended to the fully nonlinear model by Wei and Kirby (1995), which better predicts the peak frequency of the model, since the wave amplitude is over predicted for waves of high nonlinearity. The fully nonlinear equations are provided in appendix A. Gobbi and Kirby (1998) derived a fourth order Pade approximation of the dispersion relation by including high order dispersive terms into the Boussinesq model. Other researchers also defined their own

dispersive terms to balance increasing nonlinearity. As waves crash upon the shoreline nearshore circulation of the fluid is induced. The entrainment of air within the fluid, and the bottom friction and undertow significantly affect the nearshore circulation. The equations can be further modified to handle undertow currents created by the breaking and runup of waves. A current model was developed by Wei and Kirby Wei and Kirby (1998). Wei and Kirby (1998) further developed the Boussinesq equations to handle sediment transport. Extremely large amplitude waves may be modelled using Boussinesq theory. Since the wave length increases with respect to the wave amplitude for Tsunamis. the extended equations remain valid for the prediction of Tsunami propagation over variable depth. It is the intent of the research to model massive Tsunamis like Fukushima.

5.1.2 Numerical Improvements

Several improvements may be made to the numerical method to increase the accuracy. Kaihatu and Kirby (1998) derived the Boussinesq equations for the frequency domain. Further research such as seakeeping using Boussinesq theory will require a frequency domain derivation of the equations for the computation of added mass and dampening. Shi, Dalrymple, Kirby, Chen, and Kennedy (2001) derived the equations in curvilinear coordinates. The generalized coordinates allow for irregularly shaped shorelines and also provided more efficient computation for near shore regions. The spatial discretization may be improved by modifying the size and structure of the grid. The grid construction significantly influences the accuracy of the numerical method. The numerical accuracy may be improved by reducing the time step and grid size. The time step and grid size are correlated with respect to the stability of the numerical method through the resulting CFL value. Lin (2008) developed a staggered grid finite difference method to calculate the velocities at offset locations from the

free surface variable to improve the accuracy of the model. Other numerical methods have been derived to allow for complicated boundaries and complex geometries using an unstructured grid. Unfortunately, structured girds are a requirement for using a finite difference method to compute the results. Sorensen and Schaffer (2002) derived a numerical method for Boussinesq equations for an unstructured grid using a finite element method.

Other computational methods may be used instead of the finite difference method. Lin and Liu (1998) used the volume of fluid method defined by Hirtz and Nichols to model breaking waves, using the $k-\epsilon$ turbulence model. Higher accuracy in the prediction of the surface elevations may be achieved using more complex methods. Nwogu developed a finite volume method to discretize the Boussinesq methods for an unstructured grid. Walkley (1999b) and Sorensen and Schaffer (2002) both developed finite element methods for the Boussinesq equations. The finite element equations allow for an unstructured grid to represent the domain. Grilli and J. Skourup (1989) implemented a Boussinesq model using a boundary element method. Nwogu coupled his Boussinesq method with a panel method to simulate waves generated by high speed vessels. Turbulence modelling for extremely shallow water regions in which viscosity becomes a significant influence on the evolution of the wave may be modelled using RANS, LES, DNS, and other turbulence models.

5.2 Other Improvements

Nwogu's derivation was used over other highly accurate models, such as those by Bingham, Madsen, Fuhrham, and Schaeffer, as referenced in the preceeding chapters. Kirby took an alternate approach to Madsen and added only a few highly nonlinear

terms to increase the accuracy of the model, but then focused on high order dispersion using Gobbi's model. All of these models still do not fully represent the physical phenomenon. Svendsen furthered his own research and combined it with Kirby's research. He included vorticity into the Boussinesq equations to describe the rotation of the fluid disrupting the region in the front face of the wave. The path of research defined by Svendsen was followed, though the trails left by the other researchers mentioned are also significant and should be further investigated. Nowgu's model was used due to its computational efficiency, and its flexibility to be incorporated into other models.

The results have shown that the Boussinesq model is an excellent choice for modelling dispersive long waves, such as those travelling in shallow water, or extremely large waves like tsunamis. The given method could be extended with the previous recommendations to give highly accurate waveforms in extremely shallow regions as well as in deep water.

Appendix A

Full Nonlinearity

Wei and Kirby (1995) and Schaffer, Madsen, and Deigaard (1993) derived fully nonlinear Boussinesq equations for variable depth. The weakly nonlinear equations over predict the amplitude dispersion. The high nonlinearity of shoaling waves requires equations that retain higher order nonlinear terms. Wei and Kirby derived the fully nonlinear momentum equation in terms of the velocity at an arbitrary depth.

$$\eta_t + \nabla F = 0$$

Where F is the depth integrated volume flux.

$$F = \int_{-h}^{\eta} u_i dz$$

$$F \to 0 \quad \text{as} \quad h + \eta \to 0$$

The higher nonlinear terms are integrated into the the free surface equation.

$$F = (h+\eta)\mathbf{u}+(h+\eta)\left[\frac{z_\alpha^2}{2} - \frac{1}{6}(h^2 - h\eta + \eta^2)\right]\nabla(\nabla\cdot\mathbf{u})+(h+\eta)\left[z_\alpha - \frac{1}{2}(h-\eta)\right]\nabla[\nabla\cdot(h\mathbf{u})]$$

The correlating dispersive terms are added to the momentum Equation.

$$\mathbf{u}_t + \mathbf{u}\cdot\nabla\mathbf{u} + g\nabla\eta + V_1 + V_2 = 0$$

Where V_1 and V_2 are the dispersive terms.

$$V_1 = \frac{z_\alpha^2}{2}\nabla(\nabla\cdot\mathbf{u}_t) + z_\alpha\nabla[\nabla\cdot(h\mathbf{u}_t)] - \nabla\left[\frac{1}{2}\eta^2\nabla\cdot\mathbf{u}_t + \eta_t\nabla\cdot(h\mathbf{u}_t)\right]$$

$$V_2 = \nabla\left[(z_\alpha - \eta)\nabla\cdot\mathbf{u}[\nabla\cdot(h\mathbf{u})] + \frac{1}{2}(z_\alpha^2 - \eta^2)\mathbf{u}\nabla(\nabla\cdot\mathbf{u})\right] + \frac{1}{2}\nabla\left[[\nabla\cdot(h\mathbf{u} + \eta\nabla\cdot\mathbf{u}]^2\right]$$

Appendix B

Surf Zone

B.1 Surf Zone

As a wave breaks, it enters the surf zone region. In this region, the physical process is drastically different than the effects of shoaling, though shoaling determines the initial wave velocity and setup as it enters the region, so the accurate prediction of shoaling significantly affects the breaking process. Wave breaking is difficult to model due to the discontinuity in the free surface elevation. As a wave propagates toward the shore, the wave height increases as the front of the wave steepens. Eventually, the extreme steepness of the wave causes it to break and collapse. The wave height decreases, and the wave energy dissipates into the nearshore circulation.

B.1.1 Artificial Dissipation

Numerical dissipation is used to model the effect of wave breaking. An eddy viscosity term is added to the momentum equation. The mixing length and velocity scale are used to predict the turbulent kinetic energy for the front face of the wave where the wave properties have met the breaking criteria. Zelt (1991) proposed an eddy viscosity

formula with a transport equation to model the turbulent kinetic energy. Empirical values are used to evaluate the dissipation terms for the mixing length and breaking point. The added terms to the momentum represent energy dissipation.

$$F_{br} = (\nu u_x)_x + (\nu u_y)_y$$

$$G_{br} = (\nu v_x)_x + (\nu v_y)_y$$

$$\nu = -B\delta^2(h+\eta)^2\nabla \cdot u_o$$

Where ν is the eddy viscosity, B is the breaking point coefficient, δ is the mixing length.

$$B = \begin{cases} 1 & \text{if} \quad \nabla \cdot u \leq 2u_x^* \\ \left(\frac{\nabla \cdot u}{u_x^*} - 1\right) & \text{if} \quad 2u_x^* < \nabla \cdot u \leq u_x^* \\ 0 & \text{if} \quad \nabla \cdot u > u_x^* \end{cases}$$

$$u_x^* = -0.3\sqrt{\frac{g}{h}}$$

Artificial dissipation does not represent the actual physics of the wave transformation. It produces highly accurate results for specific wave breaking situations, but without the inclusion of vorticity, the generation of the energy required to induce wave breaking is not well represented.

B.1.2 Vorticity

Schaffer, Madsen, and Deigaard (1993) developed the concept of the surface roller due to the increase in flux in the roller region. Svendsen and Veeramony (1996) proposed

a physical vorticity model for the breaking of waves in the surf zone. The vorticity transport equation is depth integrated and solved numerically or analytically. The velocity variable is decomposed into two separate variables to account for both the potential and rotational fluid flow. Dissipative and convective terms are added to the momentum equation to model the vorticity. The vorticity is generated beneath the toe of the roller.

$$u = u_r + u_p$$

$$u_r = \int_{-h}^{z} w dz + O(\mu^2)$$

$$w_t = [\nu_t w_z]_z$$

The transport equation is solved using surface and bottom boundary conditions.

$$w(-h) = 0 \qquad w(\eta) = w_t$$

Where w_t is the vorticity taken at the toe of the roller.

B.2 Swash Zone

The boundary location of the shoreline changes continuously as waves crash upon the beach. Bottom friction becomes significant in the swash zone due to the shallow water depth.

B.3 Wave Runup

The runup of waves along the shore is determined by computational cells, where dry cells are assumed to be porous regions. After the volume averaged velocities and elevation exceeds a threshold, the cell is treated as a wet cell in the following computation. When the free surface elevation drops below the threshold, the cell is assumed to be dry and porous region for the next time step. K is the friction coefficient proportional to the bottom roughness and the velocity profile.

$$F_b = -\frac{K}{h+\eta}\sqrt{u^2+v^2}u$$

The shoreline boundary is divided into wet and dry computational cells to allow for the variation in the shoreline. A singularity exists at zero total water depth, so a minimum water thickness is used for dry cells. The bottom friction and gravitational force causes the minimal amount of water to remain stationary.

B.3.1 Viscous Dampening of Solitary Waves

The effect of shear stress at the bottom boundary may be added to the depth integrated conservation of momentum equation (Mei 1989).

$$\frac{\partial \eta}{\partial t} + \frac{\partial [(h+\eta)u]}{\partial x} = 0$$

$$\frac{\partial u}{\partial t} + u\frac{\partial u}{\partial x} + g\frac{\partial \eta}{\partial x} + \frac{h^2}{2}\frac{\partial^3 u}{\partial x^2 \partial t} + \nu\frac{\partial u}{\partial z} = 0$$

$$\eta = a\,\mathrm{sech}^2\left[\frac{\sqrt{3a}}{2}\left(\sigma - \frac{a}{2}\tau\right)\right]$$

Appendix C

Wave Generation

C.1 Incident Waves

Wave generation is performed inside of the domain. A source term included in the continuity equation generates the waves internally. A Gaussian shape function and a magnitude of the source function dependent on time are used. The analytical solution for the magnitude of the source function is determined by Green's function. β is the shape coefficient, and I is an integral constant.

$$f(x, y, t) = D \exp\left[-\beta(x - x_s)^2\right] \sin\left(\lambda y - \omega t\right)$$

$$D = \frac{2a_0 \cos\theta[\omega^2 - (\alpha + \frac{1}{3})gk^4h^3]}{\omega^2 kI(1 - \alpha k^2 h^2)}$$

$$I = \int_{\infty}^{\infty} \exp\left(-\beta x^2\right) \exp\left(-il x\right) dx = \sqrt{\frac{\pi}{\beta}} \exp -\frac{l^2}{4\beta}$$

$$\beta = \frac{80}{\delta^2 L^2} \qquad \text{where} \quad \lambda = k \sin\theta \quad \text{and} \quad l = k \cos\theta$$

Appendix D

Absorbing Boundary

A sponge layer may be used as an absorbing boundary condition to dampen the wave energy for a wide range of frequencies and directions. The wave should propagate out of the domain without any reflection from the outgoing boundary. The wave energy is absorbed through dampening terms added to the momentum equations. The dampening layer width is proportional to the wavelength. The magnitude of dissipation by artificial sponge layers can be defined by spatial functions.

$$F_r = -w_1 u + (w_2 u_x)_x + (w_2 u_y)_y + w_3 \sqrt{\frac{g}{h}} \eta$$

Linear friction (or Newtonian cooling) and linear viscosity are represented by w_1 and w_2, respectively. The third term, w_3, is a sponge filter that predicts the effect of radiation on linear friction. These values are set to zero when no energy dissipation is needed. The sponge layer function is used to determine the contribution for each term.

$$w_i = \begin{cases} c_i \exp \frac{[(x_P)^N - 1]}{\exp(1) - 1} & \text{for} x_S < x < x_L \\ 0 & \text{for} 0 < x < x_S \end{cases}$$

Where c_i is a constant and x_P is the coordinate.

$$x_p = \frac{x - x_S}{x_L - x_S}$$

The open boundary may be further improved numerically by using a different form of absorbing boundary. A perfectly matched layer (PML) permits all incident waves to be completely absorbed so there is no reflection back into the domain.

Bibliography

Agnon, Y., P. A. Madsen, and H. A. Schaffer (1999). "A New Approach to High Order Boussinesq Models". *Journal of Fluid Mechanics* Vol. 399 pp. 319–333.

Airy, G. B. (1841). *Tides and Waves.*

Beji, S. and J. A. Battjes (1994). "Numerical Simulation of Nonlinear Wave Propagation over a Bar". *Coastal Engineering* Vol. 23 pp. 1–16.

Bingham, H. B. and Y. Agnon (2005). "A Fourier-Boussinesq Method for Nonlinear Water Waves". *European journal of Mechanics. B/Fluids* Vol. 24 pp. 255–274.

Bingham, H. B., P. A. Madsen, and D. R. Fuhrman (2009). "Velocity Potential Formulations of Highly Accurate Boussinesq-type Models". *Coastal Engineering* Vol. 56 pp. 467–478.

Boussinesq, J. (1871). "Théorie de l'intumescence liquide, applelée onde solitaire ou de translation, se propageant daus un canal rectangulaire". *Comptes Rendus de l'Academie des Sciences* Vol. 72 pp. 755–759.

Boussinesq, J.(1872). "Theorie des ondes et des remous qui se propagent le long d'un canal rectangulaire horizontal, en communiquant au liquide contenu dans ce canal

des vitesses sensiblement pareilles de la surface au fond". *Journal de Mathematiques pures et appliquees 2e serie* Vol. 17 pp. 55–108.

Chen, Y. and P.L.F Liu (1995). "Modfied Boussinesq Equations and Associated Parabolic Models for Water Wave Propagation". *Journal of Fluid Mechanics* Vol. 288 pp. 351–381.

Debnath, M. W. (1994). *Nonlinear Water Waves.* San Diego: Academic Press, Inc.

Dingemans, M. W. (1994). "Comparison of Computations with Boussinesq-like Models for Water Wave Propagation". *Technical Report. Mast G8-M.* p. 32.

Dingemans, M. W.(1997). "Comparison of Computations with Boussinesq-like Models for Water Wave Propagation". *Advanced Series on Ocean Engineering*, p. 1016.

Ducrozet, G., H. B. Bingham, A. P. Ensig-Karup, and Pierre Ferrant (2010). "High-order Finite Difference Solution for 3D Nonlinear Wave-Structure Interaction". *9th International Conference on Hydrodynamics* Vol. 22(5), pp. 225–230.

Engquist, B. and A. Majda (1977). "Absorbing Boundary Conditions for Numerical Simulation of Waves". *Proceedings from the National Academy of Scicnce* Vol. 74(5), pp. 1765–1766.

Engsig-Karup, A. P., H. B. Bingham, and O. Lindberg (2009). "An Efficient Flexible Order Model for 3D Nonlinear Waves". *Jounral of COmputational Physics* Vol. 228 pp. 2100–2118.

Euler, L. (1757). "Principes généraux du mouvement des fluides". *Mémoires de l'académie des sciences de Berlin* Vol. 11 pp. 274–315.

Friedrichs. K. O. (1946). "Water Waves on a Shallow Sloping Beach". *Computations on Pure and Applied Mathematics* Vol. 1 pp. 109-134.

Fuhrman. D. R. and P. A. Madsen (2008). "Simulation of Nonlinear Wave Run-up with a High Order Boussinesq Model". *Coastal Engineering* Vol. 55 pp. 139 154.

Gerstner. F. J. von (1809). "Theorie der wellen". *Annalen der Physik* Vol. 32(8). pp. 412 445.

Gobbi. M. F. and J. T. Kirby (1998). "A New Boussinesq-Type Model for Surface Water Wave Propagation". *Center for Applied Coastal Research.*

Grilli. S. T. and I. A. Svendsen J. Skourup (1989). "An Efficient Boundary Element Method for Nonlinear Water Waves". *Engineering Analysis with Boundary Elements* Vol. 6(2). pp. 97-107.

Grilli. S. T. and R. Subramanya (1993). "Nonlinear wave modelling in very shallow water". *Proceedings of the 15th International Conference of Boundary Elements in Engineering*. pp. 196 204.

Kaihatu. J. M. and J. T. Kirby (1998). "Two-Dimensional Parabolic Modeling of Extended Boussinesq Equations". *Journal of Waterway. Port. Coastal. and Ocean Engineering* Vol. 124(2). pp. 57 67.

Kennedy. A. B. and J. T. Gobbi (2002). "Simplified higher-order Boussinesq Equations. I. Linear Simplifications". *Coastal Engineering* Vol. 44 pp. 205 229.

Kennedy, A. B., J. T. Kirby, Q. Chen, and R. A. Darymple (2001). "Boussinesq-Type quations with Improved Nonlinear Performance". *Center for Applied Coastal Research*. pp. 225–243.

Kirby, J. T., W. Long, and F. Shi (2003). "Funwave 2.0: Fully Nonlinear Boussinesq Wave Model on Curvilinear Coordinates Documentations and User's Manual". *Center for Applied Coastal Research.*

Kirby, J. T., G. Wei, Q. Chen, A. B. Kennedy, and R. A. Dalrymple (1998). "Funwave 1.0: Fully Nonlinear Boussinesq Wave Model Documentations and User's Manual". *Center for Applied Coastal Research.*

Korteweg, D. J. and G. de Vries (1895). "On the Change of Form of Long Waves Advancing in a Rectangular Canal, and on a New Type of Long Stationary Waves". *Philosophical Magazine* Vol. 7 pp. 441–455.

LeVeque, R. J. (2007). "Finite Difference Methods for Ordinary and Partial Differential Equations", p. 341.

Lewy, H. (1946). "Water Waves on Sloping Beaches". *Bulletin of the American Mathematical Society* Vol. 52(9), pp. 737–775.

Lin, P. (2008). *Numerical Modeling of Water Waves*. New York: Taylor & Francis.

Lin, P. and P. L. F. Liu (1998). "A Numerical Study of Breaking Waves in the Surf Zone". *Journal of FLuid Mechanics* Vol. 359 pp. 239–264.

Lo Re. C., R. E. Musumeci, and E. Foti (2012). "A Shoreline Boundary Condition for a Highly Nonlinear Boussinesq Model for Breaking Waves". *Coastal Engineering* Vol. 60 pp. 41–52.

Lynett, P. and P. L. F. Liu (2004). "A Two-Layer Approach to Wave Modelling". *Proceedings of the Royal Society* Vol. 460 pp. 2637–2669.

Madsen, P. A., D. R. Fuhrman, and B. Wang (2006). "A Boussinesq-type Method for Fully Nonlinear Waves Interacting with a Rapidly Varying Bathymetry". *Coastal Engineering* Vol. 53 pp. 487–504.

Madsen, P. A., Russel Murray, and O. R. Sorensen (1991). "A New Form of the Boussiensq Equations with Improved Linear Dispersion Characteristics". *Coastal Engineering* Vol. 15 pp. 371–388.

Madsen, P. A. and O. R. Sorensen (1992). "A New Form of the Boussiensq Equations with Improved Linear Dispersion Characteristics. Part 2. A Slowly-Varying Bathymetry". *Coastal Engineering* Vol. 18 pp. 183–204.

Mei, C. C. (1989). "The Applied Dynamics of Ocean Surface Waves". *Advanced Series on Ocean Engineering* Vol. 1 p. 740.

Mei, C. C. and B. Le Mehaute (1966). "Note on the Equations of Long Waves Over an Uneven Bottom". *National Engineering Science Company* Vol. 71(2). pp. 393–400.

Mei, C. C., M. Stiassnie, and K. P. Y. Yue (2005). "Theory and Applications of Ocean Surface Waves". *Advanced Series on Ocean Engineering* Vol. 23 p. 506.

Musumeci, R. E., I. A. Svendsen, and J. Veeramony (2005). "The Flow in the Surf Zone: A Fully Nonlinear Boussinesq-type of Approach". *Coastal Engineering* Vol. 52 pp. 565–598.

Newman, J. N. (1978a). *Marine Hydrodynamics*. Massachusetts Institute of Technology. p. 402.

Newman, J. N.(1978b). "The Theory of Ship Motions". *Advances in Applied Mechanics* Vol. 18 pp. 221–283.

Nwogu, O. (1993). "Alternative Form of Booussinesq Equations for Nearshore Wave Propagation". *Journal of Waterway, Port, Coastal and Ocean Engineering* Vol. 119(6), pp. 618–638.

Nwogu, O.(2007). "Numerical Modeling of Waves Generated by High-Speed Vessels in Shallow Water with a Coupled Boussinesq-Panel Method". *International Conference on Numerical Ship Hydrodynamics* Vol. 119(331-343).

Nwogu, O. and Z. Demirbelik (2001). "BOUSS-2D: Aboussinesq Wave Model for Coastal Regions and Harbors". *US Army Corps of Engineers*, p. 92.

Peregrine, D. H. (1967). "Long Waves on a Beach". *Journal of Waterway, Port, Coastal and Ocean Engineering* Vol. 27(4), pp. 815–827.

Peregrine, D. H.(1972). "Equations for Water Waves and the Approximation Behind Them". *Waves on Beaches and Resulting Sediment Transport*. Ed. by R. E. Meyer, pp. 95–122.

Phillips, O. M. (1977). *The Dynamics of the Upper Ocean*. 2nd ed. London: Cambridge University Press. p. 336.

Rayleigh, J. W. S. Lord (1876). "On Waves". *Philosophical Magazine*. pp. 311 390.

Russell, J. S. (1844). "Report on Waves". *Report of the British Association for the Advancement of Science*. pp. 311 390.

Schaffer, H. A., P. A. Madsen, and Rold Deigaard (1993). "A Boussinesq Model for Waves Breaking in Shallow Water". *Coastal Engineering* Vol. 20 pp. 185 202.

Schäffer, H. A. and P. A. Madsen (1995). "Further Enhancements of Boussinesq-type Equations". *Coastal Engineering* Vol. 26 pp. 1 14.

Shi, F., A. Dalrymple, J. T. Kirby, Q. Chen, and A. Kennedy (2001). "A Fully Nonlinear Boussinesq Model in Generalized Curvilinear Coordinates". *Coastal Engineering* Vol. 42 pp. 337 358.

Sommerfeld, A. (1949). *Partial Differential Equations in Physics*. New York. p. 335.

Sorensen, O. R. and H. A. Schaffer (2002). "Wave Breaking in a Boussinesq Model with Unstructured Grids". *Coastal Engineering*. pp. 369 379.

Stoker, J. J. (1947). "Surface Waves in Water of Variable Depth". *Quarterly of Applied Mathematics* Vol. 5 pp. 1 55.

Stoker, J. J.(1957). *Water Waves*. Vol. 4. New York: Institute of Mathematical Sciences.

Stokes, G. G. (1847). "On the Theory of Oscillatory Waves". *Transactions of the Cambridge Philosophical Society* Vol. 7 pp. 441–455.

Svendsen, I. A. (2006). *Introduction to Nearshore Hydrodynamics.* Vol. 24. London: World Scientific Publishing Co. Pte Ltd., p. 722.

Svendsen, I. A. and J. Veeramony (1996). "A Boussinesq Breaking Wave Model with Vorticity". *Coastal Engineering.* pp. 1192–1204.

Thomas, J. W. (1995). *Numerical Partial Differential Equations: FD Methods.* New York: Springer-Verlag, p. 437.

Ursell, F. (1953). "The Long Wave Paradox in the Theory of Gravity Waves". *Proceedings of the Cambridge Philosophical Society* Vol. 49(4), pp. 685–694.

Veeramony, J. and I. A. Svendsen (2000). "The Flow in Surf-Zone Waves". *Coastal Engineering* Vol. 39 pp. 93–122.

Venant, B. St. (1871). "Théorie du movement non-permanent des eaux". *Comptes Rendus Academie des Sciences* Vol. 73 pp. 147–237.

Walkley, M. A. (1999a). "A Finite Element Method for the One Dimensional Extended Boussinesq Equations". *International Journal for Numerical Methods in Fluids* Vol. 29 pp. 143–157.

Walkley, M. A.(1999b). "A Numerical Method for Extended Boussinesq Shallow-Water Wave Equations". *PhD Thesis.*

Wehausen, J. V. and E. V. Laitone (1960). *Surface Waves.* Springer-Verlag, p. 778.

Wei, G. and J. T. Kirby (1995). "Time Dependent Numerical Code for Extended Boussinesq Equations". *Journal of Waterway Port Coastal Ocean Engineering. ASCE* Vol. 121(5). pp. 251 261.

Wei, G. and J. T. Kirby(1998). "Simulation of Water Waves by Boussinesq Models". *Center for Applied Coastal Research.*

Wei, G., J. T. Kirby, S. T. Grilli, and R. Subramanya (1995). "A Fully Nonlinear Boussinesq Model for Surface Waves, Part 1. Highly Nonlinear Unsteady Waves". *Journal of Fluid Mechanics* Vol. 294 pp. 71 92.

Whitham, G. B. (1974). *Linear and Nonlinear Waves.* John Wiley & Sons. Inc., p. 636.

Witting, J. M. (1984). "A Unified Model for the Evolution of Nonlinear Water Waves". *Journal of Computational Physics* Vol. 56 pp. 203 236.

Yu, K. and I. A. Svendsen (1995). "Breaking Waves in Surfzones". *Coastal Dynamics.* pp. 329 340.

Zelt, J. A. (1991). "The Run-up of Nonbreaking and Breaking Solitary Waves". *Coastal Engineering* Vol. 15 pp. 205 246.